# Motor Cortex Encodes Forelimb Joint Movements According To Contextual Relevance

---

**Dissertation**

**zur**

**Erlangung der naturwissenschaftlichen Doktorwürde**

**(Dr. sc. nat.)**

**vorgelegt der**

**Mathematisch-naturwissenschaftlichen Fakultät**

**der**

**Universität Zürich**

**von**

**Wolfgang Omlor**

**aus**

**Deutschland**

**Promotionskomitee**

Prof. Dr. Fritjof Helmchen (Vorsitz)

Prof. Dr. Martin Schwab

Prof. Dr. Giacomo Indiveri

**Zürich, 2016**

# Contents


SUMMARY ..... 5

ZUSAMMENFASSUNG ..... 7

1. INTRODUCTION TO THE MAMMALIAN MOTOR SYSTEM ..... 9

1.1 CONCEPT OF NEURONAL NETWORKS ..... 13
1.2 DISCOVERY AND CHARACTERIZATION OF THE PRIMARY MOTOR CORTEX ..... 15
1.3 IDENTIFICATION OF THE PRE- AND SUPPLEMENTARY MOTOR CORTEX ..... 19
1.4 ACTION MAPS AS NEW PERSPECTIVE TO CONCEPTUALIZE MOTOR CORTEX FUNCTION ..... 21
1.5 REPRESENTATION OF MOVEMENT VARIABLES IN THE MOTOR CORTEX ..... 23
1.6 CURRENT THEORIES ABOUT THE MAMMALIAN MOTOR SYSTEM ..... 24
*1.6.1 Neuronal tuning to useful fragments of motor behaviour ..... 24*
*1.6.2 Optimal feedback control theory as concept to interpret voluntary motor behaviour 25*
*1.6.3 The dynamic systems perspective ..... 28*
1.7 SPECIFIC AIMS OF THIS STUDY ..... 29

2. GENERAL EXPERIMENTAL APPROACH: A WINDOW TO THE BRAIN ..... 33

2.1 OPTOGENETIC STIMULATION ..... 33
2.2 TWO-PHOTON CALCIUM IMAGING OF GENETICALLY ENCODED CALCIUM INDICATORS (GECIS) ..... 35
*2.2.1 Principles of two-photon microscopy ..... 35*
*2.2.2 Fluorescent calcium indicators ..... 38*
*2.2.3 Calcium dynamics during action potentials ..... 39*
*2.2.4 GECI properties and side-effects on cell homeostasis ..... 40*
*2.2.5 Selection of a calcium indicator for our study ..... 41*

3. MATERIAL AND METHODS ..... 43

3.1 SURGERY ..... 43
3.2 BEHAVIORAL SETUP AND TRAINING ..... 43
3.3 MOTION TRACKING DURING M1 MAPPING AND CALCIUM IMAGING ..... 45
3.4 OPTOGENETIC MOTOR MAPPING ..... 45
3.5 TWO-PHOTON IMAGING ..... 46
3.6 GRASP TYPE CLASSIFICATION AND GRASP-TO-GRASP VARIABILITY ..... 46
3.7 SIMILARITY MEASURE OF INDIVIDUAL GRASPS ..... 49
3.8 TWIN MOVEMENT ANALYSIS ..... 49
3.9 ELECTROPHYSIOLOGICAL CONTROL EXPERIMENT ..... 51
3.10 CALCIUM IMAGING ANALYSIS ..... 52
3.11 POPULATION CODING AND CLASSIFICATION WITH CROSS-VALIDATION ..... 52
3.12 STATISTICS ..... 53

4. RESULTS ..... 55

4.1 ANALYSIS OF BEHAVIOURAL VARIABLES ..... 55
4.2 OPTOGENETIC MAPPING OF THE MOTOR CORTEX ..... 59
4.3 CALCIUM IMAGING AND ANALYSIS OF NEURONAL ACTIVITY IN M1 L2/3 ..... 61
4.4 POPULATION CODING OF JOINT ANGLES ON THE REGULAR AND IRREGULAR PATTERN ..... 64
4.5 POPULATION CODING DURING SPECIFIC GRASP TYPES ..... 65
4.6 POPULATION CODING OF JOINT ANGLES DURING EQUIVALENT MOVEMENT SUBSETS DEPENDS ON THE BEHAVIOURAL CONTEXT ..... 67

5. DISCUSSION ..... 71

5.1 NEURONAL TUNING DURING SIMPLIFIED MOVEMENT SETS AND NATURAL BEHAVIOR ..... 72
5.2 GRASP-TO-GRASP VARIABILITY OF INDIVIDUAL JOINT MOTION AS CONTEXTUAL SIGNATURE ..... 73
5.3 ENCODING IN M1 L2/3 WITH REGARD TO DIFFERENT GRASP TYPES ..... 74

**5.4 Does M1 L2/3 function to purposefully integrate contextual, motor and somatosensory features into the motor command?** ..... 74
**5.5 Conclusion** ..... 75

**6. OUTLOOK** ..... **77**

**6.1 Applicability of our results for the investigation of Parkinson's disease** ..... 77
***6.1.1 Current and potential future approaches to treat Parkinson's disease*** ..... *78*
***6.1.2 Rationale to decipher and modulate motor cortex networks in reference to the basal ganglia loop*** ..... *79*
***6.1.3 Concrete experiments for the investigation of Parkinson's disease*** ..... *81*
**6.2 Applicability of our results for the investigation of motor cortex stroke** ..... 83
***6.2.1 Principles of cortical plasticity after stroke*** ..... *84*
***6.2.2 Concrete experiments to analyse cortical plasticity at the level of neuronal networks*** ..... *85*
**6.3 Concluding remarks: General significance of this study** ..... 89

**7. APPENDIX** ..... **91**

CURRICULUM VITAE ..... 92
**Publication list (peer-review articles)** ..... 94
**Acknowledgement** ..... 95
**References** ..... 96

## Summary

Primary motor cortex (M1) contributes to the control of limb movements which have to be applied not only in isolation but also within purposeful sequences during everyday life. How the M1 neuronal network encodes motion of individual limb joints and in particular how their encoding depends on contextual features of a movement sequence remains unclear. Here we combined two recent techniques to investigate these questions, optogenetic stimulation and two-photon calcium imaging of genetically encoded calcium indicators. Using transgenic mice which express the light-excitable cation channel channelrhodopsin-2 in cortical layer 5 neurons, we first applied optogenetic stimulation through a chronic cranial window to map the motor cortex. Without having to impair the architecture of the underlying neuronal networks with electrode penetrations, we were thus able to identify equivalent motor cortex circuits across mice that are involved in the control of proximal and distal forelimb joints. In the focal area of these M1 circuits, we subsequently employed two-photon calcium imaging to record the activity in neuronal networks of layer 2/3 (L2/3) while head-fixed mice moved across regularly or irregularly spaced rungs on ladder wheels. During skilled locomotion of the animals, we also tracked the motion in proximal and distal forelimb joints using high-speed videography. By predicting kinematics of the individual forelimb joint angles from M1 L2/3 network activity we discovered that finger motion was represented under both conditions whereas encoding of shoulder motion increased for the irregular pattern. Condition-related encoding differences of individual joints correlated with condition-related differences of their grasp-to-grasp variability during the entire movement sequence. This correlation persisted when we only considered discrete grasping actions on the regular and irregular pattern that featured equivalent kinematics in both conditions. We additionally classified three salient forelimb grasp types that occurred under both conditions ('standard', 'corrective', and near-slip 'digit tip' grasps). While the representation of finger motion was particularly high during digit tip grasps, the encoding of shoulder motion on the irregular pattern originated mainly from corrective grasps. Additionally, corrective and digit tip grasps, both of which are associated

with an impending fall, could be directly predicted from the activity in neuronal networks of M1 L2/3.

Our results suggest that neuronal populations in M1 L2/3 encode motion of individual joints according to their contextual relevance. In a learned movement sequence, neuronal networks incorporate the required grasp-to-grasp variability of individual joints as contextual signature to strengthen the representation of joints with frequent amplitude recalibration. Moreover, the encoding of motion in a joint is upregulated when its control seems to be especially relevant during the execution of a particular grasp type. Our findings are also associated with the forelimb deficits rodents modelling motor cortex stroke or Parkinson's disease exhibit on the rung ladder, thereby providing a novel framework to investigate the cortical pathophysiology in these motor disorders.

## Zusammenfassung

Der primär-motorische Kortex (M1) ist entscheidend für die Umsetzung von feinmotorischen Armbewegungen, die nicht nur isoliert, sondern meist in sinnvollen Sequenzen ausgeübt werden müssen. Wie die einzelnen Armgelenke von M1 kodiert werden und insbesondere wie ihre Kodierung von Kontextmerkmalen einer Bewegungssequenz abhängt, ist jedoch ungeklärt. In unserer Studie haben wir mit „Optogenetik“ und „2-Photonen-Kalzium-Imaging“ zwei innovative Methoden kombiniert, um diesen Fragen nachzugehen. Optogenetische Stimulation durch ein chronisches Glasfenster wurde in transgenen Mäusen durchgeführt, die den lichtaktivierbaren Kationenkanal Channelrhodopsin-2 in M1 Schicht 5 exprimierten. Auf diese Weise konnten wir in allen Tieren vergleichbare neuronale Schaltkreise in M1 identifizieren, die in die Koordination aller wichtigen proximalen und distalen Armgelenke eingebunden sind und deren Architektur nicht durch Elektrodenpenetrationen beschädigt wurde. Im Bereich dieser Schaltkreise wurde danach die Aktivität von neuronalen Netzwerken in M1 Schicht 2/3 mittels 2-Photonen-Kalzium-Imaging untersucht, während sich kopffixierte Mäuse auf einem Laufrad über Leitersprossen mit regelmässigem oder unregelmässigem Abstand bewegten. Wir benutzten anschliessend mathematische Modelle, um anhand der neuronalen Netzwerkaktivität die Bewegungen der einzelnen proximalen und distalen Gelenke des rechten Arms vorauszusagen. Diese Analyse ergab, dass Fingerbewegungen sowohl in der regulären als auch in der irregulären Bedingung stark vom motorischen Kortex kodiert werden, während die Repräsentation von Schulterbewegungen speziell in der irregulären Bedingung signifikant anstieg. Bedingungsbezogene Unterschiede in der Kodierung der einzelnen Armgelenke im motorischen Kortex korrelierten positiv mit entsprechenden Unterschieden in ihrer Variabilität während der gesamten Bewegungssequenz. Die Korrelation blieb auch dann bestehen, wenn nur Teilmengen von identischen Bewegungen in beiden Bedingungen betrachtet wurden. In einer detaillierteren Analyse haben wir basierend auf kinematischen Merkmalen drei Greifbewegungen klassifiziert, die in verschiedener Häufigkeit in beiden Bedingungen vorkamen: Standard-Griff, korrektiver Griff sowie Fingerspitzen-Griff. Die Kodierung von Fingerbewegungen war in beiden Bedingungen insbesondere beim

Fingerspitzen-Griff ausgeprägt, während die M1-Repräsentation von Schulterbewegungen in der irregulären Bedingung insbesondere mit dem korrektiven Griff assoziiert war. Zusätzlich waren der korrektive Griff und der Fingerspitzengriff, die beide mit einem drohenden Fall assoziiert sind, stärker in neuronalen Netzwerken von M1 L2/3 repräsentiert.

Unsere Ergebnisse legen nahe, dass neuronale Populationen im motorischen Kortex Gelenkbewegungen gemäss ihrer Relevanz im Bewegungskontext repräsentieren. Neuronale Netzwerke gliedern dabei die erforderliche, sequenzspezifische Variabilität der einzelnen Gelenke als Kontextsignatur in ihr Kodierungsschema ein und verstärken die Repräsentation von Gelenken mit häufigen Amplitudenänderungen. Daher können Gelenkbewegungen der gleichen motorischen Einzelaktion je nach Kontext anders in neuronalen Netzwerken von M1 kodiert werden. Darüber hinaus werden Bewegungen in bestimmten Gelenken stärker kodiert, wenn sie besonders relevant für die Ausführung eines spezifischen Greifbewegungstyps sind. Unsere Ergebnisse zeigen auch einen möglichen Zusammenhang mit den Armbewegungsdefiziten, die Mäuse mit einem Schlaganfall oder Parkinson-Modell auf dem „Leiterspossen-Test“ zeigen, und eröffnen dadurch neue Möglichkeiten, kortikale Fehlfunktionen motorischer Krankheiten zu entschlüsseln.

## 1. Introduction to the mammalian motor system

**"I move, therefore I am"**

***Haruki Murakami (2011)***

Moving enables interaction with the world. We walk, speak, manipulate objects around us and convey social gestures by moving specific parts of our body. Therefore, life quality can be dramatically reduced when our movement repertoire is compromised owing to neurologic disease. Even though our understanding of the mammalian motor system substantially increased in the past 140 years, the operation principles of key units such as the primary motor cortex still remain unclear.

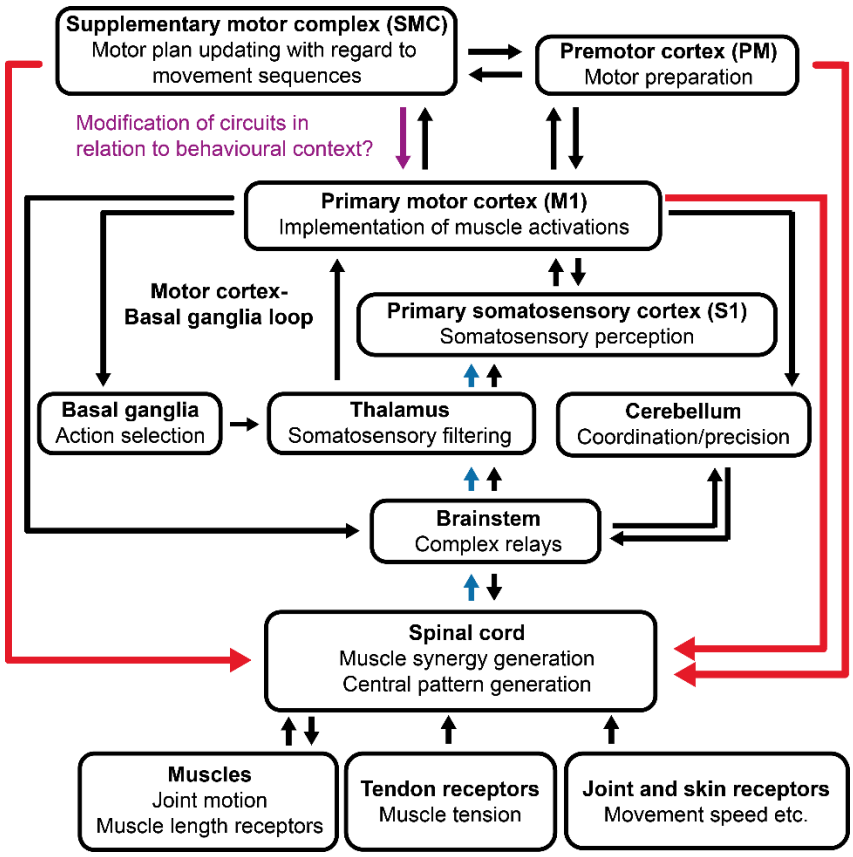


**Figure 1: Brain circuits for voluntary limb control**
Simplified scheme of functional units that process different aspects of limb movements, along with a selection of relevant connectivities; for each unit, one or two major functions regarding voluntary limb control are indicated; in reality, both the functions of each unit and the connectivity between units are by far more complex. The corticospinal tract is highlighted in red, the medial lemniscus pathway in blue. Our study asks if and how the behavioural movement context affects the processing in M1; SMC is a potential candidate to modify M1 circuits by conveying information about the movement sequence context.

In mammals, production and control of voluntary movements requires the coordinated interplay of many functional units that influence each other directly or indirectly within a complex circuitry (Fig. 1). This study deals with the operation mode of the primary motor cortex (M1) which is why I will outline in the subsequent sections mainly the current conception of the mammalian M1 and of its most important interconnecting structures. Since modern notions of mammalian motor cortex function have been largely derived from primate studies, monkey literature will prevail in the following review, but the key concepts will also be related to rodents which have been investigated in our study.

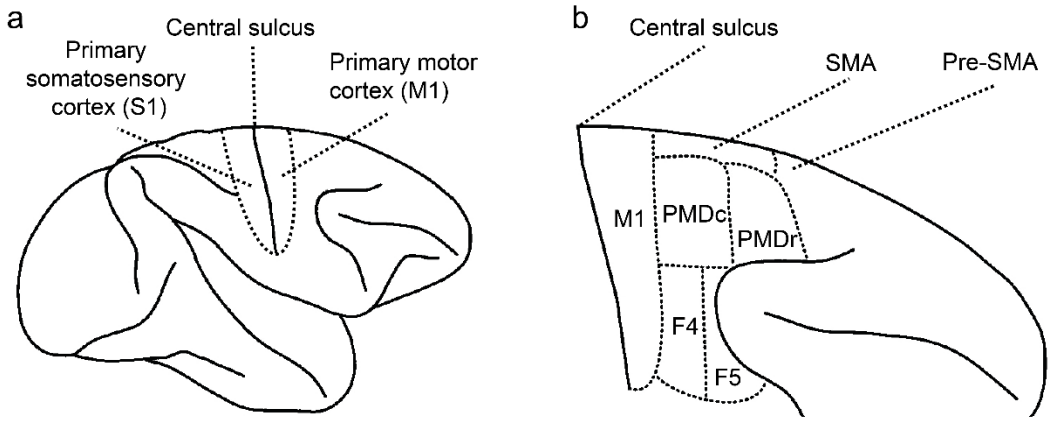


**Figure 2: Cortical sensorimotor areas in the primate brain**
**a**, Primary motor cortex (M1, anterior to the central sulcus) and primary somatosensory cortex (S1, posterior to the central sulcus) are shown for the monkey brain. **b**, Enlargement of *a* illustrating M1, the different premotor areas (PMDc, PMDr, F4, F5), the supplementary motor area (SMA) and the pre-supplementary area (Pre-SMA). SMA and Pre-SMA are collectively termed supplementary motor complex (SMC). Adapted from Graziano (2006).

In primates, the motor cortex is an area of the frontal lobe and can be divided into the primary motor cortex (M1), premotor cortex (PM) and into the supplementary motor complex (SMC), which is in turn subclassified into the supplementary motor area (SMA) and the pre-supplementary motor area (Pre-SMA, Fig. 2). All three subregions (M1, PM and SMC) are involved in the generation of final motor commands and are particularly important for the production of dexterous limb movements (Graziano, 2006). Based on histological features, M1, PM and SMA as well as other neocortical areas such as the primary somatosensory cortex (S1) can be formally divided into 6 neuronal layers (Fig. 3). While the presence of layer 4 (L4) defining granule cells is faint in SMA and PM, L4 is essentially non-existent in M1, which is

therefore also called “agranular” cortex (Kandel, 2013). In all motor areas, layer 2/3 (L2/3) mainly mediates intracortical communication through reciprocal horizontal projections, while output pathways to subcortical structures emerge from layer 5 (L5). L3, in turn, provides strong excitatory projections to L5 (Weiler et al., 2008). In addition to the layer-structure, neurons in the neocortex are organized into columns that are on the order of hundred microns wide, traverse all layers and are presumed to represent computational modules (Kandel, 2013). Each column habours principal neurons which are excitatory and often project to distant targets as well as different inhibitory interneurons with local connectivity (Harris and Mrsic-Flogel, 2013). Several types of interneurons, for instance basket cells or chandelier cells, can be distinguished based on their connectivity pattern and their co-transmitters (Kepecs and Fishell, 2014). These excitatory and inhibitory neurons interact based on a complex connectivity scheme to generate inter alia versatile behavioural functions.

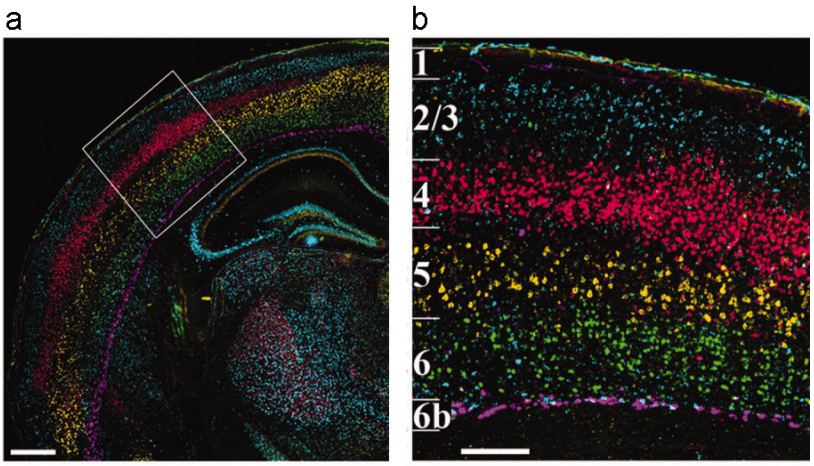


**Figure 3: Layers in the mouse neocortex**
**a**, Section through the primary somatosensory cortex of mice in which each cortical layer is labelled by a fluorescent marker; **b**, Enlarged view of the white rectangle marked in a, showing the laminar segregation of neurons into six layers. Scale bars = 500 µm in a, 200 µm in b. Adapted from Boyle et al. (2011).

To understand the current conceptions of voluntary motor control, the following closed loop between cortex and spinal cord is central (Fig. 4): L5 neurons from M1, PM and SMC connect to the spinal cord via the corticospinal tract (Fig. 4a), impinging on interneurons or directly on alpha-motoneurons (only in some non-human primates and in humans) which in turn activate muscles (Lemon and Griffiths, 2005). Muscles provide proprioceptive information about their length and tension via peripheral nerves that project back to the spinal cord, cross as part of

the medial lemniscus pathway (Fig. 4b) again to the contralateral side and are relayed via brainstem and thalamus to S1 (Trepel, 2004). S1 L2/3 reciprocally connects to M1 L2/3, thereby closing the loop. Additionally, M1 L2/3 features reciprocal horizontal connections with L2/3 of PM and SMC (Graziano, 2009). Fibers of the corticospinal tract also originate from S1, the posterior parietal cortex, the parietal operculum and cingulate motor areas (Lemon and Griffiths, 2005). Projections from S1 thereby connect to spinal neurons in the dorsal horn to filter and modify arriving somatosensory input (Ralston and Ralston, 1985, Kandel, 2013).

In comparison to primates or humans, the motor system of rodents is organized similarly, albeit there are also some notable differences. Similar to primates or humans, rodents are thought to possess counterparts of M1, PM and SMC, which are phylogenetically less sophisticated but in general subserve similar functions (Passingham et al., 1988, Lemon and Griffiths, 2005, Yin, 2009, Sul et al., 2011, Gremel and Costa, 2013). While the primary motor cortex of mice is also abbreviated as M1, PM and SMC are subsumed to the secondary motor cortex (M2) (Yin, 2009, Gremel and Costa, 2013). In contrast to some primates and humans, the corticospinal tract of rats and mice does presumably not possess direct, monosynaptic excitatory connections to alpha-motoneurons (Yang and Lemon, 2003, Alstermark and Ogawa, 2004). These so-called cortico-motoneuronal projections allow the selective control of small muscle groups and have been associated with increased dexterity and improved independent control of fingers (Kuypers, 1978, Lemon and Griffiths, 2005). In general, the motor behaviour of rodents is less reliant on the corticospinal tract since many aspects of their movement repertoire recover after interruption of this pathway (Lemon and Griffiths, 2005). Even though the corticospinal tract of rodents is involved in the organization of dexterous motor control (Metz and Whishaw, 2002), many effects on limb motoneurons are generated by cortico-reticulospinal pathways (Alstermark and Ogawa, 2004, Alstermark et al., 2004).

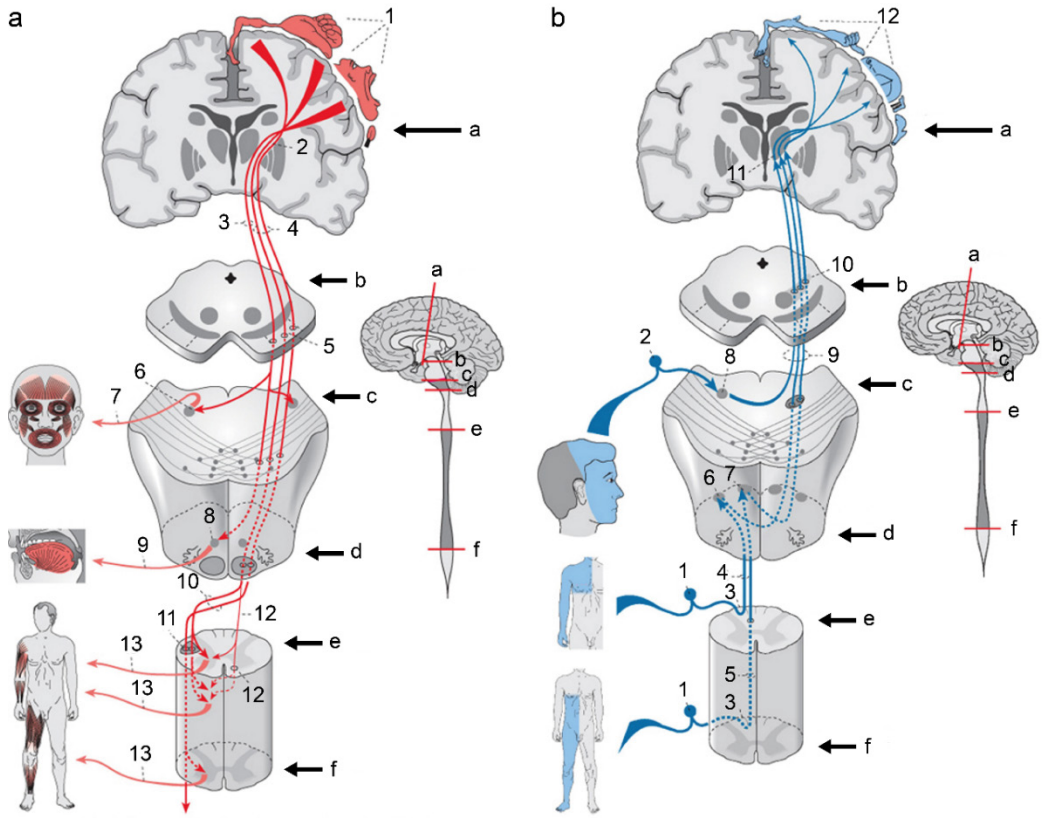


**Figure 4: Corticospinal tract and medial lemniscus pathway**
**a**: Corticospinal tract, starting in somatotopic order from M1 (1); capsula interna (2), tractus corticonuclearis (3), tractus corticospinalis (4), crus cerebri (5), cranial nerves and respective nuclei (6-9), crossing (10) of the tractus corticospinalis lateralis (11), tractus corticospinalis anterior (12), motoneuron axons (13); **b**: Medial lemniscus pathway; dorsal root ganglion (1), ganglion trigeminale (2), posterior column in the spinal cord (3), fasciculus cuneatus (4) receiving information inter alia from arm and hand, fasciculus gracilis (5), relay nuclei (6,7,8), medial lemniscus (9,10), thalamus (11), S1 in somatotopical order (12). Adapted from Trepel (2004) .

### 1.1 Concept of neuronal networks

Over a century ago, Cajal and Sherrington postulated that the individual neuron represents the structural and functional unit of our brain (Cajal, 1888, Sherrington, 1906). This view was further promoted by the concept that individual neurons were characterized by their own receptive field which can be activated by a specific sensory feature (Maturana et al., 1960). However, many characteristics of the brain such as the generation of spontaneous activity in the absence of sensory stimuli (Steriade et al., 1990, Kenet et al., 2003, Miller et al., 2014) are difficult to explain from the perspective of single cells and their receptive fields (Yuste, 2015). In particular the generation of spontaneous activity indicates that neurons could be engaged in intrinsic functions which do not relate to specific motor actions or a certain sensory stimulus

(Yuste, 2015). Moreover, the application of novel multi-neuronal recording techniques such as two-photon calcium imaging increasingly suggests that activity states of neuronal populations accounts for mammalian behaviour rather than the firing of single cells (Harvey et al., 2012). Therefore, the concept of neuronal networks more and more eclipses the focus on individual neurons. This concept assumes that neural circuit function arises from the activity of large neuronal ensembles that feature a complex connectivity scheme (Churchland and Sejnowski, 1992). In mammalian brains most neural circuits are characterized by distributed connectivity with each excitatory or inhibitory neuron sending output to a large number of cells and with most neurons receiving input from many cells (Shepherd, 1990). This architecture is thought to entail recursive and reverberating activity patterns of neuronal assemblies that occur in closed loops and generate functional states of the brain (Hebb, 1949). Coincident activation of pre- and postsynaptic neurons can then strengthen their connection, essentially enabling circuits to learn activity patterns (Hebb, 1949, Stellwagen and Shatz, 2002, Butts et al., 2007).

In attempts to model these networks properties, neurons are represented as abstract nodes and divergently linked by connections that change through learning rules (Churchland and Sejnowski, 1992). Based on their architecture, feed-forward models can be distinguished from recurrent networks. Feedforward models consist of several layers that are linked by unidirectional connections and are able to classify or categorize inputs (Rosenblatt, 1958, Yuste, 2015). In contrast, recurrent networks feature pronounced feedback connectivity of neurons (Hopfield, 1982). When asymmetric connections with certain weights are assumed, recent recurrent networks exhibit temporally organized activity that can be generated in the absence of input, thereby explaining the intrinsic firing properties of neuronal populations (Maass et al., 2002, Mante et al., 2013).

The concept that ensembles of neurons, rather than single cells, form flexible functional units to enable complex processing and behaviour, becomes increasingly prevailing (Yuste, 2015). Cortical areas such as M1, PM or SMC can be regarded as large neuronal networks that consist of numerous functional subunits. Still, how concrete behaviour is encoded in neuronal networks, particularly in motor cortex areas, remains poorly understood. All the more

important is the generation of experimental data that observes the activity of large neuronal ensembles. Particularly two-photon calcium imaging thereby represents one of the spearheads to gain deeper insight into the organisation principles of neuronal networks.

### 1.2 Discovery and characterization of the primary motor cortex

In 1744, the Swedish philosopher Emanuel Swedenborg was arguably the first to hypothesize that movement was controlled by the cerebral cortex according to a topographic map (Gross, 1997). Given that the cerebral cortex was assumed to be a nutritive rind without a mental function at that time, his theories about the cerebral cortex were remarkably innovative. The first well-documented experimental evidence of a somatotopically organized M1 followed around 130 years later when several researchers applied electrical surface stimulation to the cerebral cortex of dogs, cats, guinea pigs, rabbits and monkeys (Fritsch and Hitzig, 1870, Ferrier, 1873, 1874). Within the precentral gyrus, distinct electrical stimulation sites evoked movements in different contralateral body parts, thereby forming a motor map in the anterior part of the cerebral cortex. In the following years, a sequence of experiments on monkeys and apes promoted the view that each separate fragment of the body is represented in a discrete area of M1 (Beevor and Horsley, 1890, Grunbaum and Sherrington, 1903, Foerster, 1936, Woolsey et al., 1952). After visualization through the homunculus (Penfield and Boldrey, 1937), a manlike creature whose body proportions are distorted according to the amount of cortical representation, this motor cortical “muscle map” was popularized and is still engraved into the memory of every neurologist (Fig. 4a). Similar maps of the motor cortex with somatotopic representation of body parts have been reported inter alia in rats and mice (Neafsey et al., 1986, Tennant et al., 2011). To reduce the spread of applied electrical currents and to increase the spatial resolution of motor maps, surface stimulation of the cerebral cortex was eventually replaced by intracortical microstimulation, in which fine, hair-like microelectrodes stimulate only a small sphere of tissue around the electrode tip (Asanuma and Ward, 1971, Asanuma and Rosen, 1972).

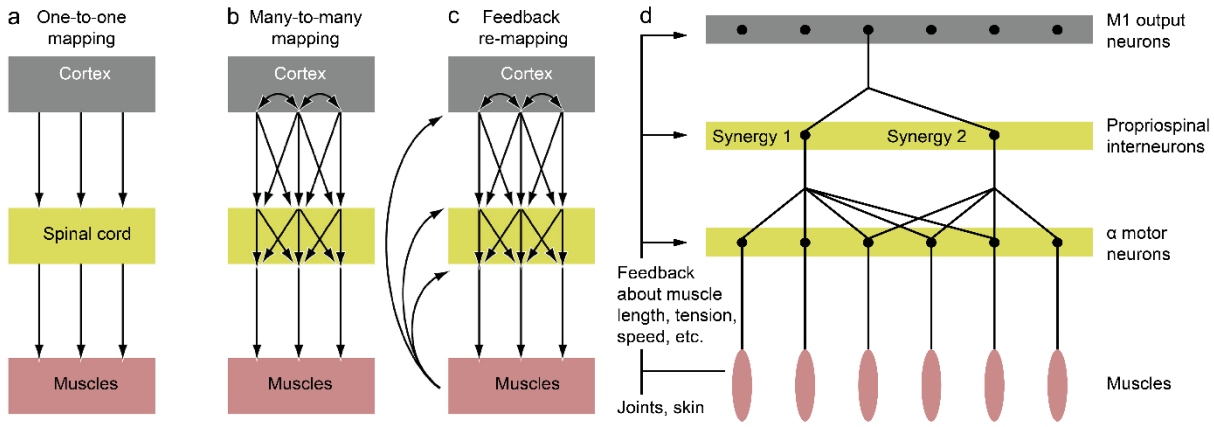


**Figure 5: Wiring concepts in the corticospinal system**
**a,** Traditional concept of one-to-one mapping in which the spinal cord simply relays signals from the motor cortex to muscles. **b**, Concept of many-to-many mapping, according to which divergent and lateral connections enable each cortical neuron to affect many muscles and each muscle to be affected by many cortical neurons. **c**, Modern concept of feedback re-mapping in which the mapping from cortical neurons to muscles can be modified by somatosensory feedback from muscles and joints. **d**, Scheme illustrating the cortical recruitment of muscle synergies and feedback re-mapping. Adapted from Graziano (2006) and Graziano (2009).

The formerly suggested muscle maps (Beevor and Horsley, 1890, Grunbaum and Sherrington, 1903, Foerster, 1936) were corroborated by the first intracortical microstimulation studies in M1 when Asanuma and colleagues proposed cortical columns that connected preferentially to a single muscle (Asanuma, 1975). Asanuma and colleagues used threshold stimulation in which the stimulation current is lowered until the muscle activity is just detectable to the experimenter. However, Cheney and Fetz (1985) challenged Asanuma's view by using microelectrodes to record the naturally occurring activity of single neurons in the monkey M1 while simultaneously recording EMG activity of wrist and finger muscles. The action potential of a single neuron generated diminutive activity of the muscles that could be seen by averaging across thousands of neuronal spikes. This technique of spike-triggered averaging also revealed latencies as short as 5 milliseconds between neuronal and muscular activity, thereby indicating that the signals have been conveyed by the corticospinal tract. Each neuron correlated with several muscles that could include flexors and extensors of one joint or even muscles across many joints. Thus, a *many-to-many mapping* from M1 neurons to muscles exists rather than a *one-to-one mapping* as suggested by Asanuma and many other researchers before (Fig. 5a, b).

Cheney et al. (1985) corroborated their findings by using “stimulus triggered averaging” in which stimulation pulses applied to M1 induce tiny activity in muscles, that similarly become visible though averaging across thousands of pulses. In the light of these findings, Graziano (2009) suggested the “tip-of-the-iceberg” hypothesis to explain Asanuma’s columns for individual muscles (Asanuma, 1975): Due to Asanuma’s use of threshold stimulation only the strongest muscle component of a movement that actually featured activation of several muscles, remains observable, thereby pretending simpler movements and activation of single muscles. Further intracortical microstimulation and anatomical tracing studies then elaborated, that neurons in M1 are related to muscles from many limb joints and that the motor cortex representations of body parts are extensively overlapping and intermingled (Donoghue et al., 1992, Schieber and Hibbard, 1993, Park et al., 2001, Park et al., 2004, Rathelot and Strick, 2006). The amount of somatotopic overlap within M1 can also be modified by experience as demonstrated for instance by the increased overlap in the M1 representation of joints that have been extensively used in combination (Nudo et al., 1996).

The divergence of connectivity from motor cortex neurons to muscles emerges at several stages. In the spinal cord, one propriospinal interneuron excites a set of alpha-motor neurons which in turn activate different muscles (Fig. 5d). The fixed ratio of excitation among muscles that is induced by the activity of one propriospinal interneuron, is termed muscle synergy and can span several joints (Giszter et al., 1993, Tresch et al., 1999, d'Avella et al., 2003, Ting and Macpherson, 2005, Torres-Oviedo and Ting, 2007). Motor cortex neurons, in turn, are thought to recruit several propriospinal interneurons (Fig. 5d), thereby combining their muscle synergies and creating more complex, composite synergies (Graziano, 2009). In humans and some primates, some cortical motor cortex neurons also bypass the interneurons to project directly to alpha-motor neurons and are thought to facilitate the activation of individual limb muscles and to increase limb dexterity (Lemon and Griffiths, 2005). In addition to the implementation of muscle synergies, the spinal cord harbours complex neuronal networks that generate inter alia alternating limb movements for locomotion. These so-called “central pattern generators (CPGs)” organize rhythmic patterns of motor activity which can be

modified by sensory information and supraspinal commands (Goulding, 2009). Brainstem centers such as the mesencephalic locomotor region are involved in the initiation of CPGs and details of their activity pattern such as the timing of signals are adapted to current demands inter alia by M1 (Kandel, 2013). In this regard, a several studies in cats have demonstrated that motor cortical neurons change their activity when the gait has to be modified (Amos et al., 1990, Beloozerova and Sirota, 1993, Drew, 1993, Drew et al., 1996, Drew et al., 2008). During skilled locomotion in complex environments with obstacles, motor cortex neurons presumably integrate the purposeful recruitment of various spinal muscle synergies with the currently required CPG-pattern (Drew and Marigold, 2015).

The *many-to-many mapping* from M1 neurons to muscles implies that activity in motor cortex neurons is conveyed to muscles along a fixed arrangement of wires, but this concept has been derived by Cheney and Fetz (1985) during motor tasks with preferably constant feedback from the periphery. Several studies on rodents, monkeys and humans by now indicated that the mapping from M1 neurons to a set of muscles can change depending on the joint angle configuration of the limb (Sanes et al., 1992, Lemon et al., 1995, Graziano et al., 2004). According to this concept of “feedback remapping” (Fig. 5c, d), somatosensory feedback of varying joint angles to the cortical and spinal network modulates the mapping from M1 neurons to muscles that actuate the respective joints. The concept of feedback remapping is thought to enable the motor cortex network to learn the control of any useful action fragment and to adapt to various scenarios (Graziano, 2006). During motor learning, the motor cortex is indeed known to undergo considerable plasticity that is related to improvement of behavioural performance (Nudo et al., 1996, Rioult-Pedotti et al., 2000, Sanes and Donoghue, 2000, Rokni et al., 2007, Xu et al., 2009, Yang et al., 2009, Komiyama et al., 2010, Huber et al., 2012, Masamizu et al., 2014, Peters et al., 2014, Chen et al., 2015). For instance, calcium imaging in M1 L2/3 of mice revealed that learning of a forelimb lever-press task is associated with the emergence of reproducible spatiotemporal activity in excitatory neuronal populations (Peters et al., 2014). Another study using calcium imaging in mice showed that neuronal ensembles in M1 layer 5 predict the lever trajectory during learning of a lever-pull task with increasing

accuracy (Masamizu et al., 2014). Regarding non-dexterous sequential limb movements, the motor cortex seems to be primarily involved in their learning by tutoring subcortical controllers while being nearly dispensable for the execution of such motor tasks (Kawai et al., 2015). In contrast, both rodents and monkeys are reliant on intact motor cortex networks for the accurate execution of dexterous limb movements, be it in isolation or embedded in a sequence (Passingham et al., 1983, Bortoff and Strick, 1993, Metz and Whishaw, 2002, Alaverdashvili and Whishaw, 2008, Lemon, 2008).

### 1.3 Identification of the pre- and supplementary motor cortex

In addition to the primary motor cortex (M1), the existence of two areas organizing more complex movements than M1 has been suggested in the twentieth century (Fig. 2b): The supplementary motor complex (SMC) located anterior and medial to M1 and also featuring an overlapping somatotopic map of the body (Penfield and Welch, 1951, Woolsey et al., 1952, Muakkassa and Strick, 1979, Macpherson et al., 1982, Gould et al., 1986, Mitz and Wise, 1987, Luppino et al., 1991) as well as the premotor cortex located anterior and lateral to M1 (Campbell, 1905, Fulton, 1935, Foerster, 1936).

The supplementary motor complex (SMC) has been associated with coordinating temporal action sequences (Roland et al., 1980a, Roland et al., 1980b, Gaymard et al., 1990, Mushiake et al., 1990, Jenkins et al., 1994, Gerloff et al., 1997, Lee and Quessy, 2003) and bilateral body movements (Brinkman, 1981, Serrien et al., 2002) as well as with the initiation of internally generated in contrast to stimulus driven movement (Roland et al., 1980a, Roland et al., 1980b, Matsuzaka et al., 1992, Halsband et al., 1994). In addition, the SMC has been suggested to encode specific movement sequences and to be involved in contextual control of voluntary behaviour (Tanji and Shima, 1994, Nachev et al., 2008, Kandel, 2013). Due to its direct input from the prefrontal cortex and output to SMA which in turn projects to M1, particularly the Pre-SMA part from the SMC (Fig. 2b) is situated at a suitable position to link information about the behavioural context to motor processing (Fuster, 1989, Passingham, 1993). In this regard, the Pre-SMA has been suggested to update motor plans before new

sequences have to be executed (Shima et al., 1996). More generally, novel concepts ascribe "executive control" functions to the SMC, which include switching from one motor plan to another and decreasing the interference of irrelevant features to optimize motor control (Nachev et al., 2008). Due to the reciprocal connectivity between SMC and M1, the relation of SMC to the behavioural context of movement sequences might also affect the M1 circuitry (Fig. 1), and this aspect becomes later important for the interpretation of our results. Similar to the findings of monkey studies, a recent study associated M2, the mouse counterpart of SMC, with the organization of movement sequences (Yin, 2009).

The premotor cortex has been subdivided into the rostral and caudal dorsal part (PMDr and PMDc, respectively) as well as into the rostral and caudal ventral part (F5 and F4, respectively). F4 or the "polysensory zone" features multimodal neurons that respond when an object is perceived within a defined space surrounding the body, regardless if through somatosensory, visual or auditory input (Rizzolatti et al., 1981, Gentilucci et al., 1983, Gentilucci et al., 1988, Graziano et al., 1994, Fogassi et al., 1996, Graziano et al., 1997a, b, Graziano et al., 1999, Graziano and Gandhi, 2000). These multimodal neurons have been suggested to spatially guide movements (Rizzolatti et al., 1981, Gentilucci et al., 1988). F5 contains neurons that preferentially respond to a certain grasp type such as the precision grip, leading to the notion that they encode a library of useful hand actions (Rizzolatti et al., 1988, Murata et al., 1997, Raos et al., 2006). Despite the lack of dense projections to the spinal cord, F5 is able to generate and possibly modulate motor output via lateral connections to M1 and is therefore thought to stand at a hierarchically higher level than the primary motor cortex (Shimazu et al., 2004, Graziano, 2009). Additionally, the F5 area has been shown to harbour "mirror neurons" which respond when the animal executes a specific movement or views someone else performing the same act (di Pellegrino et al., 1992, Gallese et al., 1996). Mirror neurons are thought to provide a mechanism by which the animal comprehends the actions of others through simulating how it would execute the action itself (Gallese et al., 2004, Rizzolatti and Craighero, 2004). Interestingly, people with autism who typically exhibit deficits in understanding the social gestures of others feature below-normal activity in the mirror neuron

network (Williams et al., 2001, Dapretto et al., 2006, Iacoboni and Dapretto, 2006). The dorsal premotor cortex (PMD) has been suggested to participate in the learning of associations between sensory stimuli and motor responses (Weinrich and Wise, 1982, Wise et al., 1983, Weinrich et al., 1984, Passingham, 1985, 1986). Additionally, the caudal dorsal premotor cortex (PMDc) has been shown to possess dense projections to the spinal cord (He et al., 1993) and to feature pronounced neuronal activity during reaching movements, which is why PMDc is assumed to be at a similar hierarchical level as M1 (Hocherman and Wise, 1991, Crammond and Kalaska, 1996, Johnson et al., 1996, Messier and Kalaska, 2000, Cisek and Kalaska, 2005, Churchland et al., 2006, Graziano, 2009). In contrast, the rostral premotor cortex (PMDr) lacks dense projections to the spinal cord (He et al., 1993), exhibits activity that is related to movement preparation and is thought to stand hierarchically above M1 (Brasted and Wise, 2004, Muhammad et al., 2006, Graziano, 2009).

In a nutshell, the traditional conception of pre- and supplementary motor cortex assumes that they process distinct higher-order aspects of movements while the primary motor cortex is responsible for implementing the required muscle activations. Although correct by trend, differences regarding the hierarchical level or the processing of movement aspects are graded and blurred, both between primary, pre- and supplementary cortex and among premotor subregions (Graziano, 2009). In the following sections, I will therefore use the term “motor cortex” to subsume primary, pre- and supplementary motor cortex.

### 1.4 Action maps as new perspective to conceptualize motor cortex function

In 2002, Graziano and colleagues (2002) reported the emergence of coordinated, ethologically meaningful multi-joint movements when different sites in M1 were electrically stimulated. In contrast to previous studies, in which electrical stimulation bursts lasting 50 ms or less were used, the experimenters had extended the stimulation duration to 500 ms, approximately the timescale over which monkeys perform common reaching and grasping actions. Using this prolonged stimulation, a sequence of studies elaborated that different cortical zones within M1, PM and SMC emphasize specific, ethologically relevant movement categories. Defensive

movements were typically observed in F4 (Graziano et al., 2002, Cooke and Graziano, 2004b, a), where multimodal neurons have been suggested to spatially guide movements. Multimodal neurons might therefore also support maintaining a margin of safety around the body (Graziano, 2009). Hand-to-mouth movements were also observed in F4, manipulation movements involving fingers and wrist were evoked in M1, reach-to-grasp movements were typically induced in PMDc and climbing or leaping actions occurred in SMC (Fig. 6a), suggesting a role in locomotion through an obstacle-strewn environment (Graziano, 2006, Graziano and Aflalo, 2007). Other experimenters observed that locomotion can also be evoked by electrically stimulating a medial anterior area of the rat cortex, indicating that a rodent counterpart of the monkey SMC might exist (Tehovnik and Yeomans, 1987). The coordinated multi-joint movements evoked by prolonged electrical stimulation lead to the conception that in cortical motor areas, an ethological action map coexists with the traditionally suggested blurred map of the body.

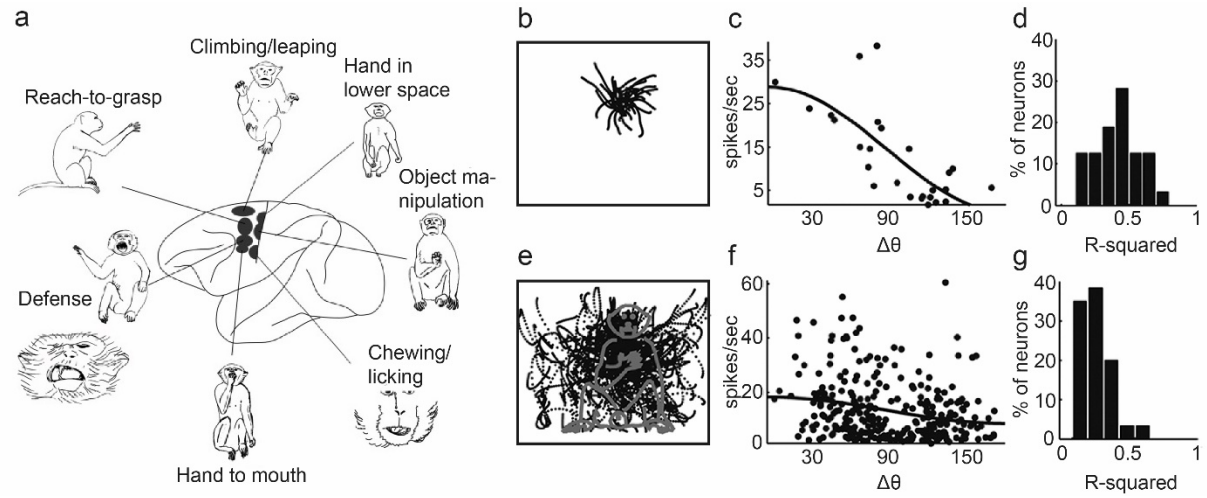


**Figure 6: Action map and local versus global direction tuning**
**a,** Action map of the monkey motor cortex; electrical stimulation at different motor cortex sites evokes common movement categories, when the stimulation duration is extended to 0.5 seconds. Each image illustrates the final posture of the animal during electrical stimulation. **b**, From the various movements during the natural behaviour of the monkey, the experimenters selected a subset that resembled the center-out reaching task and consisted of 26 arm movements. Each movement shown originated centrally and extended any direction in three-dimensional Cartesian space for a distance between 6 cm and 15 cm. **c**, Direction tuning of one example neuron within the selected movement subset. Angular difference between the preferred direction and the direction of each movement is illustrated on the x-axis; mean firing rate during each movement and cosine fit is shown on the y-axis ($R^2$ = 0.43). **d**, Histogram of $R^2$-values for all neurons when only the selected movement subset is regarded. **e**, All 320 arm movements during the natural behaviour of the monkey. **f**, Direction tuning of the same neuron as in c, but within the full movement set ($R^2$ = 0.05). **g**, Histogram of $R^2$ values for all neurons when the full movement set is considered. Adapted from Graziano (2015) and Aflalo and Graziano (2007).

By now many studies, which applied the prolonged stimulation of cortical motor areas, suggest that the action map represents a fundamental principle of motor cortex organization across many mammalian species (Graziano, 2015). In rats and mice, different ethological forelimb movements such as grasping, retracting and locomotion-like rhythmic motor actions have been reported (Ramanathan et al., 2006, Harrison et al., 2012, Brown and Teskey, 2014, Hira et al., 2015). Moreover, ethological actions were evoked by stimulation of the cat, squirrel and human motor cortex (Ethier et al., 2006, Cooke et al., 2012, Desmurget et al., 2014). Recent studies investigating the macaque motor cortex even suggest, that different action zones can be distinguished within the ethological category of hand actions (Overduin et al., 2012, 2014). However, the evoked complex movements have also been proposed to be artifacts of the prolonged stimulation for half a second or more: Since the sustained stimulation spreads in the cortex, neurons not naturally linked may be activated and induce artificial co-contraction of muscles which are actually represented separately, but near each other in the cortex (Cheney et al., 2013, Van Acker et al., 2014). Which interpretation is true, remains a matter of debate.

### 1.5 Representation of movement variables in the motor cortex

When monkeys are trained to move their hand from a central starting position to one of eight surrounding positions, the activity of individual neurons in the motor cortex is related to a preferred direction (Georgopoulos et al., 1982, Georgopoulos et al., 1986, Georgopoulos et al., 1988, Schwartz et al., 1988). The authors suggested that the activity of each neuron biases the hand in a different direction and that the many conflicting directions sum approximately linearly, thereby forming a population vector to yield the actual direction of the hand (Georgopoulos et al., 1986). However, this M1 population code that is purely related to hand direction was then questioned since neurons responded differently when the hand direction was held constant but the joint configuration of the arm was changed by raising or lowering the elbow (Scott and Kalaska, 1995, 1997). Additionally, further studies revealed that neuronal activity in motor cortex is correlated with intrinsic coordinates such as muscle activity (Holdefer and Miller, 2002, Townsend et al., 2006), extrinsic coordinates such as the spatial movement

direction (Kakei et al., 1999), the starting position of the hand during reach (Caminiti et al., 1990, Sergio and Kalaska, 2003), the direction of force applied by the hand to a holder (Georgopoulos et al., 1992, Sergio and Kalaska, 2003) and the hand velocity during reach (Moran and Schwartz, 1999, Reina et al., 2001, Paninski et al., 2004). These studies indicated that the tuning of M1 neurons to movement variables is versatile and strikingly dependent on the motor task being performed. A recent study also suggests that a variety of grip types can be differentiated based on neuronal activity in M1 (Schaffelhofer et al., 2015).

Simplified, restricted movement sets such as the center-out reaching task emphasize the relevance of selective movement variables such as the movement direction, thereby potentially leading to exaggerated representation of the respective variables in M1. During natural motor behaviour of monkeys, direction tuning of neurons is low (Fig. 6e-g) when all movements are taken into consideration (Aflalo and Graziano, 2007). However when the experimenters selected a movement subset that resembled the center-out reaching task, many cells exhibited increased direction tuning (6b-d). The authors concluded that neurons are only tuned to the movement direction when the variance of other parameters such as the initial hand position is minimized which would then also minimize the effects of feedback re-mapping. When all variables are at play, neurons are most significantly tuned to individual joint angles of preferred arm-postures (Graziano, 2009) and single neurons frequently encode various combinations of both proximal and distal joint angles (Vargas-Irwin et al., 2010). However, the encoding of any movement variable is comparably limited during natural behaviour (Aflalo and Graziano, 2006).

## 1.6 Current theories about the mammalian motor system

### 1.6.1 Neuronal tuning to useful fragments of motor behaviour

The tuning of motor cortex neurons to diverse kinematic features has led to pronounced disagreement regarding which movement variables are actually encoded in cortical motor areas. In the last few years, novel conceptions emerged which focus on the dynamic versatility of neuronal networks instead of emphasizing the meaning of neuronal tuning to fixed

movement variables. According to Graziano (2009), the statistics of natural behaviour is shaped by acquisition and maintenance of specific joint configurations around which the joints are frequently adjusted, which is why most neurons in the motor cortex are tuned to a set of joint angles that define these canonical postures. In that perspective, each motor cortex neuron is tuned to some fragment of complex behaviour and is able to impel the motor output toward its complex preferred movement. Thus, the basis set of movements incorporated in the population code would not be a set of hand directions as suggested by Georgopolous et al. (1986), but instead a set of action fragments spanning the normal motor repertoire. A typical action fragment of monkey behaviour would for instance be an arm posture in front of the trunk, that is often employed during manipulation of tools or food. Since muscle output from different motor cortical sites sums approximately linearly (Ethier et al., 2006), the neurons' complex fragments of motor behaviour can sum at the level of muscle output and thereby contribute to a population average (Graziano, 2009). Feedback remapping could thereby provide a mechanism by which motor cortex networks can learn to control any useful fragment of motor behaviour (Graziano et al., 2004). Whatever movement variable is relevant for the respective action, be it direction, speed or arm posture, becomes represented in the cortical motor networks based on feedback remapping of circuits within the corticospinal network. This conception is consistent with the optimal feedback control theory (see below), according to which the motor system controls only the task-relevant variables of a specific task while neglecting others (Todorov and Jordan, 2002, Scott, 2004, 2012).

### 1.6.2 Optimal feedback control theory as concept to interpret voluntary motor behaviour

An expanding branch of neuroscience is dedicated to describing the strategy and versatile behaviour of our sensorimotor system mathematically (Todorov, 2004, Diedrichsen et al., 2010, Scott, 2012). How voluntary motor control is generated by neuronal activity in the brain is not directly investigated, rather a principle understanding and mathematical modelling of the behavioural movement strategies themselves is in the focus. For instance, a fundamental

feature of coordination, defined as movements that involve multiple effectors such as muscles or joints, is that the number of effectors usually by far exceeds the dimensionality of the task requirements (Franklin and Wolpert, 2011). This means that a simple movement goal such as pushing a button can be achieved in countless ways, for example by using different trajectories. That the sensorimotor system employs a narrow set of solutions despite this redundancy of possibilities is one of the features this branch in neuroscience tries to account for.

One recent conceptual framework in the field is the optimal feedback control theory (OFC) according to which motor commands of the sensorimotor system optimise behaviour with regard to biologically relevant task goals (Todorov and Jordan, 2002, Todorov, 2004, Franklin and Wolpert, 2011). The OFC is a mathematical construct that implements the current body state and the task goal to infer the best possible control signals of the sensorimotor system in consideration of goal accuracy and effort (Todorov, 2004). The OFC thereby makes specific predictions about the motor strategy in different situations and also explains why the sensorimotor system selects stereotypic movement types out of the redundancy of possibilities (Guigon et al., 2007) . An example for a typical strategy of the mammalian sensorimotor system that follows from the OFC, is the minimal intervention principle (MIP). According to the MIP, the sensorimotor system selectively corrects movement deviations along task-relevant dimensions while deviations along task-irrelevant dimensions are ignored (Diedrichsen et al., 2010). For instance, when a nail is hit by a hammer into a wall, the end position of the hammer head is highly task-relevant and its variability will be minimized by the sensorimotor system. However, the starting point of the hammer head before each hit and the exact trajectory during hitting are less critical for task-performance, which is why the sensorimotor system will allow more variability of these parameters. By predicting a position-control scheme when the target limb position needs to be achieved or a force-control scheme when the organism is required to exert a target force, the OFC accounts for the flexibility and versatility of the mammalian sensorimotor system (Todorov, 2004). Many additional features of natural motor behaviour are predicted by the OFC framework, for instance the temporal shape of movements (Harris and Wolpert, 1998), the trajectories of arm movements (Braun et al., 2009), the solution to new

task environments (Izawa et al., 2008), the distribution of work across multiple muscles (Fagg et al., 2002) and the reactions of the organism to perturbations (Liu and Todorov, 2007, Kurtzer et al., 2008, Pruszynski et al., 2008).

In the OFC, task goals are mathematically defined as “cost functions” consisting of two parts. One part of the cost function encodes the external goal of the organism and a second part, the regularisation term, penalises the movement effort and should be minimal (Todorov, 2004, Franklin and Wolpert, 2011). In recent versions of OFC, the regularisation term is the sum the squared motor commands. In this context, motor commands are conceptualized as neural drive to muscles that can be quantified by rectified EMG. On the one hand, the sum of the squared motor commands is thought to reflect the effort of the organism during the execution of movements (Diedrichsen et al., 2010). On the other hand, the endpoint movement variability grows with the sum of the squared motor commands, and minimizing the sum of the squared motor commands therefore minimizes the endpoint variability of movements (Harris and Wolpert, 1998, Diedrichsen et al., 2010). Decreased variability of kinematic parameters during the final state of movements is typical for numerous natural motor actions and beneficial for their successful execution. Another typical strategy of the mammalian motor system is the even distribution of activity across several muscles even if the same movement could be achieved by stronger activation of a single muscle (Fagg et al., 2002). Since the sum of the squared motor commands is minimised when the muscle activity is distributed evenly across muscles, this natural behaviour is correctly predicted by the above mentioned cost function of the OFC (Diedrichsen et al., 2010). In summary, the mathematical construct of the OFC is based on finding the optimal balance between effort and accuracy, both in relation to a specific goal. The OFC thereby correctly predicts many features and control strategies of our natural motor behaviour.

### 1.6.3 The dynamic systems perspective

Another modern approach to account for the versatile neuronal tuning properties in the motor cortex refers to the dynamic systems perspective. According to this conception, the activity in the motor system reflects a mix of signals. A subset of these signals is directly related to output which drives the spinal cord and muscles, thereby leading to neuronal representation of the respective movement variables in M1. However, many of these signals will reflect a large basis set of patterns which support building the final motor commands without being overtly related to movement variables (Shenoy et al., 2013). In this regard, trajectories of neuronal firing rate configurations ("neuronal state space trajectory") have been shown to rotate with a phase and amplitude set by the preparatory state, and these rotational components form a basis set for building more complex patterns of muscle activation (Churchland et al., 2012). The quality of preparatory states in turn is determined by convergence of the neuronal state space trajectory to a tight subspace (Fig. 7a, b) that is specific for different movements (Churchland et al., 2006, Mandelblat-Cerf et al., 2009, Rickert et al., 2009, Churchland et al., 2010).

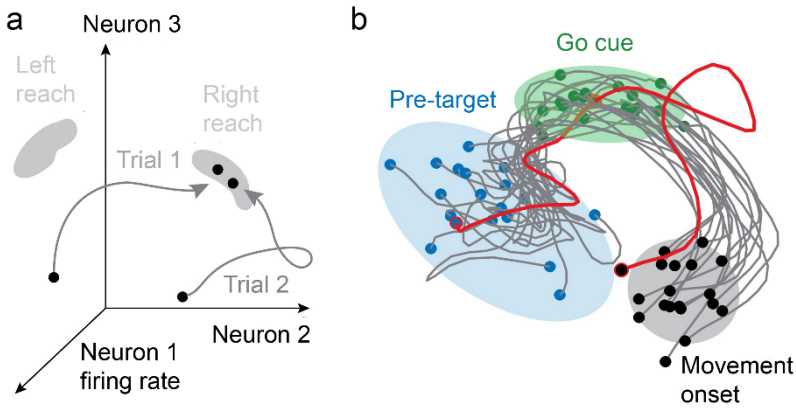


**Figure 7: State space trajectories of neuronal firing rates**
**a,** For three neurons, the state space trajectory of the firing rate configuration during movement preparation is plotted during two trials; during movement preparation, the configuration of firing rates converges (arrows) to lie within the optimal subspace for the intended movement (shaded grey areas); **b,** Neuronal state space trajectories move from the preparatory stimulus via the Go cue to the movement onset. Trajectories between blue and green dots refer to movement planning and feature decreasing variability until the preparatory state (green) is reached. Red trace shows an outlier trial in which the monkey hesitated for an abnormally long duration before beginning to reach. Adapted from Shenoy et al. (2013).

### 1.7 Specific aims of this study

To summarize, experimenters have tried to relate numerous kinematic variables to the simultaneously recorded neuronal activity in the motor cortex, both during restricted movement sets and during natural behaviour, but no agreed-upon conceptual framework has yet emerged. In particular during discrete movements of natural motor behaviour, the encoding of any movement variable becomes limited, and much of the neuronal variance remains unexplained (Aflalo and Graziano, 2006). The question therefore arises if the relationship between neuronal activity in the motor cortex and the concurrently occurring discrete motor action captures the whole picture. An intriguing possibility is that features of the behavioural context retroact on the encoding during discrete motor actions, thereby confounding relationships between neuronal activity and kinematic variables. However, principles according to which the behavioural context affects the kinematic encoding in the motor cortex remain poorly understood.

To investigate how the behavioural context affects the encoding of movement variables in M1, in this thesis I therefore combined skilled locomotion on regularly and irregularly spaced rungs with simultaneous calcium imaging of neuronal networks in the mouse motor cortex. To move across regular and irregular rung ladders, rodents are required to apply different discrete grasping actions in a sequence. Even though many of these discrete grasping actions feature similar or equivalent kinematics on the regular and irregular rung pattern, they have to be applied in two different behavioural contexts, respectively (the context of the regular or irregular pattern). To consistently identify equivalent motor cortex circuits across mice which control movements in all forelimb joints I decided to functionally map M1 in advance using optogenetic stimulation. I subsequently aimed at applying calcium imaging of neuronal networks in M1 L2/3 while head-fixed mice moved across regularly or irregularly spaced rungs and all relevant forelimb joint angles are recorded. Due to its input from the SMC which is involved in contextual control of motor behavior (Nachev et al., 2008, Kandel, 2013) and its excitatory output to M1 L5 (Weiler et al., 2008, Anderson et al., 2010), M1 L2/3 is ideally situated to incorporate contextual information streams into the motor command.

The specific aims of our experiments were as follows:

- Render the combined use of two-photon calcium imaging and optogenetic motor mapping in the same animals possible to enable recording the activity of well-characterized neuronal networks in M1 whose architecture has not been compromised by electrode penetrations.
- Employ two-photon calcium imaging to investigate how neuronal networks in M1 L2/3 encode motion in individual forelimb joints during two different movement sequences (skilled locomotion on regularly or irregularly spaced ladder rungs).
- Elucidate how the encoding of motion in individual forelimb joints depends on the type of the discrete grasping actions within the sequence.
- Investigate how different types of discrete grasping actions within the sequence are represented in neuronal networks of M1 L2/3.
- Clarify how contextual features of the movement sequence (regular vs. irregular rung pattern) affect the encoding of motion in individual forelimb joints during its discrete grasping actions. In other words, is the motion of individual joint angles encoded differently, when the same discrete grasping action is applied in the regular or irregular movement sequence? If so, do features that characterize the entire movement sequence explain these differences in encoding?
- Compare the obtained results with the conceptual frameworks of neuronal coding in the motor cortex.
- Create a novel experimental framework to investigate the pathophysiology of different cortical circuitries in mice modelling Parkinson's disease and motor cortex stroke. Moving across regular and irregular rung ladders is a frequently used test to identify forelimb deficits in rodents modelling motor cortex stroke or Parkinsonism (Metz and Whishaw, 2002, Farr et al., 2006, Zorner et al., 2010) and the combination of calcium

imaging with genetic labelling techniques allows dissecting the activity patterns in discrete circuitries within cortex-spinal cord loop or within the cortex-basal ganglia loop.

## 2. General experimental approach: A window to the brain

**"If the human brain were so simple that we could understand it,**
**we would be so simple that we couldn't."**
***Emerson Pugh***

With about 100 billion ($10^{11}$) neurons that interact elaborately via an estimated 200 trillion ($2x10^{14}$) contacts, the human brain has been called the most complex known entity in the universe (Buzsáki, 2006). A complete understanding of mammalian or even human brain function might therefore be impossible for us to achieve, or is a distant prospect at the very least. Nonetheless researchers never got tired in trying to come closer to this aim and achieved many seminal advances so far. Often, groundbreaking progress in neuroscience was associated with technical innovations that allowed viewing brain function from a different perspective. We therefore aimed for probing the mouse motor cortex with the combination of two modern optical techniques that are used in conjunction with chronic glass windows on the brain surface: Optogenetics and two-photon calcium imaging.

### 2.1 Optogenetic stimulation

The significance of optogenetics for neuroscience was foreshadowed by Nobel laureate Francis Crick decades before its actual implementation. He concluded that a profound understanding of the brain requires a "method by which all neurons of just one type could be inactivated, leaving the others more or less unaltered" (Crick, 1979). Extracellular electrical stimulation lacks specificity for cell types, does not achieve true inactivation and requires the penetration of neural tissue, thereby compromising the architecture of neuronal networks (Fenno et al., 2011). In contrast, recently developed optogenetic tools permit contactless manipulation of selective neuronal systems or cell types by shining light on genetically modified neurons (Deisseroth, 2015). The concept is based on microbial opsins, a family of light-sensitive proteins that require the vitamin A-related cofactor retinal as antenna for photons (Nagel et al., 2003, Zhang et al., 2007a, Fenno et al., 2011). When retinal is attached to functional opsins, they are termed "rhodopsins". Channelrhodopsin-2 (ChR2), a nonspecific

cation channel controlling phototaxis in the green alga Chlamydomonas reinhardtii (Nagel et al., 2003), as well as other microbial opsins can be delivered to mammalian neurons using Lenti- and adeno-associated viral vectors (Zhang et al., 2010). Upon illumination with blue light, ChR2 opens its pore, thereby allowing the entry of mainly sodium ions and to a lesser degree of calcium ions (Fig. 8a). The ion influx depolarizes the membrane potential which can surpass the threshold so that an action potential is generated in the respective neuron. The pore then closes within a few milliseconds and the flow of ions is terminated (Nagel et al., 2003, Zhang et al., 2007a). When ChR2 is expressed in mammalian neurons, their activity can thus be controlled with millisecond precision using pulses of blue light (Boyden et al., 2005).

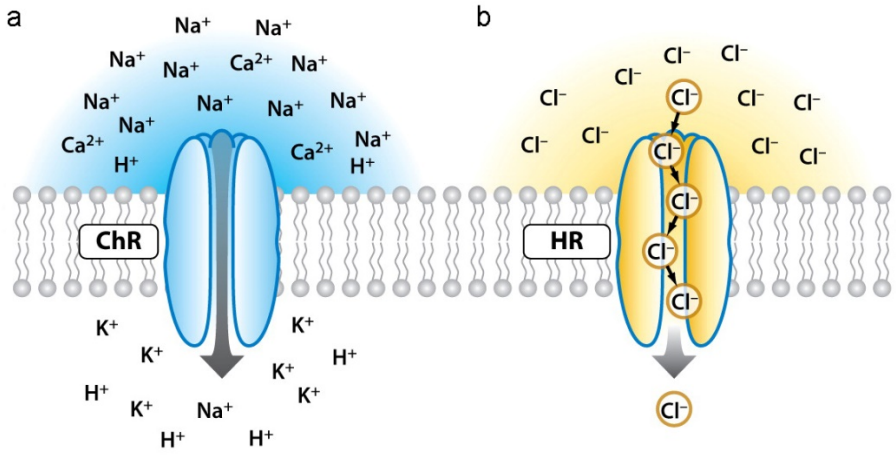


**Figure 8: Optogenetic tools to excite or inhibit neuronal activity**
**a**, Upon blue light illumination, channelrhodopsins conduct cations into the cytoplasm of the neuron, resulting in its depolarization and in the generation of action potentials. **b**, Upon yellow light illumination, halorhodopsins conduct chloride anions into the cytoplasm of the neuron, thereby hyperpolarizing the cell. Adapted from Fenno et al. (2011).

In addition to excitation, optogenetic tools can induce neuronal inhibition. The halorhodopsin NpHR from the halobacterium Natronomonas pharaonis, is an electrogenic chloride pump (Fig. 8b) that hyperpolarizes respective neurons following yellow light illumination (Zhang et al., 2007b, Gradinaru et al., 2008, Gradinaru et al., 2010). Other opsins have been engineered that are able to modify excitability levels in neuronal groups. In step function opsins (SFO), a blue light pulse raises the membrane potential in the neuronal target group to increase their firing probability for prolonged time periods until this effect is neutralized by an additional yellow light pulse (Yizhar et al., 2011). In contrast to ChR2, step function opsins only increase the

excitability of the targeted cells but do not force the stimulated neuronal groups into defined temporal discharge patterns. By now, the optogenetic toolbox has been extended beyond the examples described above and the combination with genetic tools has also allowed the selective targeting of specific cell subtypes or projection systems (Tye and Deisseroth, 2012, Deisseroth, 2015). For instance, selective optogenetic stimulation of cortical parvalbumin-expressing fast-spiking interneurons suggested their involvement in the generation of gamma oscillations (Cardin et al., 2009, Sohal et al., 2009) while optogenetic control of direct- and indirect-pathway medium spiny projection neurons (MSNs) in the striatum dissected their role in Parkinsons's disease (Kravitz et al., 2010). In a nutshell, light-sensitive optogenetic probes allow the activation, inhibition or modulation of selective neuronal systems in the millisecond-to-minute timescale and are therefore suited to link neuronal activity in specific circuits and behaviour causally. So far, optogenetics has led to new insights regarding inter alia the malfunction of neuronal circuits in depression, autism and Parkinsonism (Tye and Deisseroth, 2012).

Using the Thy1 promotor, a transgenic opsin-expressing mouse line has been created in which ChR2 is expressed throughout neocortical layer 5 projection neurons (Arenkiel et al., 2007, Ayling et al., 2009). This transgenic mouse has also been used in our study to map M1 by focusing blue laser light through a chronic glass window at different spots on the cortical surface while limb movements were recorded simultaneously. Using the optogenetic mapping approach instead of electrical stimulation enabled us to later apply calcium imaging in specific, well-characterized M1 circuits whose architecture were not destroyed by electrode penetrations.

## 2.2 Two-photon calcium imaging of genetically encoded calcium indicators (GECIs)

### 2.2.1 Principles of two-photon microscopy

Two-photon excited fluorescence for laser-scanning microscopy of brain tissue *in vivo* (Denk et al., 1990) is a rapidly expanding field in neuroscience. Two-photon excitation in general is based on the concept that a fluorophore can be excited by the "simultaneous" (within ~0.5 femtoseconds) arrival of two photons, each of which carries approximately half the energy

required for one-photon excitation (Denk et al., 1995). Compared to traditional optical microscopy techniques that use one-photon absorption for fluorophore excitation, two-photon excitation has several advantages. First, since two photons combine their energies to promote the respective molecule to an excited state, they feature a longer wavelength compared to one-photon excitation and are therefore less scattered (Helmchen and Denk, 2005). Secondly, due to the absorption of two photons during excitation of the fluorophore, the probability for fluorescent emission (S) from the fluorophores increases supralinearly ($S \propto I^2$) with the excitation intensity (I) (Helmchen and Denk, 2005). Consequently, two-photon absorption is spatially confined to the focal volume of the laser beam (Fig. 9a) and does not occur in out-of-focus planes (Denk et al., 1990, Helmchen and Denk, 2005, Svoboda and Yasuda, 2006). In contrast, the single photon absorption used in confocal microscopy (Fig. 9a) entails absorption within the entire excitation light cone (Svoboda and Yasuda, 2006). Out-of-focus excitation also increases photodamage of functional tissue and is therefore particularly disadvantageous for long-term imaging (Squirrell et al., 1999). Thirdly, the density of scattered excitation photons is in general too low to induce significant signal which is why the tight localization of excitation is preserved even in extensively scattering tissue (Helmchen and Denk, 2005). This further reduces the sensitivity of two-photon excitation to light scattering (Fig. 9a) when compared to traditional microscopy techniques. These features make two-photon excitation well suited for deep imaging of tissue at high resolution. While scattering effects restrict the use of one-photon based microscopy techniques to depths of around 100 µm from the tissue surface, two-photon microscopy can generate high-resolution images at depths up to one millimeter (Theer et al., 2003). The simultaneous absorption of two photons requires a laser system that emits ultrashort pulses, typically 100 femtosecond pulses at about 100 MHz (Denk et al., 1995). Excitation of commonly used fluorescent markers thereby occurs in the near-infrared wavelength range (700-1000 nm) and the fluorophores then emit photons in the visible range (Helmchen and Denk, 2005).

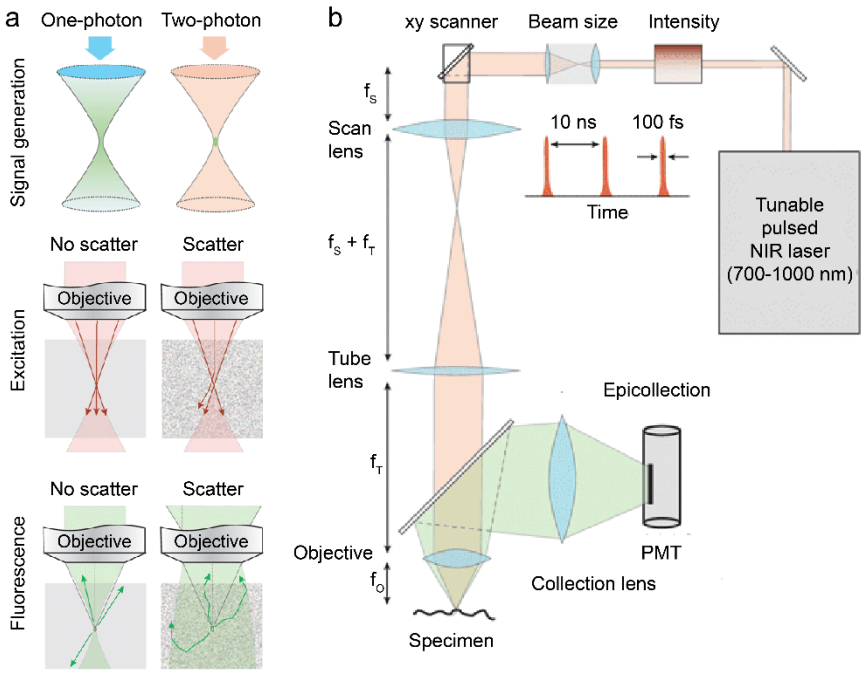


**Figure 9: Concept of two-photon microscopy**
**a**, Upper panel: While a complete cone of fluorescence light is generated in one-photon microscopy, the excited fluorescence in two-photon microscopy is localized in the vicinity of the focal spot. Middle panel: In contrast to clear tissue, scattering tissue deflects light rays from their original direction which then miss the focus and are lost for signal generation. Lower panel: Scattering tissue also deflects the direction of fluorescence light, which might even turn around. **b**, Example setup of a laser-scanning microscope: Near infrared ultrashort pulses are generated by a laser and directed to spots in the specimen in which fluorescence is generated. The emitted fluorescence is then collected in the epi-collection mode by means of photomultiplier tubes (PMTs). Focal lengths of the scan lens ($f_S$), the tube lens ($f_T$) and the objective ($f_O$) are shown. Adapted from Helmchen and Denk (2005).

In a typical two-photon microscope for calcium imaging, a pair of galvanometric scanners directs the focused laser beam to different spots on the specimen, leading to local excitation of fluorophores (Fig. 9b). The excitation at each spot is collected with a “whole-area” epi-detection scheme that guides the light collected by the objective to the detector system (Mainen et al., 1999, Oheim et al., 2001, Beaurepaire and Mertz, 2002). The fluorescence profile of the scanned area is then assembled to a coherent image. For *in vivo* imaging of neuronal activity, two-photon microscopy is used in combination with fluorescent sensors that have been delivered to the brain tissue and that change their fluorescence in response to neuronal activity. The most prominent type of these sensors, so-called calcium indicators, will be introduced in the next section.

### 2.2.2 Fluorescent calcium indicators

Neuronal action potentials induce rapid calcium influx via voltage-gated calcium channels located throughout the cell membrane (Hille, 1992, Jaffe et al., 1992). These intracellular calcium concentration changes can be measured with calcium indicators and exploited to infer the spiking activity of neuronal populations *in vivo* and *in vitro* (Helmchen and Konnerth, 2011). Loading of living neuronal tissue with synthetic calcium indicators allows the visualisation of intracellular calcium dynamics with high signal-to-noise ratio, but they damage neuronal tissue after several hours and are therefore not suitable for repeated, chronic *in vivo* measurements (Yuste et al., 1992, Svoboda et al., 1997, Fetcho et al., 1998, Stosiek et al., 2003, Gobel et al., 2007). Moreover, synthetic calcium indicators cannot be easily targeted to specific neuronal subtypes or projection systems (Helmchen and Konnerth, 2011). However, genetically encoded calcium indicators (GECIs) which have been engineered in the last years overcome these limitations (Grienberger and Konnerth, 2012). Through the combination with viral tools, GECIs can be targeted to specific neuronal subtypes, projection systems or even subcellular compartments (Palmer and Tsien, 2006). Additionally, in the best case, GECIs do not damage neuronal function for several weeks or months and thereby allow chronic imaging of neurons, synapses, axons and dendrites through implanted cranial glass windows (Hires et al., 2008, Margolis et al., 2014).

In general, GECIs consist of a calcium-binding recognition element that is coupled to an optical reporter element (Hires et al., 2008). GECI recognition elements such as Calmodulin feature pronounced calcium dependent conformational changes which are enhanced by a conformational actuator such as the M13 peptide (Miyawaki et al., 1997, Nakai et al., 2001). GECI reporter elements are either single fluorescent proteins or fluorescence resonance energy transfer (FRET) donor-acceptor pairs. In single fluorescent proteins (Fig. 10a), calcium binding triggers a conformational change of calmodulin, thereby leading to the formation of the calmodulin-M13 peptide complex and increasing the fluorescence of the single fluorescent protein (Baird et al., 1999, Nagai et al., 2001, Nakai et al., 2001). In FRET donor-acceptor pairs (Fig. 10b), calmodulin and the M13 peptide are bracketed by a FRET pair (Hires et al., 2008).

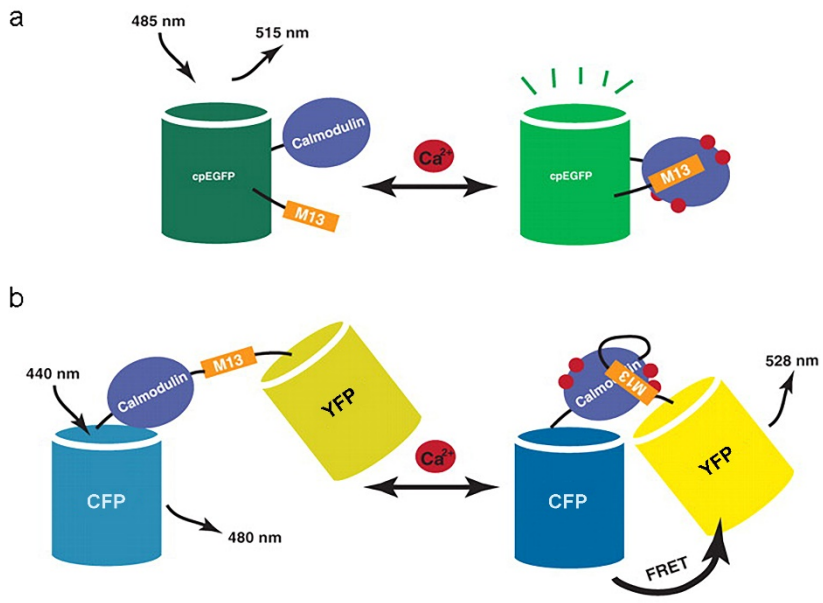


**Figure 10: Scheme of GECI classes**
**a**, G-Camp-type sensing mechanism: Calcium binding induces conformational changes in calmodulin, leading to the calmodulin-M13 complex and entailing a fluorescence increase in the circularly permuted enhanced Green Fluorescent Protein (cpEGFP). **b**, Sensing mechanism of FRET-based indicators such as Yellow Cameleon nano 140 (*YC-Nano140*): Upon calcium binding, calmodulin undergoes a conformational change and the generation of the calmodulin-M13 complex induces an increase in FRET between Cyan Fluorescent Protein (CFP) and Yellow Fluorescent Protein (YFP). Adapted from Hires et al. (2008).

Upon calcium binding, calmodulin undergoes a conformational change and the formation of the calmodulin-M13 complex brings donor and acceptor closer together, leading to a fluorescence increase in the acceptor and a fluorescence decrease in the donor (Miyawaki et al., 1997, Heim and Griesbeck, 2004, Palmer et al., 2006). The firing rate of neurons can then be inferred based on the fluorescence ratio between acceptor and donor. This ratiometric measurement of calcium signals with FRET-based GECIs has the advantage to be less sensitive to motion artifacts (Helmchen and Konnerth, 2011).

### 2.2.3 Calcium dynamics during action potentials

Typical sodium action potentials in excitatory neurons of the CNS last approximately 1 ms and occur over a wide range of frequencies (Hires et al., 2008). Through brief opening of voltage-gated calcium channels, each action potential is associated with a brief influx of calcium ions. While each calcium transient is independent during sparse generation of single action

potentials, calcium transients sum when the action potentials are closely spaced (Helmchen et al., 1996). The exact relationship between instantaneous firing rate and evolution of calcium transient depends on the used GECI and must be calibrated by simultaneous electrophysiology (Chen et al., 2013). An example of such a calibration is shown in Fig. 11 for the GECI YC-Nano140, that was also employed in this study. The calcium dynamics evoked by calcium influx during an action potential exhibits a rapid increase followed by a slower prolonged decay. Using a simplified single-compartment model of intracellular calcium dynamics, this time course can be modelled by the following set of equations (Hires et al., 2008, Helmchen and Konnerth, 2011):

$$\Delta[Ca^{2+}]_i = A * e^{-t/\tau}$$

$$\tau = \frac{1 + \kappa_S + \kappa_B}{\gamma}$$

$$A = \frac{\Delta[Ca^{2+}]_T}{1 + \kappa_S + \kappa_B}$$

where t = time, ɣ = calcium extrusion rate, $\kappa_S$ = buffering capacity of endogenous buffers, $\kappa_B$ = buffering capacity of the GECI, $\Delta[Ca^{2+}]_T$ = total amount of calcium current injected by the action potential (Hires et al., 2008). When brief trains of action potentials occur, calcium fluxes from action potentials sum linearly (Helmchen et al., 1996).

### 2.2.4 GECI properties and side-effects on cell homeostasis

Since fluorescence responses rely on calcium binding by the recognition element, GECIs inherently perturb the naturally occurring calcium dynamics in a neuron (Helmchen and Konnerth, 2011). Increasing the indicator concentration will therefore more and more buffer the calcium transients (Hires et al., 2008). The result is a reduction of the peak amplitude of the calcium transient and a prolongation of its time course. On the other hand, higher GECI concentrations increase the number of collected photons and thereby improve the signal-to-noise ratio (Yasuda et al., 2004), so that the optimal GECI concentration is always a trade-off

between signal-to-noise ratio and buffering. Since calcium ions are second messengers regulating cellular signalling events, altered calcium dynamics due to buffering might also affect respective signalling pathways (Tian et al., 2009).

The fluorescence response of a GECI to calcium dynamics is influenced by the affinity, kinetics and dynamic range of the sensor. Effective dynamic range thereby means the ratio between the signal at saturating calcium level and that at baseline calcium level (Hires et al., 2008). While high-affinity GECIs facilitate the detection of small calcium transients, they saturate more easily and resolve long spike trains poorly (Helmchen and Konnerth, 2011). Increased buffering of calcium ions leading to slower kinetics and the above mentioned side-effects is another drawback of high-affinity sensors (Mank and Griesbeck, 2008). On the other hand, a low-affinity sensor has faster kinetics, but is not suitable to indicate small calcium transients (Hires et al., 2008). Maintaining both high affinity and fast kinetics in GECI engineering is challenging due to the inverse correlation between affinity and dissociation rate (Mank et al., 2006). Calcium affinity and dynamic range of each GECI should also be calibrated under the same experimental conditions since they also depend on pH, temperature and presence of competing ions (e.g. $Mg^{2+}$) (Ogawa and Tanokura, 1984, Hires et al., 2008).

### 2.2.5 Selection of a calcium indicator for our study

In our study, we decided to use the FRET-based indicator yellow-cameleon Nano140 (*YC-Nano140,* Fig. 11), which features high signal-to-noise ratio and is resistant to motion artifacts due to the ratiometric readout (Chen et al., 2013). The latter was important for our study, since motion artifacts cannot be completely avoided during calcium imaging of mice engaged in skilled locomotion. Since we performed calcium imaging in M1 L2/3 of Thy1-ChR2 mice (Arenkiel et al., 2007), we also had to make sure that we did not inadvertently excite ChR2 expressing dendrites from M1 L5 neurons. *YC-Nano140* was suited for our application in Thy1-ChR2 mice, since it can be efficiently excited at a two-photon wavelength of 820 nm, which in turn is inefficient for the activation of ChR2 (as will be shown below).

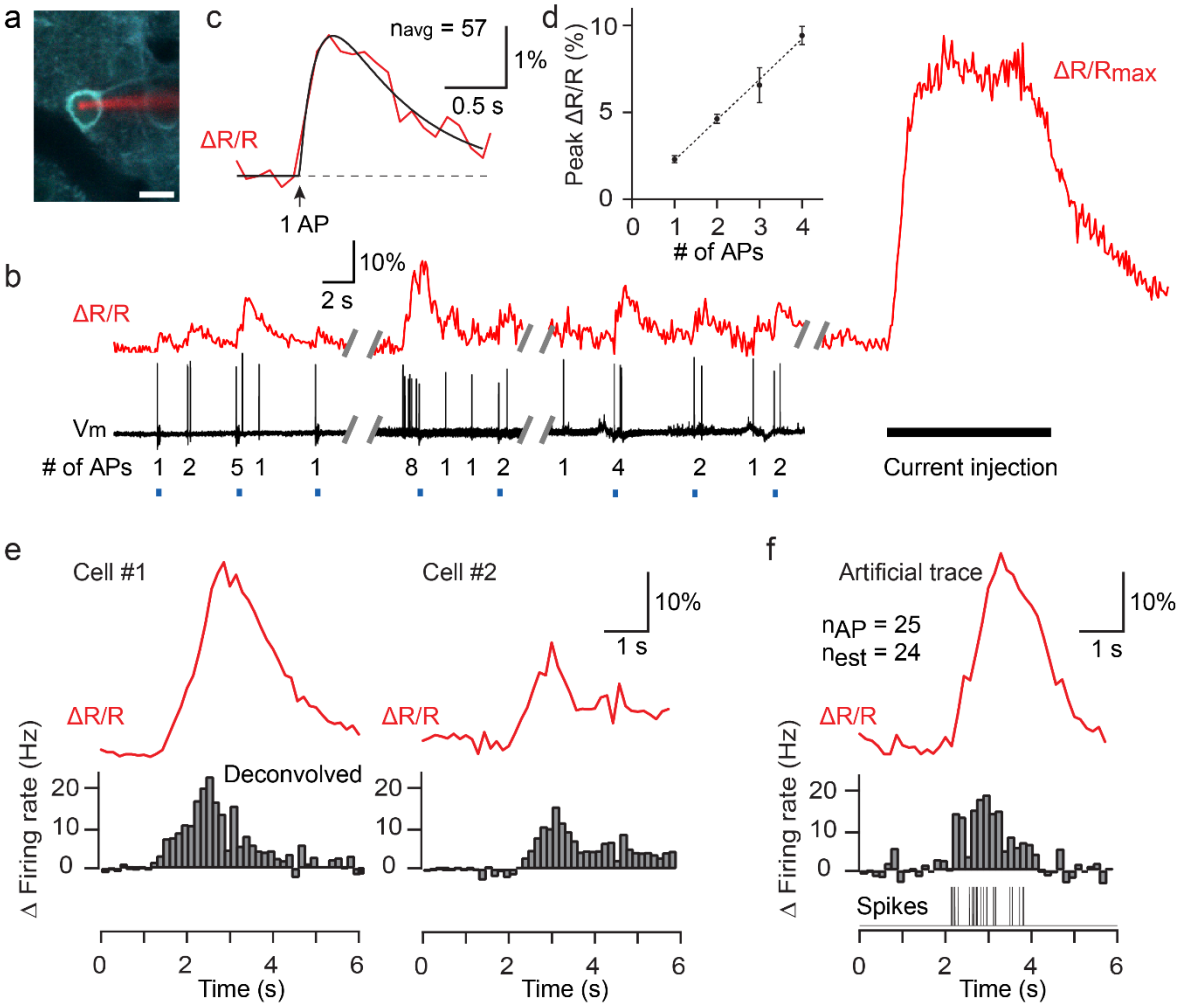


**Figure 11: *In vivo* characterization of the GECI YC-Nano140**

*In vivo* calcium imaging was performed in YC-Nano140 expressing L2/3 pyramidal neurons while the action potentials of single cells were recorded simultaneously using electrophysiology. **a**, Targeting of a YC-nano140 expressing neuron with a Alexa Fluor 594-filled pipette (red). Scale bar = 10 µm. **b**, Calcium measurements with YC-Nano140 (red) and simultaneous juxtacellular recordings (black) from 3 neurons. Number of action potentials that occur spontaneously or during air puff whisker stimulation (blue) are indicated. Far right trace: Estimate of maximum response at saturation ($\Delta R/R_{max}$) by prolonged injection of large current. On average, $\Delta R/R_{max}$ was 70.8 ± 4.4% (mean ± s.e.m.). **c**, Average calcium transient for spontaneous, isolated single action potentials. An exponential rising and decaying function was fit to the trace ($A_0$ = 4.54%, τonset = 0.186 s, $\tau_{decay}$ = 0.673 s, peak amplitude $A_{peak}$ = 2.3%). Signal-to-noise ratio ~ 1.5. **d**, Mean peak amplitudes of spontaneous calcium transients as a function of action potential number. **e**, Deconvolution of average calcium transients using the template 1 action potential-calcium transient from [c]. The mean of the first second was subtracted from the deconvolved trace to obtain the change in instantaneous action potential firing rate (IFR). The integral of the deconvolved trace then represents the number of additional action potentials that are generated during the trial period. **f**, Verification of the deconvolution approach using an artificial calcium transient produced by convolving an artificial spike train (25 action potentials uniformly distributed in middle 2 s period) with the template 1 action potential - calcium transient. In this case, deconvolution revealed the change in IFR with an estimate of 24 for the number of action potentials. Adapted from Chen et al. (2013).

## 3. Material and Methods

**"We shall not fail or falter; we shall not weaken or tire…Give us the tools and we will finish the job"**
***Winston Churchill***

### 3.1 Surgery

All experimental procedures were carried out according to the guidelines of the Veterinary Office of Switzerland and approved by the Cantonal Veterinary Office in Zurich. In young adult (P35-43) male transgenic ChR2 mice (Thy1-COP4/EYFP), AAV2/1-*EF1α-YC-Nano140* (300 nl, approximately $1 \times 10^9$ vg $\mu l^{-1}$) was delivered into L2/3 of M1 (100 µm anterior, 1900 µm lateral to Bregma, 300 µm below pial surface). 24 hours after virus injections, a circular cranial window (4 mm diameter) was implanted over M1 around the injection coordinates (Margolis et al., 2012). Contralateral to the cranial window, an aluminium head post (< 1g) for head fixation was implanted on the skull using dental cement. During the surgeries, mice were anaesthetized with isoflurane (4% induction, 2% maintenance). After the surgery the animals were treated with a the analgetic Rimadyl (Carprofen, 5mg/kg body weight, s.c.) as well as the antibiotic Rocephin (40mg/kg body weight, s.c.) and placed in the homecage for recovery. For the following 3 days, Rimadyl and Rocephin have been injected once per day and the animals's health and well-being has been evaluated at least twice per day for the first two days after surgery and thereafter at least once during the first week after the surgery.

### 3.2 Behavioral setup and training

To emulate the rung ladder test for rodents (Metz et al., 2001, Metz and Whishaw, 2002, Farr et al., 2006, Zorner et al., 2010) for head-fixed mice we built two ladder wheels (23-cm diameter), one with rungs at constant 1 cm spacing ('regular' wheel), the other with rungs placed at distances varying unpredictably between 0.5 to 3 cm ("irregular" wheel: 0.5 cm steps; 1.68 cm mean distance; 0.56 cm standard deviation). We trained five mice to perform skilled locomotion on these wheels (Fig. 13a). In the beginning of each trial, a brake blocked the wheel and prevented the animals to initiate locomotion. Animals had to initiate skilled locomotion after an auditory start cue (16000Hz for the irregular pattern, 12000Hz for the regular pattern) and

cover a predetermined distance of 15-30 cm (in one animal only 10-15 cm per run) until an auditory stop cue (8000Hz) indicated successful completion of the task. In successful trials, 2 seconds after the stop tone, the brake was reactivated and the animals, which were not water-restricted, received a reward of sweet water (2 µl). In unsuccessful trials, in which the mouse did not traverse the predetermined distance within a given time period, the animals were punished with a time-out. After one week of training all animals were successful in more than 80% of the trials on the regular and irregular rung pattern. Within successful trials the forelimb performance score (Farr et al., 2006) for the horizontal ladder reached a plateau in all mice after 10 training days (Fig. 12). After a training period of 10 days, animals were habituated to head fixation and trained well enough to perform skilled locomotion on the ladder wheels during simultaneous calcium imaging of neuronal networks in M1. During one day of the training period, one mouse was approximately between 30 minutes and 2.5 hours on the wheel, until 10 successful runs could be evaluated with the forelimb performance score in the regular and irregular condition. For each day, the forelimb performance score was averaged across the 10 runs of each condition.

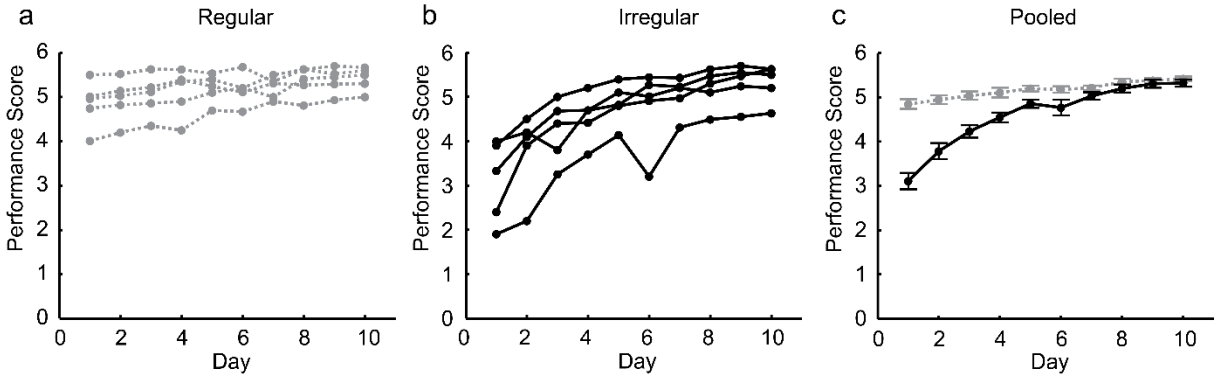


**Figure 12: Forelimb performance score during learning of the motor task**
**a,** Increase of the forelimb performance score of individual mice during learning of skilled locomotion on the regular pattern; **b**, Increase of the forelimb performance score of individual mice during learning of skilled locomotion on the irregular pattern; **c**, Comparison of the pooled performance scores on the regular and irregular pattern; initially, mice exhibited better performance on the regular pattern, but achieved comparable performance on the irregular pattern after 10 training days. Rating scale of forelimb placement as described in Metz et al. (2002): 0 = Total miss; 1 = Deep slip; 2 = Slight slip; 3 = Replacement; 4 = Correction; 5 = Partial placement; 6 = Correct placement.

### 3.3 Motion tracking during M1 mapping and calcium imaging

To allow the analysis of forelimb kinematics during light stimulation and calcium imaging of M1, the skin overlying defined anatomical landmarks of the right forelimb was shaved and tattooed with a commercially available tattooing kit (Hugo Sachs Elektronik, Harvard Apparatus GmbH). On the forelimb, we marked the vertebral border of the scapula, along with shoulder, wrist, metacarpophalangeal (MCP) joint and tip of the third digit. Limb kinematics during the optogenetic light stimulation were tracked by using a video camera that recorded the right side of the animal at 30 Hz. To allow the tracking of the limb kinematics during calcium imaging the right side of the animals was illuminated with two 940 nm infrared LED light sources and recorded at 90 Hz (1280 x 640 pixels) using a high-speed CMOS camera (A504k; Basler).

The markers on the skin of the forelimb were semi-automatically tracked offline and frame by frame, using the custom-made software ClickJoint 6.0 (ALEA solutions GmbH) which generated two-dimensional coordinates (x,y) for every marker and time point (Zorner et al., 2010). Based on these coordinates, the software modeled limb segments as rigid straight lines between markers and calculated the angles in each joint for consecutive frames. To minimize artifacts owing to divergent skin movements over the elbow joint, the position of the elbow was deduced from the shoulder and wrist coordinates as well as from the upper (~1.1 cm) and lower (~1.2 cm) forelimb length (Zorner et al., 2010). For subsequent analyses, we considered the angle changes in the shoulder, elbow, wrist and MCP joints. Hand movement was quantified by the x and y-coordinates of the MCP joint in each video frame. The reaching distance of the animals during each discrete grasping action was then calculated based on the x- and y-coordinates of the MCP-joint using Pythagorean addition.

### 3.4 Optogenetic motor mapping

2 weeks after the window implantation, mice were anesthetized with 0.02 ml ketamin/xylazine (20 mg/mL ketamine, 2 mg/mL xylazine) for the optogenetic motor mapping (Ayling et al., 2009). During the mapping, mice were placed into a hammock, with all four limbs dangling

freely (Fig. 16). Using a stereoscope with a motorized scanning system, a 473 nm laser was directed to 100 spots on the motor cortex, arranged in a 10x10 grid. Each of the 100 spots was hit in random order and stimulated for 500 ms at 100Hz (Pulse duration 4 ms). In all animals, the beam width was adjusted to 130 µm at the level of the motor cortex in the window center by using a reference micrometer grid. During stimulation of M1, the right side of the animal was monitored with a camera for subsequent offline-analysis of forelimb kinematics. The angle changes in the shoulder, elbow, wrist and metacarpophalangeal (MCP) joint during light stimulation of M1 were quantified using the custom-made software ClickJoint 6.0 (ALEA Solutions GmbH). The stimulation spot in which the maximal combined angle change in the shoulder, elbow, wrist and MCP joint occurred, was selected as “forelimb focus region” for calcium imaging.

**3.5 Two-photon imaging**

Calcium imaging was performed with a custom-built two-photon microscope controlled by HelioScan (Langer et al., 2013), equipped with a Ti:sapphire laser system (100-femtosecond (fs) laser pulses; Mai Tai HP; Newport Spectra Physics), a water-immersion objective (X16, Nikon), galvanometric scan mirrors (Cambridge Technology), and a Pockel’s Cell (Conoptics) for laser intensity modulation. For calcium imaging, YC-Nano140 was excited at 820nm to avoid simultaneous activation of ChR2 in dendrites of L5 neurons. Fluorescence of cyan fluorescent protein (CFP) was collected with blue (480/60 nm), and fluorescence of yellow fluorescent protein (YFP) with yellow (542/50 nm) emission filters. Image series were acquired at 18 Hz with 128x64 pixel resolution. The emitted fluorescence has been collected in the epi-collection mode by means of photomultiplier tubes (PMTs).

**3.6 Grasp type classification and grasp-to-grasp variability**

The classification into the three grasp types was performed using a sequence of custom-written Matlab functions. We first defined single grasp cycles based on local minima in the x-component of the reaching distance vector. To demarcate grasp cycles, which define

complete, discrete grasping actions with a reaching and pulling phase, from corrective subcycles within a discrete grasping action (as during corrective grasps, see below), only minima lower than the half between all local minima and maxima were accepted. Then, the mean finger extension as well as the number of subcycles in the reaching distance vector was computed for each grasp cycle. The number of subcycles during each grasp cycle corresponds to the count of local maxima in x- and y-component of the Savitzky-Golay-filtered reaching distance vector. Each grasp cycle was then assigned to the respective grasp type according to the following criteria:

- One subcycle, mean finger extension < 170° = standard grasp
- Two or more subcycles, mean finger extension < 170° = corrective grasp
- One or several subcycles, mean finger extension > 170° = (near-slip) digit tip grasp.

For each discrete grasping action, the amplitude in each joint was calculated as difference between the maximum and minimum. The grasp-to-grasp variability in a particular joint during a discrete grasping action was defined as amplitude difference between the ongoing and preceding discrete grasping action. To quantify the grasp-to-grasp variability of each joint angle for the whole regular or irregular movement sequence, the absolute values of the grasp-to-grasp variability in each grasping action were first averaged across all grasping actions of a single run:

$$\text{GtG-Var-single(JA)} = 1/(n-1)^* \sum_{k=2}^{n}(|A_k\text{-}A_{k-1}|)$$

GtG-Var-single = Grasp-to-grasp variability of one joint angle (JA) during one single run on the regular or irregular pattern. $A_k$ = Joint angle amplitude during the k-th-grasping cycle of one run. The resulting values were then averaged across all runs of the regular or irregular pattern, respectively, thereby leading to the final grasp-to-grasp variability of a particular joint angle on the regular or irregular pattern.

$$\text{GtG-Var(JA)} = 1/N \sum_{k=1}^{N} \text{GtG} - \text{Var} - \text{single}(\text{JA}, \text{k})$$

N = number of runs on the regular or irregular condition. If a specific joint is characterized by a high grasp-to-grasp variability during the regular or irregular movement sequence, the movement amplitude of this joint has to be frequently and extensively modified from one discrete grasping action to the next. In contrast, if a specific joint is characterized by a low grasp-to-grasp variability during the regular or irregular movement sequence, the movement amplitude of this joint can be frequently repeated from one discrete grasping action to the next and has to be modified only rarely. Untwisting the cap of a bottle during everyday life would be an example for a movement sequence with low grasp-to-grasp variability in more or less all arm joints, since their movement amplitude has to be repeated several times until the bottle is open. On the other hand, playing the Liszt sonata in b minor on the piano would be an example of a movement sequence with high grasp-to-grasp variability in more or less all arm and hand joints. When discrete tones are struck in a sequence during playing this piece, the movement amplitude of all arm and hand joints are rarely simply repeated. Instead, most discrete groups of tones require a unique combination of movement amplitudes in all arm and finger joints which are then concatenated to a sequence. Apart from these two extreme examples, numerous movement sequences during everyday life require high grasp-to-grasp variability in certain arm joints and low grasp-to-grasp variability in others.

In this regard, the grasp-to-grasp variability in all arm and hand joints represents one feature to describe a movement sequence as a whole (for instance on the regular or irregular rung pattern). Therefore, the grasp-to-grasp variability of arm and hand joints during a specific movement sequence provides a feature to describe movement context the discrete grasping actions of the sequence are embedded in. An intriguing question is therefore if and to what extent such a contextual feature or signature is represented in the motor system when for instance discrete movements are generated within a specific movement sequence.

### 3.7 Similarity measure of individual grasps

We first normalized the duration of all discrete grasping actions by interpolation to 160 sample points (k). The similarity of all grasp pairs was then quantified by summing up their sample-point-wise Euclidean distance *d* in the 4-dimensional joint angle space:

$$\boldsymbol{d}(\mathrm{n_i},\mathrm{m_i}) = \mathbf{1} - \frac{1}{\boldsymbol{max}(\boldsymbol{d}(N,N))} \sum_{i=1}^{k} \sqrt{(\mathrm{n_{iS}}-\mathrm{m_{iS}})^2+(\mathrm{n_{iE}}-\mathrm{m_{iE}})^2+(\mathrm{n_{iW}}-\mathrm{m_{iW}})^2+(\mathrm{n_{iF}}-\mathrm{m_{iF}})^2}$$

N represents all grasps, n and m denote one individual grasp, respectively. iS represents the i-th value of the z-scored shoulder angle, iE of the z-scored elbow ange, iW of the z-scored wrist angle and iF of the z-scored finger angle. The normalizing factor $\frac{1}{\boldsymbol{max}(\boldsymbol{d}(N,N))}$ yields similarity values between 1 (maximum similarity) and 0 (maximum dissimilarity).

To reduce the distracting effect of phase shifts between individual joint angles of the differerent grasping pairs, dynamic time warping (Müller, 2007) of the all joint angles (however without decoupling them) was allowed in a sliding time window of 33% of the grasp duration. Let us assume for instance, that two discrete grasping actions feature nearly the same time course in all joint angles (meaning they are virtually equivalent), but the joint angles between the two grasping actions are phase-shifted due to different starting points. The formula above would then compute an artificially high Euclidean distance between the two discrete grasping actions. Dynamic time warping compensates for phase shifts, but thereby inherently distorts the real time course of the joint angles. To limit such distortion, we restricted time warping to 33% of the grasp duration and did not allow decoupling of the four joints.

### 3.8 Twin movement analysis

Even though the same salient grasp types (“standard”, “corrective”, “digit tip”) were found in both conditions, they occurred at different frequencies (Fig. 14c). Moreover, the same grasp type clusters across conditions could still feature systematic differences in the mean, variance

and time course of individual joint angles. The condition-related encoding differences could have emerged as a consequence of these kinematic differences between the regular and irregular condition. Alternatively, the different behavioural context of the regular and irregular condition could have triggered encoding differences independent of kinematic discrepancies across conditions. To investigate to what extent the condition-related encoding differences emerged due to the behavioural context and irrespective of kinematic discrepancies across conditions, we compiled quasi-identical grasp sets for the regular and irregular pattern. The similarity between grasp pairs across conditions was quantified using the sample-point-wise Euclidean distance in the 4-dimensional joint angle space (see above). Starting with the standard grasp cluster, we first selected the most similar grasp pair across conditions. In each condition, the respective standard grasp was no longer available for further selections. From the remainder of grasps in the standard grasp cluster of each condition, we again selected the most similar pair and continued in this way until all grasps in the standard grasp cluster of one condition were consumed. We then performed the same procedure for the corrective and finger grasp cluster. After this selection procedure, each “twin” cluster in the regular condition featured the same number of grasps as its counterpart in the irregular condition. Moreover, the joint angle deviation of grasp pairs across conditions was reduced to less than 13°. We then checked if the significant differences in encoding between the regular and irregular pattern were preserved after this analysis that yielded pools of quasi-equivalent grasps across conditions. Additionally, we checked if condition-related encoding differences of individual joint angles still correlated with differences in their total grasp-to-grasp variability from the regular to the irregular condition. If so, the grasp-to-grasp variability of individual joints during a learned movement sequence represents a contextual feature that can modify the encoding of kinematics during equivalent, discrete grasping actions.

In other words, we compare the encoding of joint angles only during selections of the same movements on the regular and irregular pattern. Even though the movements in each condition are now by selection equivalent, they still have been applied in two different movement sequences, meaning in two different movement contexts. If there are now encoding differences

for the equivalent movement subsets in both conditions, these emerged due to the different context and not due to kinematic differences. As explained above, one of many features of the movement context is the grasp-to-grasp variability of joint angles. So our question is, do differences in the joint angle grasp-to-grasp variability on the regular and irregular condition explain encoding differences during discrete movements on the regular and irregular condition, that feature equivalent kinematics? If so, it means that the encoding of movement variables in M1 during a discrete motor action in a sequence can only be understood when the characteristics of the whole movement sequence are taken into consideration.

### 3.9 Electrophysiological control experiment

In a separate set of 8 ChR2 mice, we investigated, if two-photon imaging in L2/3 at the wavelength of 820 nm affects the membrane potential and spiking rate of ChR2 expressing L5 neurons via dendrites passing though L2/3. To make sure that the advantage to perform calcium imaging in optogenetically identified and thereby mechanically unharmed M1 circuits does not disturb the physiological neuronal homeostasis, we performed cell-attached recordings of L5 neurons. When we applied blue laser light (488 nm) onto the motor cortex, ChR2 expressing L5 neurons exhibited a pronounced increase in their firing rate. Following this response to blue light illumination, we imaged L2/3 above the recorded L5 neuron using a wavelength of 820 nm and our imaging light intensities (<45 mW). Following the two-photon imaging in L2/3, blue light was again shone onto M1 to confirm that the cell was still spiking. We then analysed the number of spikes during “Blue light on” and “Blue light off” as well as during “2-Photon on” and “2-Photon off” using the sixth standard deviation of the electrophysiological recording as threshold for spike detection. For statistical analysis, we performed a paired t-test with Bonferroni correction for “Blue light on” vs. “Blue light off”, “2-Photon on” vs. “2-Photon off”, “Blue light on” vs. “2-Photon on” and “Blue light off” vs. “2-Photon off”.

### 3.10 Calcium imaging analysis

Calcium imaging data from the channels of YFP and CFP was imported into MATLAB (version 7, Mathworks) for subsequent processing steps. Motion in both data channels was corrected using the Turboreg Algorithm. Individual neurons were selected manually from the mean image of each single-trial time series as regions of interest (ROIs). The mean pixel value of each ROI was extracted for both channels and applied to express neuronal calcium signals as relative YFP/CFP ratio change $\Delta R/R = (R - R_0)/R_0$ in which we employed a sliding window across the dataset to infer the baseline ratio $R_0$.

For cross-correlation and population coding analyses, calcium signals were deconvolved using the Wiener filter algorithm (Chen et al., 2013) (smoothness parameter $\alpha$ = 0.01) and time vectors of kinematic parameters were downsampled to the imaging frame rate (18 Hz) using cubic spline interpolation as implemented in Matlab.

### 3.11 Population coding and classification with cross-validation

We used the random forest algorithm (Breiman, 2001) to predict the angle motion in the shoulder, elbow, wrist and finger joints from neuronal population activity or from the activity of single neurons. After trials have been concatenated, the algorithm was trained on a subset of trials which comprised 90% of the dataset and which have been selected randomly. For cross-validation, the trained algorithm was then evaluated on the 10% of the dataset not included in the training set (the test set). To quantify the accuracy of the decoding, we computed the Pearson correlation coefficient ($p$) between the model estimate of the joint angles in the test set and the real joint angles in the test set. We repeated this procedure 100 times and defined the decoding accuracy as the mean correlation coefficient of all 100 iterations. The whole decoding approach with cross-validation was again executed, but with random sample point shuffling of the calcium traces in the training set. With regard to the population coding, this approach to quantify the decoding of forelimb joints was applied for the whole dataset as well as separately for standard, corrective and finger grasps. We also performed the same analyses

with test data sets of different sizes (20% and 30%), which did not lead to substantial differences of the results. Additionally, using a general linear model instead of the random forest algorithm did not substantially alter the results.

For the prediction of grasp types, the mean neuronal activity of each cell during a particular grasp was computed. The random forest algorithm was then trained on 90% of randomly selected grasps (the training set) to predict the three different grasp types based on the mean neuronal activity of each neuron in the network. In the training set, the count of each grasp type was equalized to avoid training bias to more frequently occurring grasps. For cross-validation, the trained algorithm was subsequently evaluated on the 10% of grasps that have not been included in the training set (the test set). To quantify the accuracy of prediction, the Matthew's correlation coefficient between real and predicted grasps was calculated, separately for each type. The prediction of grasp types with cross-validation was again executed, but with random sample point shuffling of the calcium traces in the training set.

The random forest algorithm is a multivariate, non-parametric machine learning algorithm and utilizes bootstrap aggregation of regression trees. We adopted the Treebagger function that is implemented in Matlab and specified 100 trees, a minimum leaf size of 5 as well as the default setting for the number of features selected randomly in each split (Nsplit = $N_{features}/3$). These parameters were an appropriate trade-off between computation time and decoding accuracy. For the prediction of joint angles or grasp types, the method was specified with "regression" and "classification", respectively.

### 3.12 Statistics

To test the significance of decoding differences between conditions for joint angles or grasp types, paired t-tests with post-hoc Bonferroni-correction were used. To test if decoding of joint angles or grasp types was significant per se, paired t-tests between the mean decoding values for "true" and "shuffled" across mice have been applied with post-hoc Bonferroni correction. To investigate to what extent the encoding of individual joint angles can be explained by their grasp-to-grasp variability within the learned movement sequence, we z-scored the 4 values for

grasp-to-grasp variability and encoding in each animal and condition. Separately for the regular and irregular condition, we then calculated a linear regression with clustered standard error (animal = cluster variable) of the encoding values versus the grasp-to-grasp variability values, pooled across mice. A significant positive linear relationship indicates that joint angles that feature high grasp-to-grasp variability in a movement sequence, are also characterized by increased encoding in M1 neuronal networks (e.g. the finger base angles on the regular pattern are characterized by higher grasp-to-grasp variability and encoding when compared to shoulder, elbow and wrist angles). Additionally, we asked to what extent condition-related differences in encoding of joint angles correlate with condition-related differences in their grasp-to-grasp variability. We first calculated, separately for each joint angle and animal, the differences in encoding and grasp-to-grasp variability from the regular to the irregular condition. In each animal, we then z-transformed the 4 values for differences in grasp-to-grasp variability and encoding. We then calculated a linear regression with clustered standard error (animal = cluster variable) of the condition-related grasp-to-grasp variability differences versus the condition-related encoding differences, pooled across mice. A significant positive linear relationship indicates that condition-related increases in grasp-to-grasp variability of individual joint angles are accompanied with condition-related enhancements of their encoding (e.g. the grasp-to-grasp variability of the shoulder angle increased from the regular to the irregular condition, as did its encoding in neuronal networks of M1 L2/3). In plots with data that has been averaged across animals, means with standard errors are shown.

# 4. Results

**"For me context is the key – from that comes the understanding of everything"**
***Kenneth Noland***

During skilled locomotion on regular or irregular rung ladders, mice have to apply multiple discrete grasping actions in a sequence. Even if two discrete grasping actions, one applied on the regular pattern and the other applied on the irregular pattern, feature equivalent kinematics, they are still applied in different behavioural contexts, scilicet in that of the regular or irregular condition. To investigate inter alia if and how the behavioural context affects the encoding of forelimb variables in neuronal networks of the motor cortex, we therefore made the rung ladder test for rodents compatible with simultaneous calcium imaging of cortical neurons. To emulate the rung ladder test for head-fixed mice, we employed two custom-made ladder wheels. While transverse rungs were equally spaced on the regular wheel, their distance varied unpredictably on the irregular wheel. Five mice were trained to perform skilled locomotion on these wheels during head-fixation. While the mice were engaged in skilled locomotion on the wheels, calcium imaging of neuronal networks in M1 L2/3 was employed and angle changes in shoulder, elbow, wrist as well as finger base joints were recorded.

## 4.1 Analysis of behavioural variables

While the animals were engaged in skilled locomotion on the wheels with regularly or irregularly spaced rungs, we performed calcium imaging in M1 L2/3 and used high-speed videography to track shoulder, elbow, wrist and finger-base angles along with the reaching distance for the right forelimb (Fig. 13a, b). Based on these behavioural variables, we analyzed the basic grasping features during skilled locomotion of the animals. Assessed from the local minima of the reaching distance vector, we divided the motor behavior into discrete grasping actions. On average, mice performed 11.67 ± 1.61 grasps per run on the regular pattern and

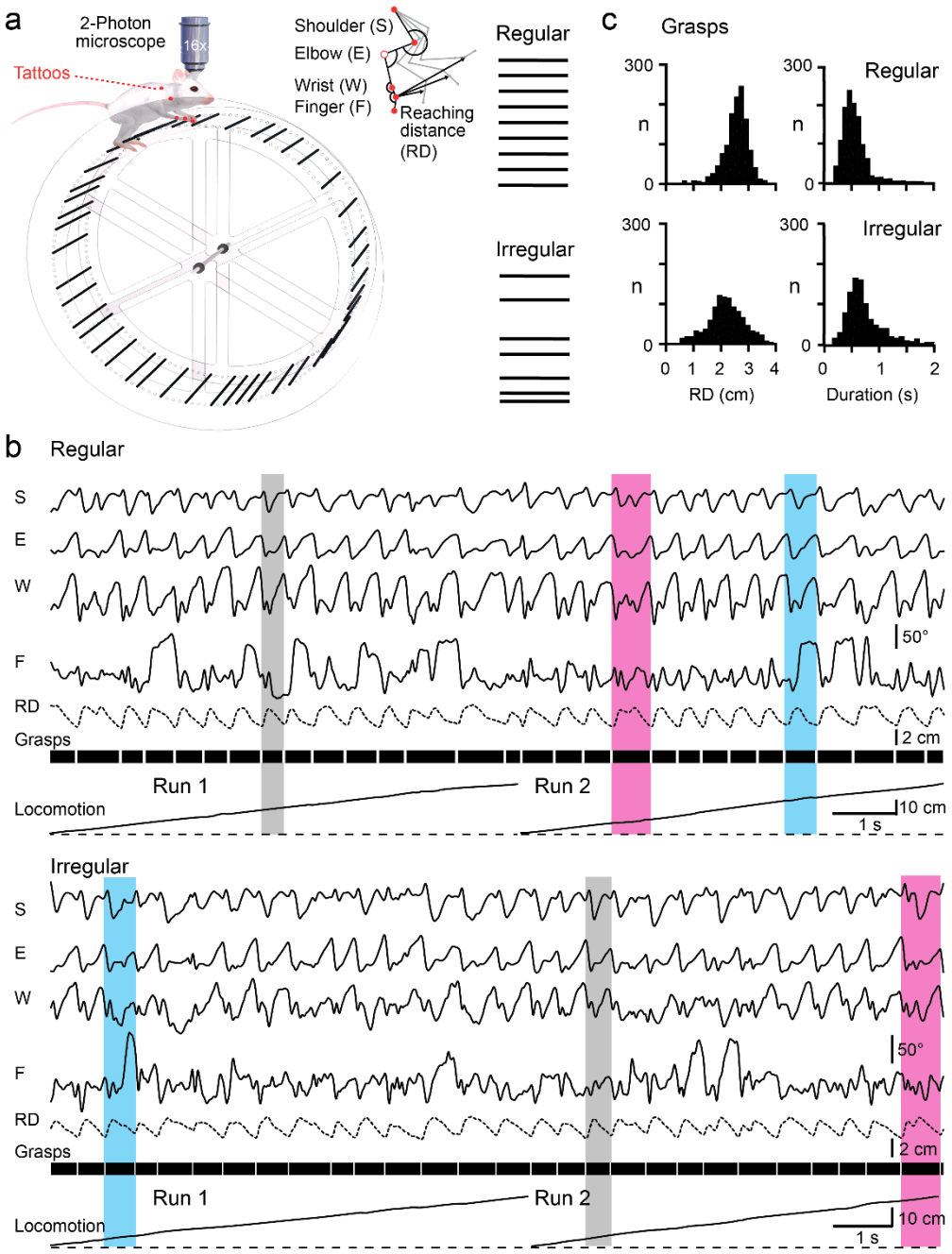


**Figure 13: Behavioural setup and recording of movement variables**
**a,** Schematic of setup. A head-fixed mouse is placed on top of a ladder wheel to move across rungs with regular or irregular spacing (here irregular wheel is shown). The setup is mounted below a two-photon microscope. A high-speed video camera tracks a set of tattoos on the right forelimb (red dots: scapula, shoulder, wrist, finger base joint, digit tip; the elbow position is calculated assuming fixed shoulder-to-elbow and elbow-to-wrist distances) to allow quantification of reaching distance (RD) and changes in shoulder (S), elbow (E), wrist (W) and finger (F) joint angles. **b**, Time course of forelimb joint angles and reaching distance during two example runs on the regular (top) and the irregular (bottom) wheel with individual grasps indicated. Three typical grasps are highlighted by dashed boxes (grey = standard grasp, magenta = corrective grasp, cyan = digit tip grasp). **c**, Histograms of the reaching distance and grasp durations during both conditions, pooled across all mice.

9.15 ± 0.97 grasps per run on the irregular condition (mean ± s.e.m.). The distributions of reaching distance and grasp duration were similar for the regular and irregular wheel, with insignificant trends of decreased reaching distance and prolonged grasp duration on the irregular wheel (Fig. 13c; $p > 0.05$; paired t-test of mean values, Bonferroni-corrected; $n = 5$ mice). Consistent with the larger difficulty to run on the irregular wheel, grasping duration varied significantly more on the irregular pattern, as judged from the standard deviation of the distribution ($P < 0.05$; Bonferroni-corrected).

Across mice and conditions, we identified three salient grasp types that could be classified based on the temporal profile of the reaching distance and the mean finger extension during each grasp (Fig. 14a): “Standard” grasps consisted of single cycle with reaching phase, correct placement of the forepaw on the rung, and terminal pulling phase; “corrective” grasps were characterized by one or multiple corrective reaches following the initial reach until the forepaw hit the targeted rung optimally and the pull proceeded; during “digit tip” grasps the targeted rung was hit with the digit tips, causing pronounced finger joint extension with the need for dexterous finger control to avoid a forelimb slip and to finish the pull (Fig. 14a). The similarity between grasp pairs within and across different types was also quantified using the mean Euclidean distance of the 4-dimensional joint angle trajectories. When grouped according to our classification (see 3.6), digit tip grasps formed a cluster clearly separate from the other grasps types under both conditions whereas the distinction between standard and corrective grasps was less obvious (Fig. 14b). For the irregular wheel significantly more grasps were classified as corrective (Fig. 14c) ($p < 0.05$, paired t-test, Bonferroni-corrected). For each class we also quantified the grasp-to-grasp variability of all joint angles as amplitude variation from one grasp to the next. Grasp-to-grasp variability was larger in all forelimb joints for the irregular pattern but this increase was significant only for the shoulder (Fig. 14c; $p < 0.05$, paired t-test, Bonferroni-corrected). This result indicates that shoulder movements can be stereotypically recalled on the regular rung pattern while the irregular condition requires grasp-by-grasp recalibration of the shoulder joint angle amplitude. Since the adjustment of the reaching distance is crucial to avoid rung misses and subsequent falls on the irregular pattern,

we also calculated the correlation between reaching distance and its defining joints, shoulder and elbow (Fig. 15).

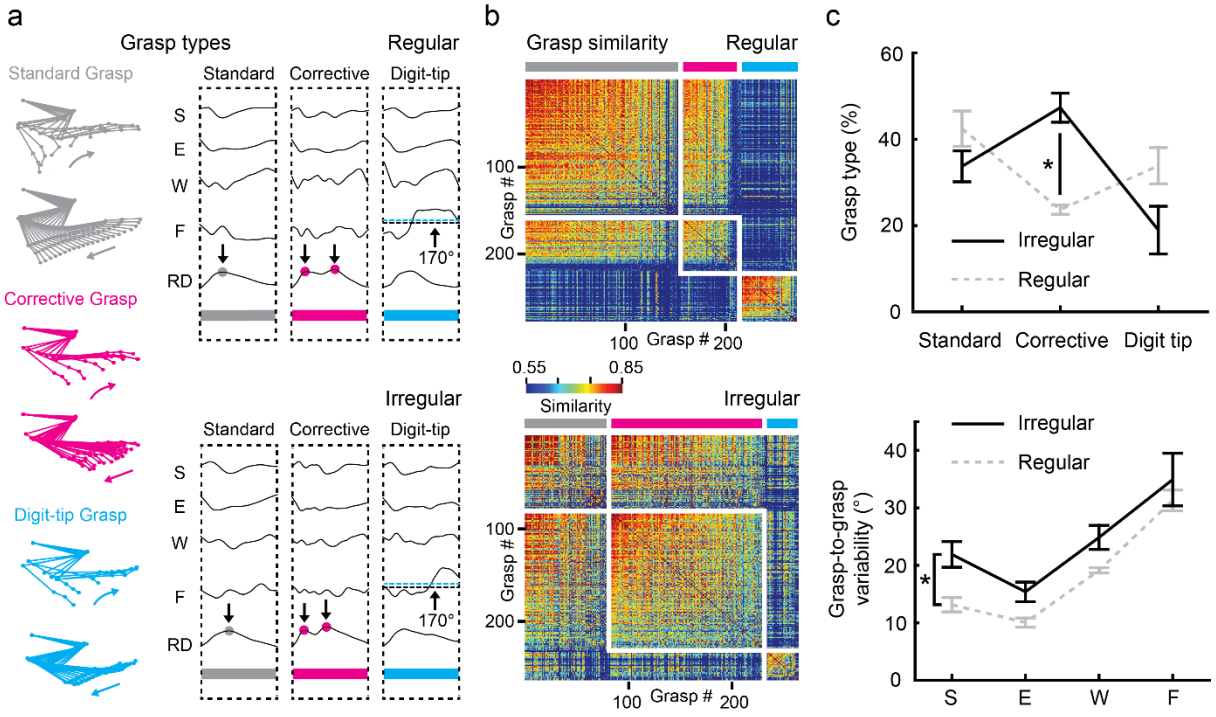


**Figure 14: Quantitative analysis of forelimb grasps**
**a,** Left panel: Limb kinematic plots for the three principal grasp types (top: reaching phase, bottom: pulling phase). Right panel: Kinematic profile of joint angles and reaching distance for examples of standard (grey), corrective (magenta), and digit tip (cyan) grasps during both conditions (expanded view of grasps marked Fig. 13b, grasp duration normalized). Dots on the reaching distance trace indicate the number of reach subcycles during the grasp; cyan dashed line in the digit tip grasp box marks the mean finger extension during the grasp. Black dashed line below marks the 170° threshold for mean finger extension used to classify digit tip grasps. **b,** Grasp similarity matrix for regular and irregular conditions sorted according to the classification in standard (grey bar), corrective (magenta bar) and digit tip (cyan bar) grasps. Matrices are subsorted according to similarity values. **c,** Top: Fraction of grasps types on the regular (dashed grey) and irregular (solid black) rung pattern. Bottom: Grasp-to-grasp variability of each joint on the regular (dashed grey) and irregular pattern (solid black). Asterisks indicate $p < 0.05$.

Interestingly, the shoulder joint showed the higher correlation with the reaching distance, especially when the reaching distance surpassed 2 cm, which was true for the majority of grasps. These results suggest that the increased grasp-to-grasp variability of the shoulder angle on the irregular pattern indeed relates to the required adjustments of the reaching distance to avoid misses and falls.

### 4.2 Optogenetic mapping of the motor cortex

Our final goal was to relate the measured behavioral variables to the simultaneously recorded activity in neuronal networks of M1 L2/3. Therefore we had to map the motor cortex in advance, on the one hand to identify cortical circuits that control all joints in the right forelimb, on the other hand to ascertain that the targeted circuits are comparable across mice. To maintain intact neuronal architecture for the subsequent calcium imaging we decided to avoid electrical stimulation with inherent impairment of neuronal tissue by electrode penetrations and employed the optogenetic mapping approach instead (Ayling et al., 2009, Harrison et al., 2012). Using transgenic mice expressing ChR2 in cortical L5 neurons (Arenkiel et al., 2007), we stimulated different spots in M1 consecutively with a blue laser and quantified the evoked forelimb joint angle changes using videography (Fig. 16a, b).

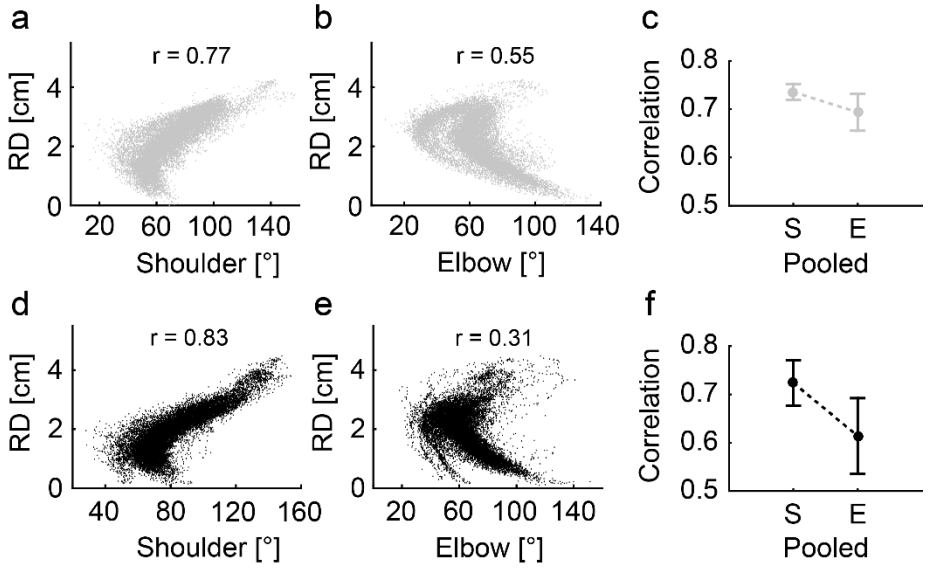


**Figure 15: Correlation of proximal joints with the reaching distance**
**a-c**, Regular pattern (grey); **a**, Correlation between shoulder angle and reaching distance for each sample point in one example mouse; **b**, Same for elbow. **c**, Correlation between shoulder and reaching distance as well as between elbow and reaching distance, pooled across mice. **d-f**, same analyses as in a-c, but for the irregular pattern (black). Both on the regular and irregular pattern, the correlation between shoulder and reaching distance is particularly high for reaches longer than 2 cm, which represent the majority of grasps.

In a circumscribed cortex area, laser stimulation elicited pronounced flexions in elbow and wrist joints as well as distinct extensions in shoulder and finger joints (Fig. 16d). All five mice featured a central subdivision within the forelimb area, in which optical stimulation evoked the most pronounced movement, involving all proximo-distal joints (Fig. 16c). This area was

selected for calcium imaging of L2/3 networks. Thus, the recorded L2/3 populations are likely to be part of comparable motor cortex circuits across mice, and their architecture has not been compromised by electrode penetrations. Before the implantation of the chronic window and the optogenetic mapping, the motor cortex forelimb area of all ChR2 mice has been injected with the genetically encoded calcium indicator YC-Nano140 (Chen et al., 2013). After optogenetic mapping calcium imaging of neuronal networks in L2/3 was applied while the animals were engaged in skilled locomotion on the regular or irregular rung arrangement.

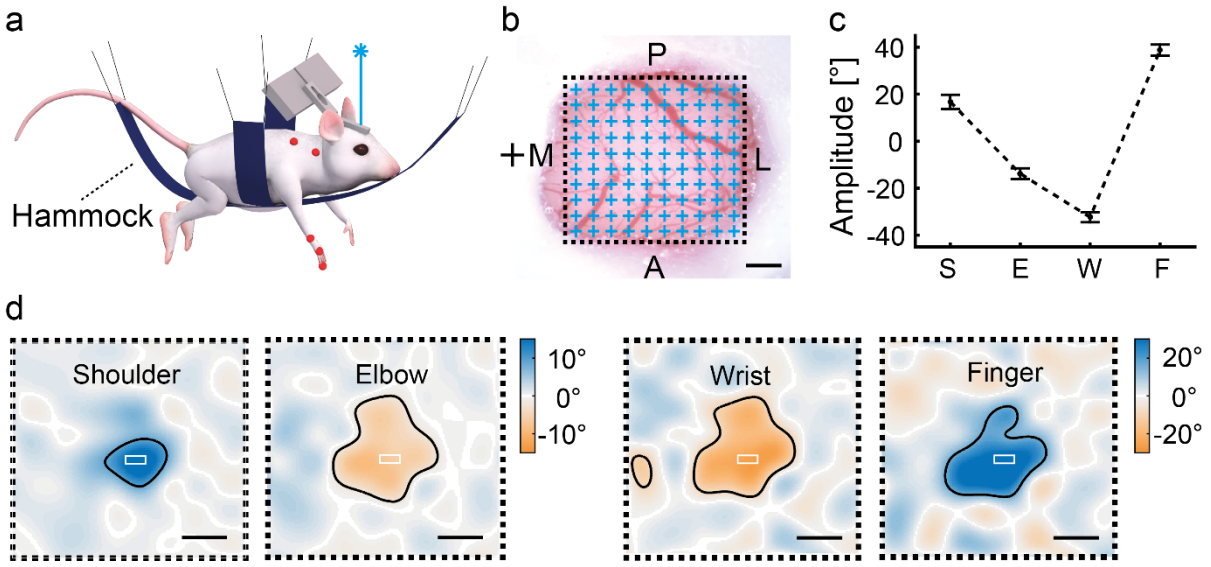


**Figure 16: Optogenetic mapping of M1**
**a,** During the optogenetic mapping, anesthetized ChR2 mice were hanging in a hammock with all four limbs dangling freely; angle changes in shoulder, elbow, wrist and finger base joints were recorded with a high-speed camera; **b**, Stimulation grid with 100 spots, overlayed with the cortex after implantation of a chronic glass window. Each spot was stimulated for 500 ms in random order; black cross on the left indicates the location of the Bregma **c**, Movement amplitude in each joint, that has been induced by optogenetic stimulation in the forelimb focus for calcium imaging, pooled across all five mice. **d**, Joint angle map of one example mouse; the superimposed white rectangles indicate the selected area for subsequent calcium imaging; in all mice, the area for calcium imaging featured the most pronounced movement amplitude in all forelimb joints ("forelimb focus"). Scale bars = 0.5 mm.

To assure that calcium imaging of M1 L2/3 populations did not inadvertently activate L5 neurons via ChR2 in dendrites penetrating L2/3 we performed cell-attached recordings of L5 cells during calcium imaging of L2/3 in a different set of anesthetized ChR2 mice (Fig. 17a, b). During stimulation with one-photon light at 488 nm, ChR2 expressing L5 cells showed strikingly increased spiking activity (Fig. 17a, upper panel). In contrast, two-photon imaging in M1 L2/3

using a excitation wavelength of 820 nm did not induce any detectable changes in the cell-attached recordings of ChR2-expressing L5 neurons (Fig. 17a, lower panel; only significant difference occurred between blue on vs. all other conditions, $p<0.05$, Bonferroni-corrected, Fig. 17b). This was expectable since ChR2 requires a two-photon wavelength of 940nm to be effectively activated.

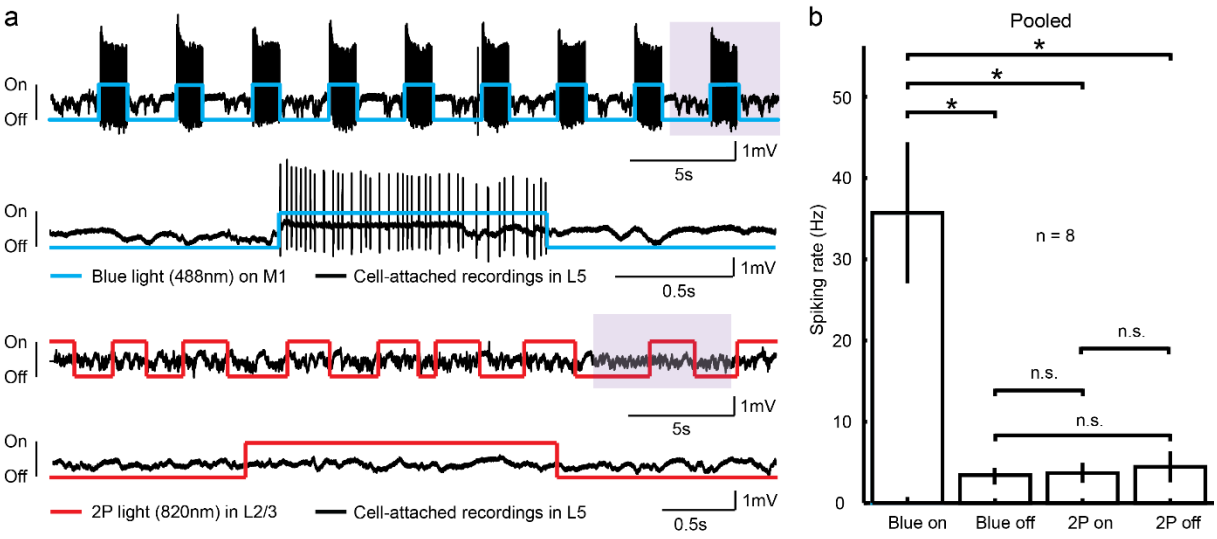


**Figure 17: Effect of blue one-photon and infrared two-photon light illumination (820nm) on spiking activity of L5 neurons**
**a,** Upper panel: Cell-attached recordings of ChR2 expressing L5 cells during the application of blue light on the motor cortex. Lower panel: Cell-attached recordings of ChR2 expressing L5 cells during scanning of L2/3 cells using two-photon light at 820 nm. **b**, Pooled data for all eight animals; while blue light stimulation induced extensive spiking of the L5 neurons, scanning L2/3 with two-photon excitation light at 820nm did not induce any detectable changes in the spiking rate of L5 neurons.

### 4.3 Calcium imaging and analysis of neuronal activity in M1 L2/3

To extract fluorescence dynamics caused by neuronal activity, regions of interest (ROIs) were drawn around all individual cells of the imaged network (Fig. 18a). Depending on the animal, the recorded networks comprised 41 to 56 neurons. We subsequently applied a deconvolution algorithm (Wiener Filter, see Methods) to transform the raw fluorescent traces to estimates of the instantaneous firing rates of neurons (Fig. 18b). All subsequent analyses were based on the time series of the instantaneous neuronal firing rates. We first investigated to what extent the activity of individual neurons is associated with each of the three grasp types. Averaging the activity of all neurons across each grasp type revealed that 5% of the cells showed significant activity during digit tip grasps on the regular pattern while 15% of the cells exhibited

significant activity on the irregular pattern (Fig. 18d, left panel). The number of cells that showed significant activity during standard and corrective grasps did not surpass chance level in both conditions.

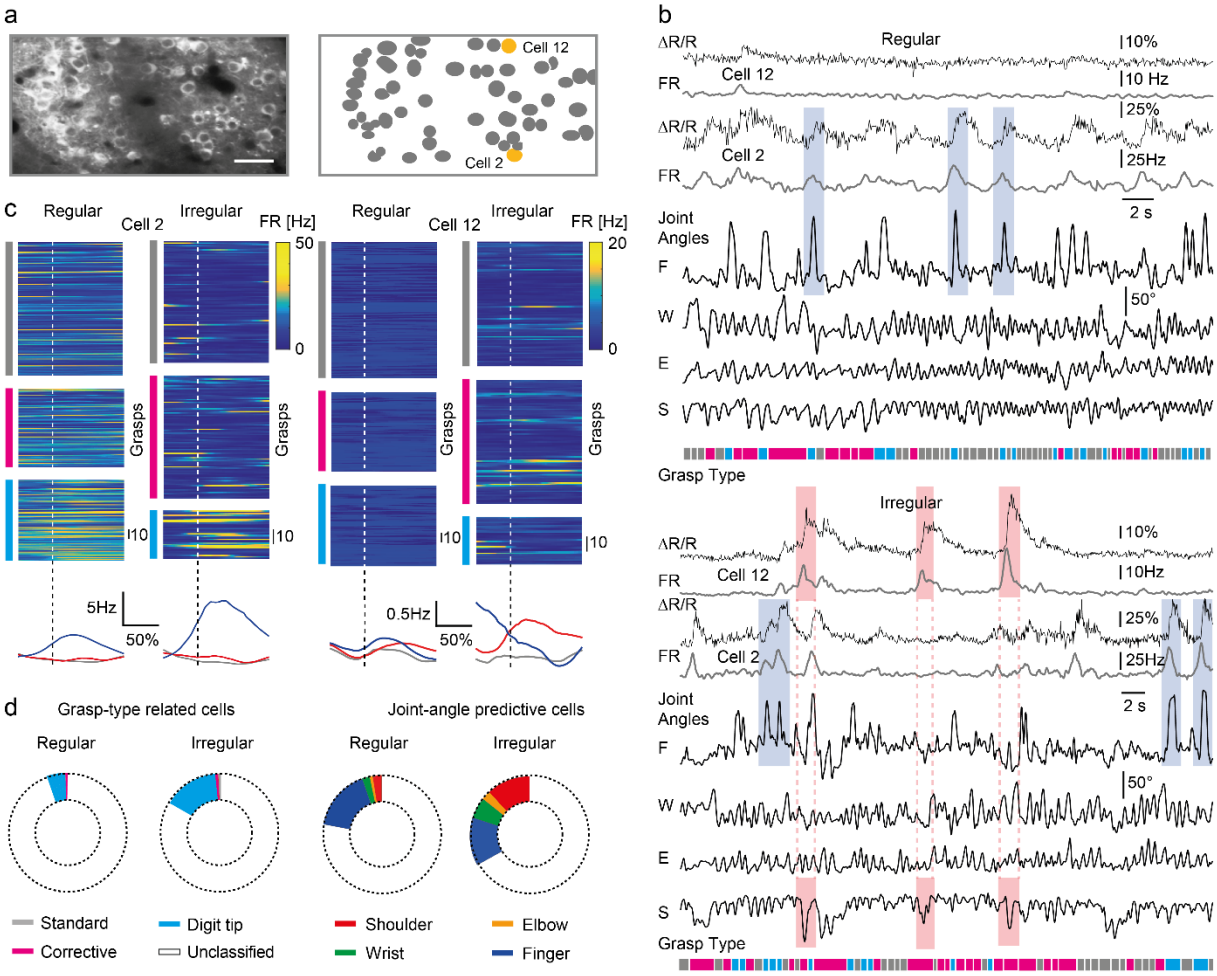


**Figure 18: Calcium imaging of neuronal networks in M1 L2/3**
**a**, Neuronal network recorded with calcium imaging (left panel) during skilled locomotion as well as schematic of the regions of interest (right panel); scale bar = 50 µm**. b**, Raw (upper trace) and deconvoluted calcium signal (lower trace) for the two cells in a, that are highlighted in yellow, along with simultaneously recorded joint angles and the classified grasp types. On the regular and irregular condition, cell 2 exhibits high activity during pronounced finger extensions (blue shaded areas). Only on the irregular pattern, cell 12 generates activity during shoulder movements. **c**, Deconvoluted activity of cell 2 and cell 12 during the three different grasp types and the corresponding averages for both conditions; **d**, left panel: Relationship of single cells to grasp types for both conditions, pooled across all mice; right panel: Cross-validated prediction of shoulder (red), elbow (orange), wrist (green) and finger base angles (blue) using single cells as predictors, pooled across mice.

We next asked to what extent single neurons encode the time course of the recorded joint angles. We trained the Random Forest Algorithm to predict each of the four joint angles based on the activity trace of individual cells. On the regular pattern, the correlation between the predicted and the real joint angle was significant for the finger angle in 17% of the neurons

(Fig. 18d, right panel). On the irregular pattern, 13% of the cells were predictive for the finger angle, 12% for the shoulder angle and 6% for wrist angle (Fig 18d, right panel, elbow angle not above chance level).

Interestingly, single cells were rarely tuned to one joint angle alone. Rather, tuning of neurons was distinctly shifted towards selective joint angles for a subset of cells (Fig. 19). On the regular pattern, pronounced neuronal tuning was observed only for the finger joints (Fig. 19a). These finger angle predicting cells showed different tuning with regard to the other three joints: They could in addition be biased to the elbow (orange), wrist (green) or shoulder angle (x-axis) or to a combination of these joints, albeit to a far lower extent than for the finger angle (Fig. 19a). The continuous tuning spectrum to combinations of the four joints was also present on the irregular pattern. However, one or more neurons in each animal strikingly increased its encoding of the shoulder angle in comparison to the regular condition (Fig. 19b). We conclude that M1 employs a versatile encoding scheme by simultaneously representing multiple degrees of freedom at the level of individual neurons.

### 4.4 Population coding of joint angles on the regular and irregular pattern

We next asked how well the collective activity of all neurons in the imaged neuronal subsets encodes angle changes in the different forelimb joints. We used the random forest algorithm to predict the motion in shoulder, elbow, wrist and finger base joints based on the neuronal firing rates of all cells in the imaged area (see Material and Methods).

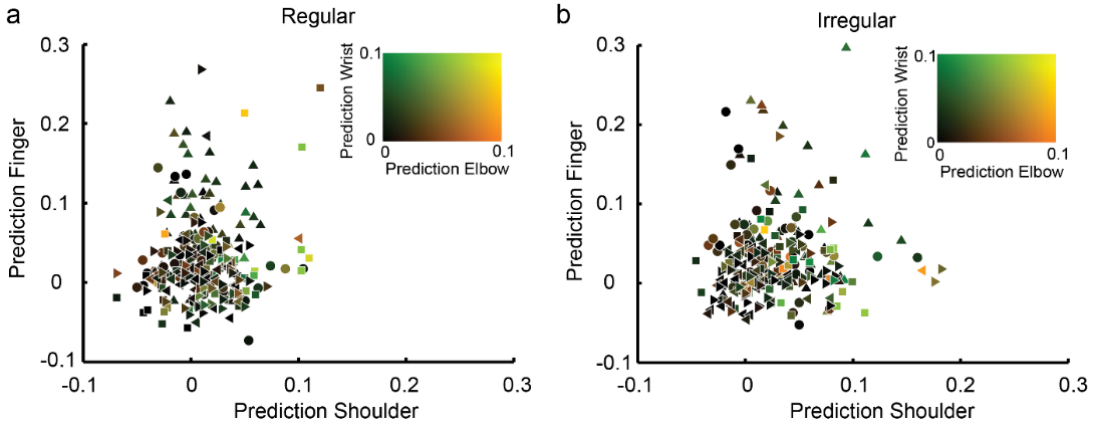


**Figure 19: Tuning of individual neurons to the four joint angles**
**a,** Prediction of forelimb joint angles by all recorded cells from the five animals for the regular pattern; for each cell, the encoding for the shoulder and finger angles can be concluded from the spatial location in the diagram while the encoding for elbow and wrist can be derived from the color code in the upper right corner **b**, same conventions as in a, but for the irregular condition.

In both conditions, the motion of all forelimb joints was significantly encoded in the recorded neuronal networks of M1 L2/3 (Paired t-test between true and shuffled cross-validation across mice; $p<0.05$ for all joints in both conditions, Bonferroni-corrected). On the regular pattern, the encoding of finger base joint motion surpassed that of all other forelimb joints (Fig. 20a, 21a**,** paired t-test against all other joints, $p < 0.05$, Bonferroni-corrected). On the irregular pattern, the same neuronal networks still featured precise prediction of finger base movements, but additionally increased their encoding of shoulder motion (Fig. 20b, 21a, paired t-test, $p < 0.05$, Bonferroni-corrected). The correlation between the encoding of each movement variable and its corresponding grasp-to-grasp variability was significant within both conditions (Fig. 21b, c, linear regression with clustered standard error, $p < 0.05$ for regular and irregular, see Methods). In-between conditions, the differences in encoding and grasp-to-grasp variability of the respective joint angles were likewise positively correlated (Fig. 21d, linear regression with clustered standard error, $p < 0.05$).

### 4.5 Population coding during specific grasp types

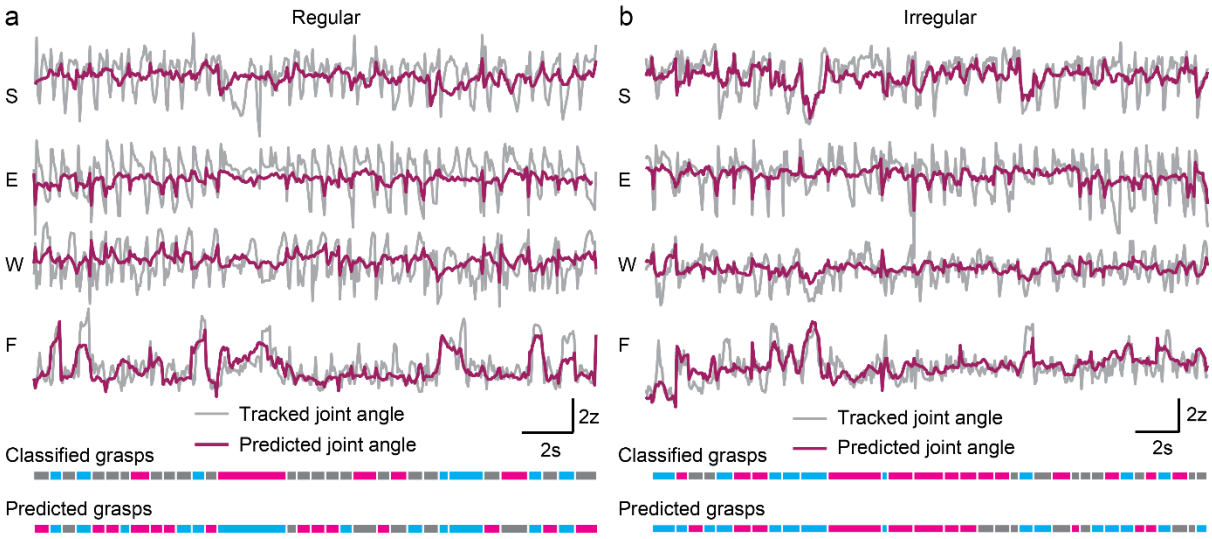


**Figure 20: Encoding of forelimb variables and grasp types for one example mouse**
**a**, Regular condition: Tracked shoulder (S), elbow (E), wrist (W) and finger base (F) angles in grey as well as predicted by the activity of neuronal networks in M1 L2/3 (purple overlays); grasps that have been classified based on kinematic criteria and predicted by network activity are shown below the kinematic traces; **b**, Same conventions as in a, but for the irregular condition. While the match between real and predicted finger angle is accurate in both conditions, the irregular condition features in addition increased precision in the prediction of the shoulder angle.

We next investigated how well forelimb joint angles are encoded within each of the three grasp types. We predicted the motion of each forelimb joint angle within each of the three movement clusters, separately for the two conditions (Fig. 22a-c). This analysis revealed that the encoding of shoulder joint motion during corrective grasps significantly increased from the regular to the irregular condition (Fig. 22b, paired t-test, $p < 0.05$, Bonferroni-corrected). To assess the representation of the three different grasp types in M1, we compared to what extent each grasp type can be directly predicted by the activity in neuronal M1 L2/3 networks. While neuronal network activity predicted digit tip grasps on the regular and irregular pattern, the representation of corrective grasps was significant only on the irregular pattern (22d, paired t-test, $p < 0.05$, Bonferroni-corrected).

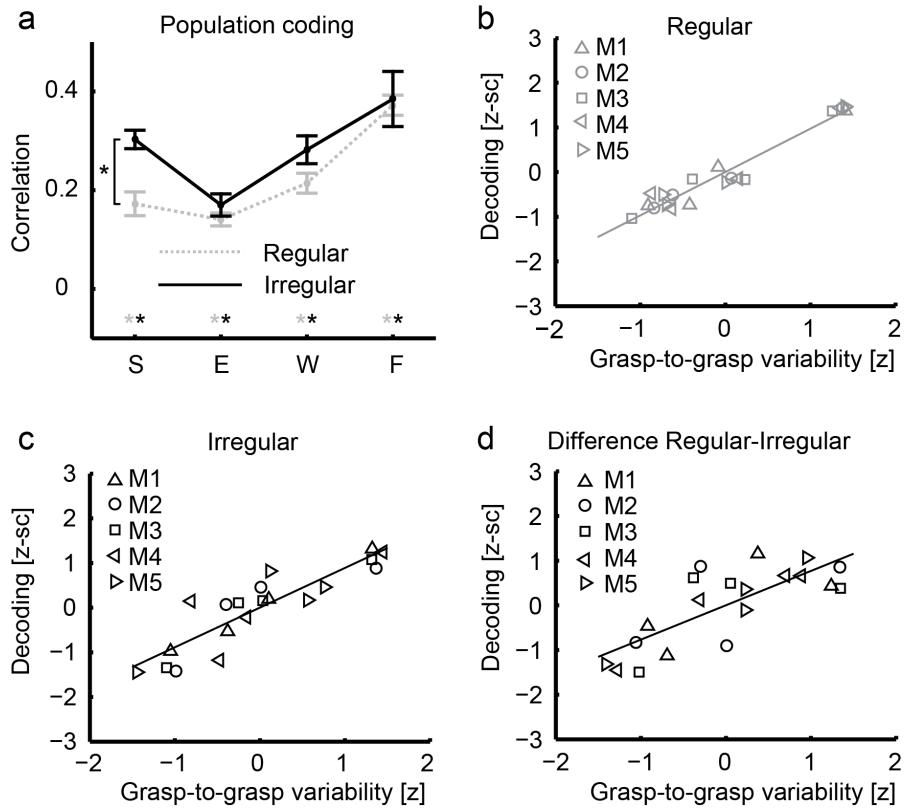


**Figure 21: Encoding of forelimb variables and its relationship with grasp-to-grasp variability**
**a**, Prediction of forelimb joint angles from neural network activity in the regular and irregular condition, averaged across all five animals; grey and black asterisks at the bottom indicate significant encoding of the joint angle on the regular and irregular condition, respectively. **b**, Grasp-to-grasp variability of forelimb joints versus their respective encoding in M1 L2/3 in the regular condition; each symbol represents values for the four joints in one animal. **c,** same conventions as in b, but for the irregular pattern. **d**, Differences in encoding of individual joint angles versus differences in their grasp-to-grasp variability from the regular to the irregular condition.

Regarding all movements, we also asked how the encoding accuracy increased as a function of the number of neurons. Starting with the best single cell predictor, we added neurons with decreasing prediction strength and calculated the encoding for the increasing population size until all cells have been incorporated. On average, saturating decoding performance was achieved after approximately 20% of the best single cell predictors have been included in the population coding (Fig. 23). These findings suggest that about 10 neurons in each imaged motor cortex area contain approximately as much information about a specific joint angle as all cells in the imaged region.

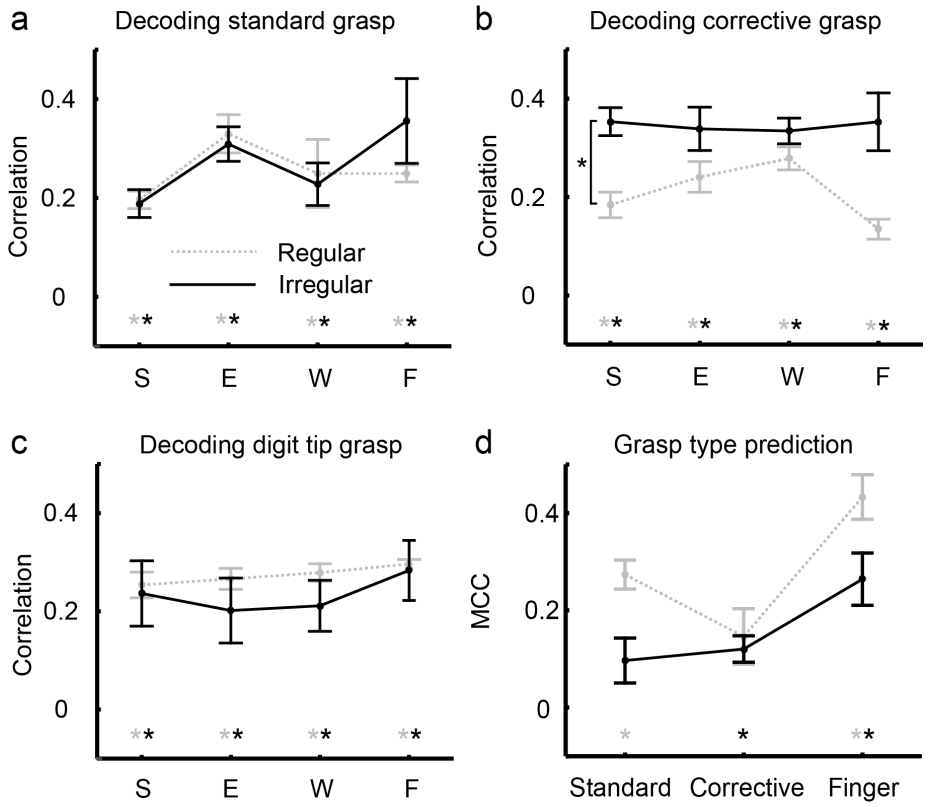


**Figure 22: Encoding with regard to different grasp types**
**a**, Prediction of forelimb joint angles from neural network activity during standard grasps, for the regular (dotted grey) and irregular condition (continuous black), averaged across all five animals; same conventions as in Figure 21a. **b**, same conventions as in a, but for corrective grasps. **c,** same conventions as is a, but for digit tip grasps. **d**, Prediction of grasp types from simultaneous states of neural network activity, quantified by calculating the Matthew's correlation coefficient (MCC) between real and predicted grasp types; same conventions as in a-c.

### 4.6 Population coding of joint angles during equivalent movement subsets depends on the behavioural context

We next asked if the encoding differences across conditions are preserved if only equivalent movements on the regular and irregular pattern are compared. Based on the sample-point-wise Euclidean distance in the 4-dimensional joint angle space (Fig. 14b), we compiled the most similar grasp pairs across conditions, separately for the standard, corrective and digit tip grasp cluster (Fig. 24a). For the regular and irregular condition, this analysis (see methods) generated a "twin" standard, corrective and digit tip grasp cluster each of which differed minimally across conditions (Fig. 24b, c). The encoding of the shoulder angle still increased for the irregular condition, when grasps from the "twin" standard, corrective and digit tip clusters were pooled in each condition (Fig. 24d).

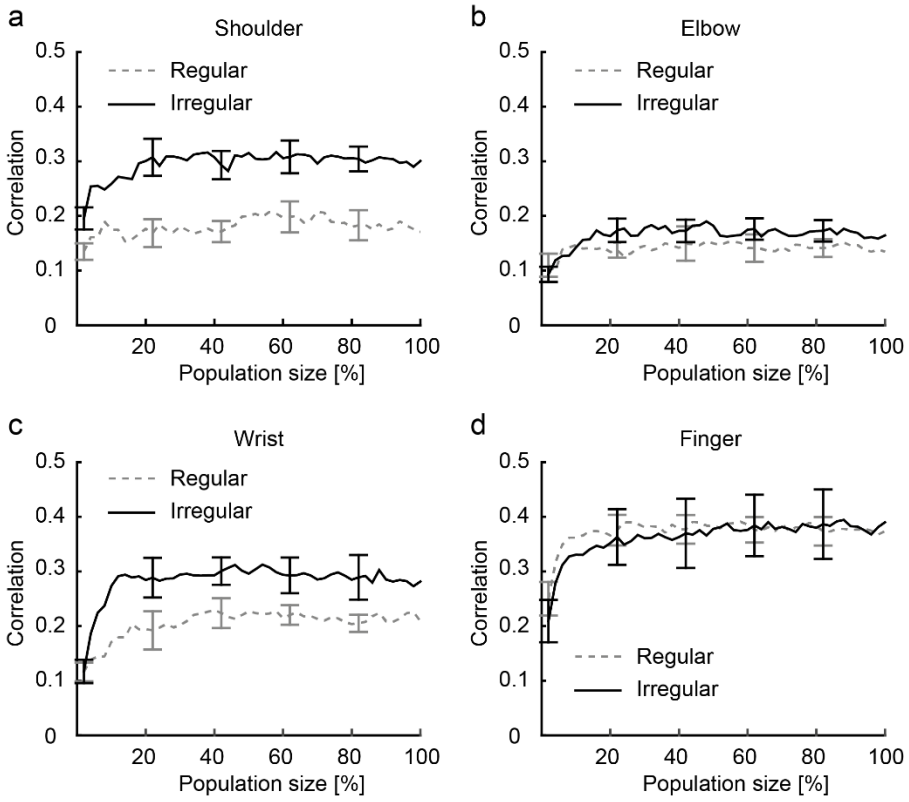


**Figure 23: Decoding accuracy of forelimb joint angles as a function of population size**
**a,** Decoding of the shoulder joint angle as a function of population size, pooled across animals; for each mouse, cells with decreasing prediction strength have been added to the population coding, starting with best single cell predictor; dashed grey curves = data for the regular condition; continuous black curves = data for the irregular condition. **b, c, d,** Data for elbow, wrist and finger joints, respectively, same conventions as in a.

For this pooled twin movements, the condition-related differences in the encoding of individual joints still correlated with differences of their grasp-to-grasp variability from the regular to the irregular condition (Fig. 24e). Additionally, the encoding of the shoulder angle remained strengthened for the irregular condition, when only grasps from the twin corrective pools were considered (Fig. 24d). Likewise, corrective grasps could be significantly predicted by neuronal networks only on the irregular pattern, digit tip grasps only on the regular pattern (Fig. 24f). Thus, all encoding differences between the regular and irregular condition are preserved when only subsets of grasps are considered that are equivalent for the regular and irregular condition with regard to their kinematic features.

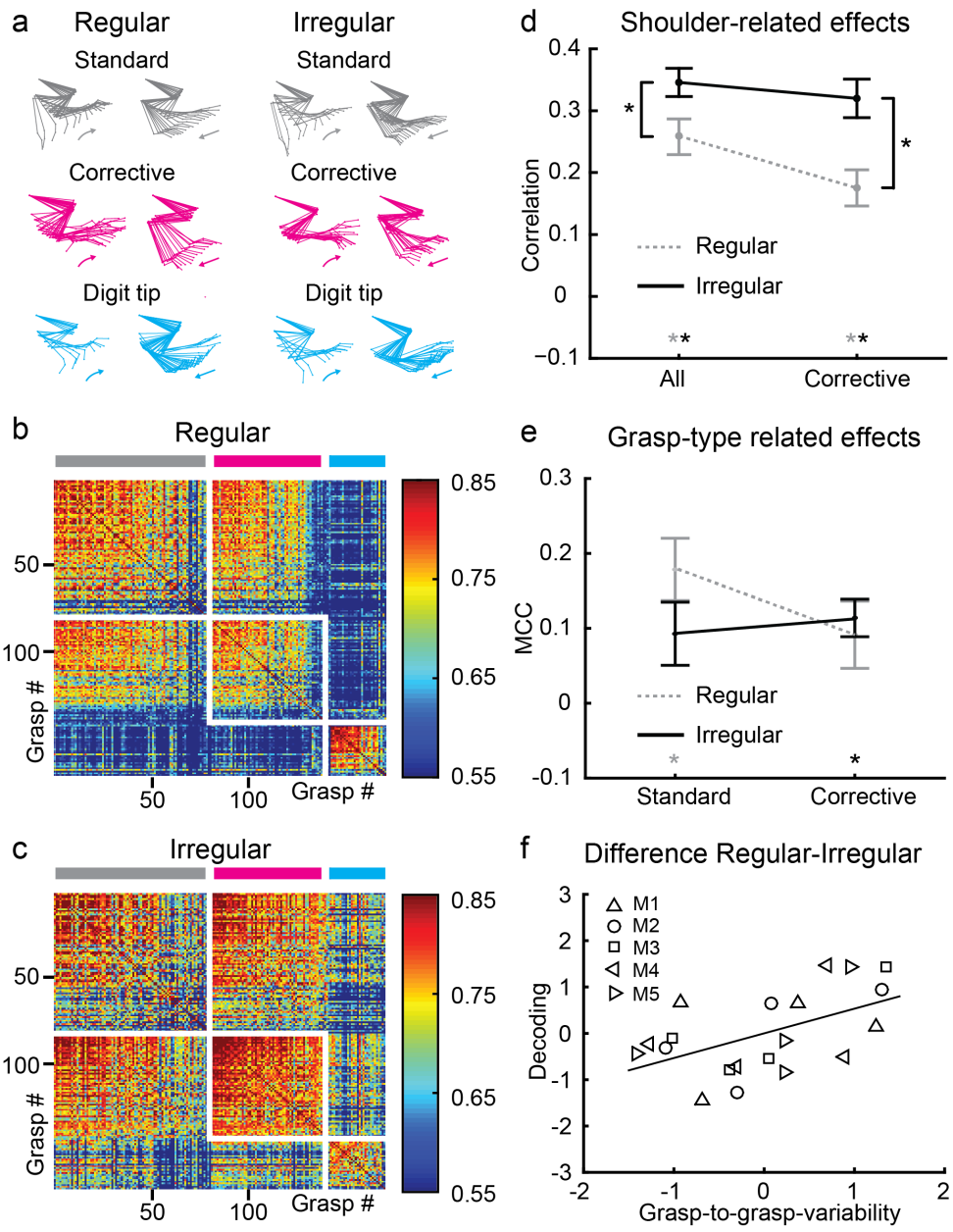


**Figure 24: Encoding of forelimb variables and grasp types for pools of "twin" grasps**
**a,** Representative examples of "twin" grasp pairs in the regular and irregular condition; **b, c,** Similarity matrices for the regular and irregular condition after the twin-movement pruning for the same example animal as in Fig. 14: For each movement (discrete grasping action) on the regular condition, an quasi-equivalent "twin"-movement on the irregular condition exists, that belongs to the same grasp type and additionally features minimal differences in the sample-point wise Euclidean distance calculated for the 4-dimensional joint angle space. **d**, Averaged across animals, prediction of forelimb joint angles in the regular (dotted grey) and irregular condition (continuous black) when grasps from each twin grasp cluster are pooled per condition (left) and when only the corrective twin cluster is regarded (right); same conventions as in Fig 22. **e**, Differences in the encoding of individual joint angles when grasps from each twin grasp cluster are pooled per condition versus differences in their total grasp-to-grasp variability from the regular to the irregular condition; **f**, Prediction of grasp types from simultaneous states of neural network activity, when only twin corrective and twin digit tip grasps are considered; chance level (33%) is indicated by the dashed line.

Given the similarity of the twin movement pools and that the dataset of the regular and irregular condition was significantly reduced by this analysis, the stability of the encoding effects across conditions suggests that the behavioural context of the irregular condition generated at least in part the increased encoding of shoulder angle and corrective grasp.

In other words, joint angles during the same movements are differently encoded in M1 L2/3 depending on the behavioural context they are embedded in. During a learned movement sequence, the required grasp-to-grasp variability of individual joint angles thereby represents a contextual signature that modifies their encoding during equivalent discrete grasping actions.

## 5. Discussion

**"Nothing in biology makes sense except in the light of evolution"**
***Theodosius Dobzhansky***

Moving is a universal function possessed by all brains. While simple organisms were endowed only with basic circuitry for movement control, multiple, parallel circuits were superimposed on the existing wiring during the course of evolution (Buzsáki, 2006). The phylogenetically oldest circuits of mammalian brains are thereby located at the bottom and the most recent structures are situated on top (Sur and Leamey, 2001, Kandel, 2013). In mammals, the neocortex rests on top and is the seat of our highest sensory, motor and cognitive abilities (Sur and Leamey, 2001). That the motor cortex controls only selective, sophisticated aspects of movement control would therefore be a logical consequence of this architectural framework. And indeed, the pronounced disagreement regarding the rules according to which movement variables are encoded in the mammalian motor cortex (Georgopoulos et al., 1986, Georgopoulos et al., 1992, Scott and Kalaska, 1995, Kakei et al., 1999, Aflalo and Graziano, 2006, Graziano, 2006, Reimer and Hatsopoulos, 2009, Vargas-Irwin et al., 2010, Shenoy et al., 2013) led inter alia to the optimal feedback control theory, according to which M1 selectively controls the relevant kinematic variables of different movements (Todorov and Jordan, 2002, Scott, 2004, Graziano, 2006, Scott, 2012). For instance, during hitting a nail with a hammer into a wall of particular resistibility, the final position of the hammer head and the hitting strength are of fundamental importance and might therefore be the targeted variables to be controlled in the motor cortex. However, the relevance of a movement variable may be not only defined by the ongoing discrete motor action itself, but also by its embedding in the context of a movement sequence. Let us consider two walls, one consisting of a hard and a soft layer and the second consisting of two soft layers. Let's further assume that for both walls, the fifth hit is consciously performed in the soft layer and with the same kinematic features, but was preceded by four strong hits with extensive trajectories in the first case and four weak hits with small trajectories in the second. Will the control scheme of the motor cortex control the fifth hit equally in both situations or will the different context play a role? Our results indeed suggest that the motor cortex

incorporates contextual variables to encode joint angles during discrete motor actions of a learned movement sequence. Our findings further demonstrate that during the entire movement sequence, the non-repetitive components of joint motion are selectively represented in neuronal networks of the motor cortex while repetitive components are comparably neglected. Purposeful incorporation of contextual features and selective orchestration of varying joint components during movement sequences demand elaborate processing schemes and would be consistent with the notion that the motor cortex is a phylogenetically sophisticated circuitry.

### 5.1 Neuronal tuning during simplified movement sets and natural behavior

Using restricted, simplified movement sets such as a set of reach directions or isometric force on a lever in different directions, different researchers suggested neuronal tuning in M1 to particular kinematic variables. From these experiments, neuronal activity has been inter alia proposed to be related to direction, force, speed, curvature of hand path, joint angle, distance and muscle activity, among others (Cheney et al., 1985, Georgopoulos et al., 1986, Caminiti et al., 1990, Hocherman and Wise, 1991, Georgopoulos et al., 1992, Fu et al., 1993, Ashe and Georgopoulos, 1994, Scott and Kalaska, 1995, Kakei et al., 1999, Li et al., 2001, Reina et al., 2001, Holdefer and Miller, 2002, Sergio and Kalaska, 2003). In contrast, the representation of these variables was minor during naturalistic movements, in which the relevance of single kinematic variables such as the movement direction is less emphasized than for example in the stereotypical center-out reaching task (Aflalo and Graziano, 2006). Even though neurons showed partial tuning to individual joint angles of preferred arm-postures, much of the neuronal variance remained unexplained and hidden or unknown variables must have been at play (Aflalo and Graziano, 2006, Graziano, 2009). In this regard, an intriguing possibility would be that contextual features such as the grasp-to-grasp variability of individual joint angles during the naturalistic motor sequences affected the encoding scheme of the motor cortex.

Another study in which monkeys were engaged in naturalistic motor behaviour suggested that single neurons frequently encode a broad spectrum of combinations between proximal and

distal joint angles (Vargas-Irwin et al., 2010). These results are consistent with our observation, that individual neurons in the motor cortex simultaneously predict several forelimb joint angles, but usually to different degrees.

### 5.2 Grasp-to-grasp variability of individual joint motion as contextual signature

The increased grasp-to-grasp variability of shoulder motion on the irregular pattern accounts for its elevated encoding in M1 while the high grasp-to-grasp variability of finger motion during digit tip grasps explains its pronounced representation in both conditions. In learned movement sequences, neuronal ensembles in M1 L2/3 thus preferentially encode motion of joints that require frequent amplitude variation from one grasp to the next. On the other hand, if movement amplitudes in specific joints are simply repeated from preceding motor actions, their representation in M1 L2/3 seems downregulated. Moreover, the different grasp-to-grasp variability of individual joints in the regular or irregular movement sequence even accounts for encoding differences during grasp pools that feature quasi-equivalent kinematics across conditions. This different, context-dependent encoding of joint angles during even equivalent movements further suggests that the control scheme of M1 operates beyond the kinematic features of the ongoing, discrete motor action in a sequence. Rather, neuronal networks in M1 L2/3 seem to adapt the encoding of motion in individual joints by incorporating their grasp-to-grasp variability in a learned movement sequence as contextual signature. As mentioned above, the optimal feedback control theory posits that M1 controls only selective task-relevant parameters instead of predefined movement variables (Todorov and Jordan, 2002, Scott, 2004, 2012). Since our findings highlight particularly the importance of the movement sequence context in defining the relevance of a variable during an ongoing, discrete motor action, we suggest that grasp-to-grasp variability of a variable quantifies its contextual relevance. Such a conception of contextual relevance might also provide an explanation for the generally decreased M1 encoding observed during naturalistic motor behavior (Aflalo and Graziano, 2006). Naturalistic motor tasks frequently feature sets of repetitive movements in which low grasp-to-grasp variability of relevant variables would account for their diminished

control in M1 (for instance, a monkey using iterative hand movements to repetitively turn a tool or fruit around for inspection). In contrast, embedding of trials in resting periods during restricted movement sets precludes reduction of grasp-to-grasp variability by a directly preceding movement and would thereby lead to higher encoding of task-relevant variables in M1.

### 5.3 Encoding in M1 L2/3 with regard to different grasp types

Our results also demonstrate distinct encoding in M1 L2/3 with regard to different grasp types. While the high population coding of the shoulder joint angle originated mainly from corrective grasps, the pronounced encoding of finger joint angles was associated with digit tip grasps. Compared to standard grasps, corrective and digit tip grasps are rather associated with impending slips, possibly leading to a situation-dependent upregulation of the encoding for relevant joints. During corrective grasps, the prevention of an impending fall is linked primarily with shoulder control which is used to adapt the reaching distance. During digit tip grasps on the other hand, the avoidance of a slip with a subsequent fall is primarily reliant on precise finger control. Increased encoding of shoulder during corrective grasps and high encoding of finger joints during digit tip grasps is therefore in line with the optimal control hypothesis (Todorov and Jordan, 2002, Scott, 2012). We could also directly predict corrective grasps for the irregular pattern and digit tip grasps for the regular pattern. These results are consistent with a recent electrophysiological monkey study in which a variety of grasp types was decoded based on neuronal activity in the motor cortex (Schaffelhofer et al., 2015).

### 5.4 Does M1 L2/3 function to purposefully integrate contextual, motor and somatosensory features into the motor command?

The SMC has been associated with motor plan updating before the execution of new movement sequences (Shima et al., 1996), fading out of irrelevant motor features (Nachev et al., 2008) and linking context information to motor processing (Fuster, 1989, Passingham, 1993, Tanji and Shima, 1994, Nachev et al., 2008). The SMC might therefore also store contextual signatures such as the required grasp-to-grasp variability of joint angles during a

learned movement sequence and modify circuitries in M1 accordingly when the respective sequence needs to be executed. This modification could be the activation of selective circuits in M1 that are wired to control shoulder motion when a specific movement sequence demands extensive recalibration of the shoulder amplitude from grasp-to-grasp. Such a function of the SMC has been betokened in the scheme of Fig. 1. M1 L2/3 receives input from the SMC as well as from the somatosensory cortex (S1) via cortico-cortical connections (Kaneko et al., 1994, Nachev et al., 2008, Mao et al., 2011, Kandel, 2013) while sending excitatory projections to output layer 5 (Weiler et al., 2008, Anderson et al., 2010). M1 L2/3 is therefore ideally situated to coordinate sensory, motor and contextual information streams for their purposeful integration into the motor command. That many conclusions about the higher-order functions of the SMC come from studies in primates or humans, adds a caveat to this interpretation. However, recent studies in mice suggest, that the murine M2 subserves functions that are similar to those of the primate SMC, particularly with regard to movement sequences (Yin, 2009, Gremel and Costa, 2013).

### 5.5 Conclusion

Overall, our results suggest that neuronal networks in M1 L2/3 learn which joint angles need to be varied in a given context and selectively reinforce their representation. This conception assumes that M1, a phylogenetically sophisticated structure of the motor system, is specialized to organize the more complex non-repetitive joint components in a movement sequence while repetitive joint components are comparably neglected and possibly left over for lower-level structures. Since motor cortex neurons are thought to integrate the recruitment of spinal muscle synergies with currently required CPGs (Drew and Marigold, 2015), the organization of repetitive movements in the respective joints might be delegated to CPGs in the spinal cord. Moreover, our findings indicate that the encoding of joint motion during discrete motor actions within a sequence is not only determined by their kinematic features, but also by the required grasp-to-grasp variability of joint amplitudes during the entire learned movement sequence.

However, it is fair to say that following the twin-movement analysis, the correlation between condition-related differences in grasp-to-grasp variability and condition-related differences in the population coding was not extremely high, albeit statistically significant. This means a major part of the population coding differences between equivalent movements on the regular and irregular pattern cannot be explained by differences in joint angle grasp-to-grasp variability. One explanation is that this relationship is actually more pronounced by was blurred by minor kinematic differences between the regular and irregular twin movement pool. However, I deem another explanation more probable. Apart from the grasp-to-grasp variability of joint angles, there is a variety of contextual signatures that characterize a specific movement sequence. For instance, grasp-to-grasp variability of movement speed, acceleration or trajectories and many other context-characterizing features presumably affect the encoding of variables in M1. Even though grasp-to-grasp variability of joint angle amplitudes was a salient feature to define a systematic difference between the regular and irregular condition, other contextual features must have been at play. In different behavioral tasks, other contextual features might be even much more appropriate to characterize systematic differences that are related to movement sequences as a whole. Anyway, the consideration of contextual signatures to account for the encoding scheme of the motor cortex incorporates the big picture and might therefore provide new insights into the operational principles of M1.

Finally, our study also provides a new conceptual framework to investigate the cortical pathophysiology of motor cortex stroke and Parkinsonism (Redgrave et al., 2010) since rodents modelling these diseases exhibit forelimb deficits on the irregular ladder (Metz and Whishaw, 2002) that are related to our findings: While the impaired forelimb placement on irregular rungs may result from the lost ability of M1 to efficiently process information of the shoulder joints, the lacking encoding of finger motion during finger grasps likely contributes to the increased number of slips. The next and final chapter will elucidate the applicability of our results with regard to Parkinson's disease and motor cortex stroke in detail.

# 6. Outlook

**“Imagination is more important than knowledge”**
***Albert Einstein***

## 6.1 Applicability of our results for the investigation of Parkinson’s disease

In behavior studies, rodents modelling Parkinsonism exhibit motor deficits on the rung ladder test that can be associated with hypokinesia, bradykinesia, impaired postural control and decreased dexterity (Metz and Whishaw, 2002). Since our experimental paradigm makes the rung ladder test compatible with simultaneous calcium imaging in M1 and recording of forelimb variables, these deficitis can be related to the simultaneous activity of neuronal networks in the motor cortex. The combination of calcium imaging and genetic labelling techniques thereby provides unique possibilities to dissect aberrant activity of different circuitries within the cortex-basal ganglia or cortex-spinal cord loop. On the one hand, plenty of evidence suggests that Parkinson’s disease entails impaired processing in M1 (Marsden et al., 2001, Williams et al., 2002, Fogelson et al., 2006, Lalo et al., 2008, Eusebio et al., 2009), on the other hand the well-known Parkinsonian symptom akinesia (Hufschmidt and Lücking, 2006) argues for an impaired ability to appropriately drive relevant muscle groups, be it during isolated motor actions or in a movement sequence. Therefore it would be of particular interest to observe how the relationship between population coding and grasp-to-grasp variability in limb joints evolves after the induction of Parkinsonism.

In a set of preliminary experiments, we employed one of the most widely used Parkinson models in mice, the stereotactic injection of 6-hydroxydopamine (6-OHDA) into the substantia nigra (Grealish et al., 2010, Francardo et al., 2011, Heuer et al., 2012) We showed, that the stereotactic injection of 6-OHDA can easily bypass an already implanted chronic glass window over M1 and leads to bradykinesia in shoulder, elbow, wrist and finger base joints (Brändli, 2014). Thus, we can apply our experimental paradigm to perform calcium imaging in the same neuronal networks of M1 before and after Parkinsonism is induced in the respective mouse.

### 6.1.1 Current and potential future approaches to treat Parkinson's disease

Currently, none of the available anti-parkinsonian therapies, alone or combined with other interventions, offers a satisfying therapeutic strategy. During the course of the disease the beneficial effects of pharmacological medications decrease while adverse effects such as drug-induced dyskinesias rise (Rascol et al., 2003). Deep brain stimulation (DBS) is a surgical alternative for advanced Parkinson's disease and acts through stimulation of subcortical structures via implanted electrodes. However, this approach does not account for the complexity of neural network organization and unfolds its predominant effect by jamming the neuronal message transmitted through the whole stimulated structure (Benabid et al., 2009). As a consequence the motor symptoms are only eliminated incompletely while the invasive stimulation additionally entails adverse effects such as hemorrhage, infection, paresthesias and others (Benabid et al., 2009, Lyons, 2011). In future, the novel and powerful optogenetic stimulation might provide a more effective improvement of Parkinsonian motor symptoms. Since this approach allows light-controlled activation or silencing of selective genetically modified neuron subtypes or projection systems from the millisecond to minute timescale, the activity of neuronal networks can be modulated far more specifically than with electrical stimulation methods (Nagel et al., 2003, Zhang et al., 2007b, Gradinaru et al., 2008, Cardin et al., 2009, Fenno et al., 2011, Yizhar et al., 2011, Tye and Deisseroth, 2012, Berndt et al., 2014). So far, some studies applied optogenetic stimulation in Parkinsonian rodents and improved the motor symptoms (Gradinaru et al., 2009, Kravitz et al., 2010). However these studies did not account for the complex organization within neural networks, they rather stimulated coarsely a certain group of projection neurons to influence motor behavior. To capitalize the potential of the diverse optogenetic options to the greatest extent a detailed knowledge about the disorganization of neural networks in Parkinson's disease is indispensable. Only the latest *in vivo* two-photon calcium imaging tools, combined with genetic labeling techniques, are able to characterize dysfunctions in selective neural networks in detail and thus hold the potential to guide specific, complex and highly effective optogenetic modulations. Without major destruction of brain tissue that would be problematic particularly

in awake behaving mice, only cortical areas are accessible for two-photon calcium imaging. One pivotal cortical entity to investigate the pathophysiology in the cortex-basal ganglia loops is M1.

### 6.1.2 Rationale to decipher and modulate motor cortex networks in reference to the basal ganglia loop

Both molecular and neurophysiological evidence suggests that the dopamine depletion in Parkinsonism distorts the equilibrium within the basal ganglia loop as well as the neuronal activity in cortical motor areas (Obeso et al., 2008). The modern conception of Parkinsonian pathophysiology is based on the conception that cortex-basal-ganglia circuits (Fig. 25) can be divided in spatially segregated loops which control goal-directed and habitual movements, respectively (Fig. 26). While the habitual system is preferentially engaged in the control of predictable, learned motor tasks, the goal-directed system orchestrates unpredictable, skilled movements. Under physiological conditions, both loops converge inter alia in the motor cortex and act in concert to perform the motor task at hand most efficiently (Redgrave et al., 2010). In the Parkinsonian state, the basal ganglia malfunction especially in the loop controlling habitual, automatic movements which sends “noisy”, distorted signals to the thalamocortical projections. At the level of the motor cortex, these distorting signals cause increased inhibition and abnormal oscillations and thereby impede the processing and expression of goal-directed actions (Redgrave et al., 2010). Whenever this noisy output of the basal ganglia is reduced, for instance by blocking the hyperactive nucleus subthalamicus with deep brain stimulation, patients can rely more efficiently on the goal-directed mode of action to compensate for the impaired habitual control system. There are observable manifestations of the distorted basal ganglia output in the motor cortex: Human Parkinsonian patients exhibit pronounced synchronized oscillations at around 20Hz between nucleus subthalamicus and cortex (Marsden et al., 2001, Williams et al., 2002, Fogelson et al., 2006, Lalo et al., 2008) which probably reflect rampant resonance in the basal ganglia-cortical network due to the decreased dopaminergic input (Eusebio et al., 2009).

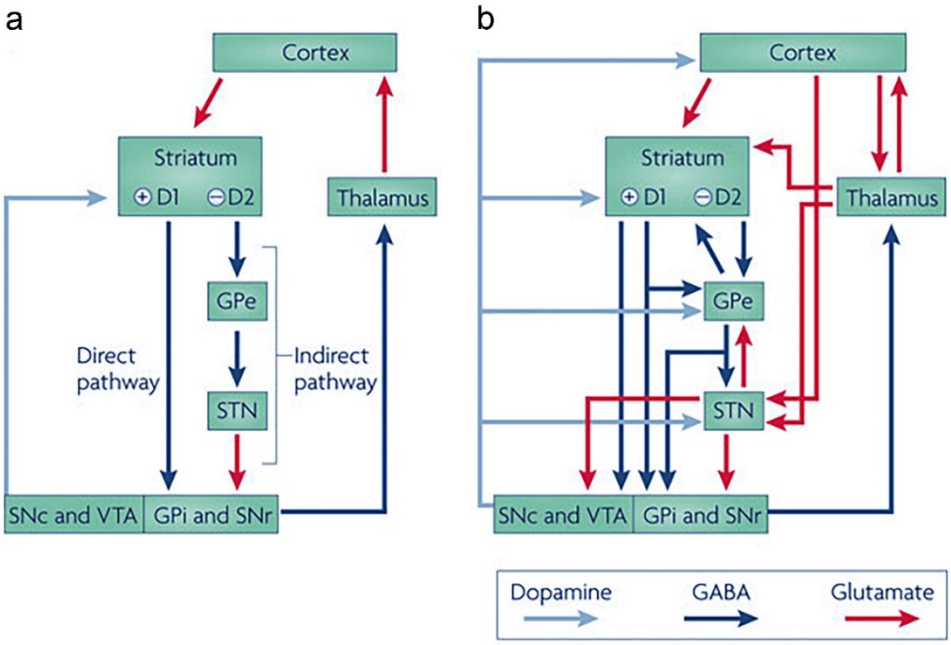


**Figure 25: Classic and modern conception of connectivity within the cortex-basal-ganglia loop** **a:** First functional model of the basal ganglia architecture: Excitatory input from motor cortical L5 cells activates the striatum. The "direct pathway" then conveys the activity of striatal neurons that express D1 receptors monosynaptically to the output nucleus globus pallidus internus (GPi). The "indirect pathway" connects striatal neurons expressing D2 receptors via relays in the globus pallidus externus and the nucleus subthalamicus to the GPi. Dopaminergic input from the substantia nigra, in turn, excites the direct pathway through D1-receptors and inhibits the indirect pathway through D2-receptors. Output from GPi neurons keeps targeted structures in the thalamus and brainstem under tonic inhibitory control (Redgrave et al., 2010). The thalamus sends fibers (inter alia) to L3 (Strick and Sterling, 1974, Shinoda and Kakei, 1989) of the motor cortex, thereby closing the basal ganglia loop. According to this model, activation of the "direct pathway" would inhibit the GPi neurons and thereby facilitate movement while activation of the "indirect pathway" at the level of the striatum would promote movement inhibition or arrest. In the Parkinsonian state, reduced dopamine input from the substantia nigra results in decreased activation of the direct pathway and reduced inhibition of the indirect pathway, resulting in excessive activation of inhibitory basal ganglia output to the thalamus. The thalamus in turn features decreased activation of M1. **b:** Recent anatomical investigations suggest a more complex connectivity and organization of the cortex-basal-ganglia loops. Adapted from Redgrave et al. (2010).

Despite these indications for aberrant activity in the Parkinsonian motor cortex the nature of this distortion is unknown at the level of local neuronal networks. The change in oscillation patterns and molecular evidence argues for aberrant activity in inter alia parvalbumin-positive interneurons which are pivotal for the generation of fast rhythms (Capper-Loup et al., 2005, Sohal et al., 2009).

### 6.1.3 Concrete experiments for the investigation of Parkinson's disease

Using our experimental paradigm, the investigation of the following three motor cortex circuitries would be of particular interest under conditions modelling Parkinson's disease: First, parvalbumin-expressing interneurons in L2/3 and L5, secondly L5 neurons projecting to the striatum and thirdly L5 neurons projecting to the subthalamic nucleus. The last two systems represent the principal motor cortex projections to the basal ganglia though which the equilibrium and processing in the basal ganglia loop can be influenced (Fig. 25b).

Before calcium imaging the three neuronal systems can be marked using viral labelling techniques. Calcium imaging can then be performed in M1 L2/3 and L5 networks while mice move across regularly or irregularly spaced rungs on a ladder wheel and multiple forelimb variables are recorded (Fig. 27a, b). While the predictable regular rung arrangement is presumably organized predominantly by habitual control systems, the unpredicable irregular pattern should demand a higher degree of goal-directed control. Since skilled locomotion on ladder rungs is known to reveal motor deficits in rodents modelling Parkinson's disease, imaging sessions of the same neuronal networks in M1 would occur before and after the induction of Parkinsonism.

The aim of these experiments could be to observe how the encoding of forelimb variables is modified by the disease state with regard to habitual and goal-directed control. In particular, our finding that neuronal networks in M1 encode joint angles according to their grasp-to-grasp variability in a movement sequence might also reflect the interplay between habitual and goal-directed control. Joint angles with high and unpredictable grasp-to-grasp variability should demand higher control of the goal-directed system while repetitive components are likely to be predominantly processed by the habitual system. For these reasons, the evolution of the relationship between population coding and grasp-to-grasp variability after the induction of Parkinsonism might provide useful insight into the cortical pathophysiology of the disease.

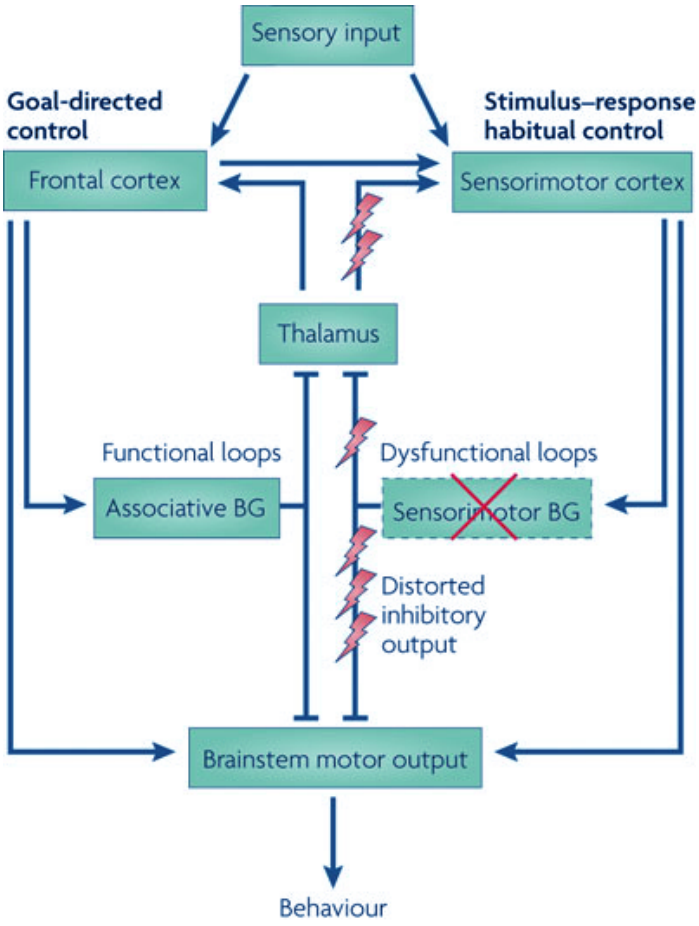


**Figure 26: Modern conception of the pathophysiology in the cortex-basal-ganglia loop during Parkinsonism**
Goal-directed and habitual control systems can be viewed as parallel-projecting, segregated loops in the cortex-basal-ganglia circuit. Goal-directed and habitual territories represented at the cortical level are maintained throughout the basal ganglia nuclei and thalamic relays. Goal-directed control emerges from associative networks though the basal ganglia, while stimulus-response habitual control relies on sensorimotor territories. Both networks independently direct behavioral output when they converge in the sensorimotor cortex. In Parkinson's disease, loss of dopamine innervation from sensorimotor territories in the basal ganglia (indicated by the red cross) entails distorted output signals from the basal ganglia (indicated by lightning symbols), which propagate via the thalamus to the motor cortex. Loss of habitual control circuits leads to increased reliance on goal-directed control whose execution is, in turn, compromised by the distorted activity in the motor cortex. Adapted from Redgrave et al. (2010).

Especially because typical Parkinsonian deficits such as akinesia argue for an impaired ability to drive relevant muscle groups in a movement sequence we would expect that Parkinsonism entails a destructed or at least modified relationship between coding of joint movements and their grasp-to-grasp variability. Depending on the observed encoding dynamics during Parkinsonism optogenetic stimulation can then be applied to selective neuronal populations to restore the physiological network activity.

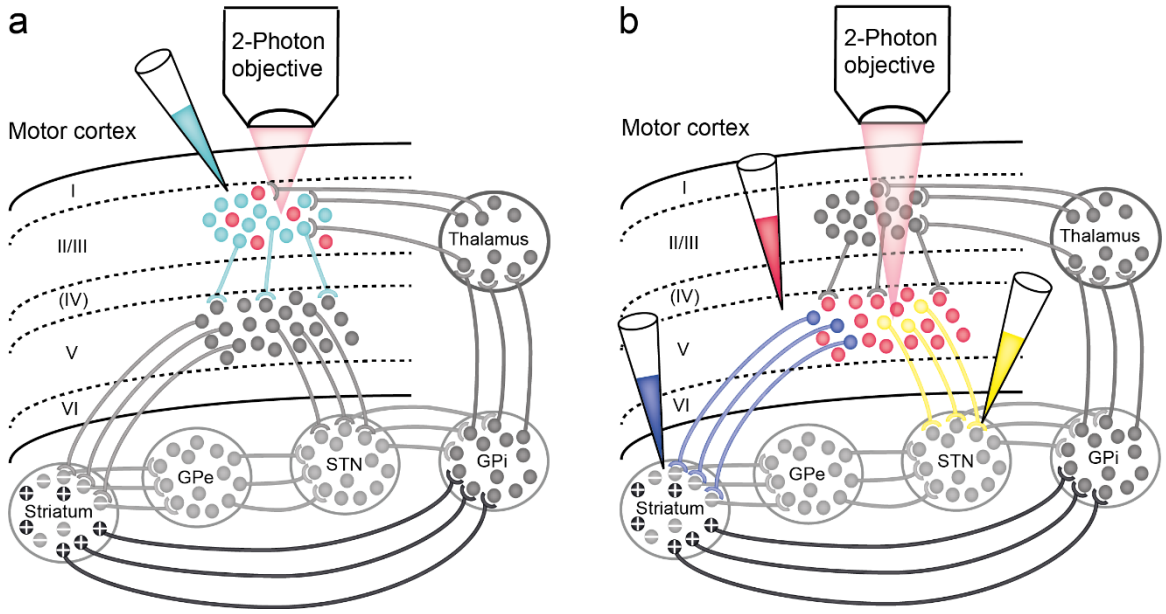


**Figure 27: Dissection of M1 circuitry dysfunction in Parkinsonian mice**
**a:** Imaging of M1 L2/3 networks with labelling of Parvalbumin-positive (PV) interneurons (red) in PV-Cre mouse lines; red labelling can be achieved by injection of a Cre-dependent marker such as td-Tomato **b:** Two-photon calcium imaging of pyramidal L5 neurons in the motor cortex, for instance by using the genetically encoded calcium indicator R-camp. Retrograde tracer injections would additionally allow the differentiation between striatum- and subthalamic nucleus-projecting neurons.

Step function opsins (see also chapter 2), which require a single light pulse to induces a sustained increase or decrease in the firing probability of stimulated neurons (Fenno et al., 2011, Tye and Deisseroth, 2012, Berndt et al., 2014) could for example equilibrate neuronal activity in the cortex-basal-ganglia loop by modifying the excitability of selective circuits. Since the light modulation would occur exclusively at a cortical level, mechanically touching or damaging brain tissue is not necessary and deep brain stimulation's unpleasant adverse effects due to the permanent electrode penetrations drop out (Benabid et al., 2009, Lyons, 2011).

### 6.2 Applicability of our results for the investigation of motor cortex stroke

Similar to rodents modelling Parkinson's disease, rats and mice with a motor cortex stroke show specific forelimb deficits during skilled locomotion on the rung ladder test (Metz and Whishaw, 2002, Farr et al., 2006, Zorner et al., 2010). Particularly on the irregular rung pattern, an increased number of rung misses and slips is typical (Metz and Whishaw, 2002). There is

a potential link between these motor deficits after motor cortex stroke and our results, according to which skilled locomotion on the irregular pattern entails increased encoding of shoulder and finger kinematics in neuronal networks of M1. Since the shoulder joint is most pivotal to adapt the reaching distance correctly, stroke-related loss of M1 circuits controlling the shoulder joint should entail an increased number of rung misses on the irregular pattern. On the other hand, it is conceivable that loss of M1 circuits for the organization of finger movements compromises the ability to prevent a slip during digit tip grasps, which require delicate control of finger angles. Since the rung ladder test for rodents also quantifies the recovery of dexterous forelimb movements after stroke, an intriguing question would be to what extent plasticity in motor cortex networks restores the encoding of shoulder and finger joints in spared cortical areas. With regard to skilled locomotion on ladder rungs, our paradigm is ideally suited to relate the activity of neuronal networks in M1 to forelimb kinematics before and several weeks after motor cortex stroke. Therefore, recording the activity of intact neuronal networks around a stroke while the animals recover their motor functions might provide valuable insights into neurophysiological plasticity mechanisms of the brain. In particular, the combination of calcium imaging with genetic labelling tools could elucidate how remodeling of spared cortical tissue is related to routing signals from intact sensory or motor areas.

### 6.2.1 Principles of cortical plasticity after stroke

Throughout life, our cerebral cortex modulates the efficacy of synaptic contacts to adapt to varying environmental demands (Nudo, 2006). This cortical plasticity also contributes to the limited recovery of function after cortical strokes. During a stroke, the blood supply to a brain area is interrupted and respective neurons are deprived of their physiological metabolic substrates (Fig. 28). While most neurons in the ischemic core will die in consequence of the metabolic deprivation, some neurons usually survive in the penumbra, the area with reduced blood flow surrounding a stroke (Hossmann, 2006, Zhang and Murphy, 2007). Particularly in this peri-infarct cortex, neurons undergo structural and functional plasticity which is in rodents especially pronounced during the first 4 weeks after stroke (Nudo, 2013). In this period, a

combination of homeostatic and Hebbian plasticity has been suggested to be involved in the remodelling of penumbra tissue (Murphy and Corbett, 2009). Homeostatic plasticity is triggered by attenuation of synaptic activity and includes upregulation of presynaptic release and postsynaptic response to neurotransmitters (Turrigiano and Nelson, 2004). Hebbian plasticity occurs during coincident activation of pre- and postsynaptic neuron and strengthens their connection (Hebb, 1949, Stellwagen and Shatz, 2002, Butts et al., 2007). In the first days or weeks after stroke, the loss of input from the perished stroke core tissue reduces physiological synaptic activity in the penumbra (Gao et al., 1999, Bolay et al., 2002, Carmichael et al., 2004, Winship and Murphy, 2008, Brown et al., 2009), thereby inducing homeostatic plasticity. As part of homeostatic processes, a number of growth promoting factors are upregulated in the peri-infarct region, leading to increased spine turnover and synaptogenesis (Carmichael et al., 2001, Carmichael, 2003, Brown et al., 2007, Brown et al., 2009). To prevent the emergence of aberrant connectivity the growth promoting factors are increasingly balanced by growth-inhibiting molecules such as the extracellular matrix factor NOGO (Papadopoulos et al., 2006, Cheatwood et al., 2008). Homeostatic plasticity also induces hyperexcitability of neurons during the first weeks after stroke (Redecker et al., 2002), thereby facilitating subthreshold input and resetting the decreased activity level of peri-infarct neurons (Turrigiano and Nelson, 2004, Murphy and Corbett, 2009). When homeostatic plasticity approached synaptic function to target levels, Hebbian plasticity can more easily occur to support the strengthening of surviving functional circuits (Hebb, 1949, Butts et al., 2007). In the competition for cortical territory, the local environment of the peri-infarct region therefore presumably favors stroke-affected neuronal circuits over healthy adjacent tissue (Murphy and Corbett, 2009).

### 6.2.2 Concrete experiments to analyse cortical plasticity at the level of neuronal networks

Following small strokes in M1, remodelling within the penumbra has been suggested to enable true recovery of motor functions, while reorganisation after large strokes is rather associated with behavioural compensation (Moon et al., 2009). Since the mechanisms of recovery are

poorly understood at the level of neuronal networks in M1, calcium imaging in the penumbra of a small stroke might be a promising approach. Before a stroke, our paradigm could be employed to relate neuronal activity in the M1 forelimb area to forelimb kinematics and neuronal activity in the M1 hindlimb area to hindlimb kinematics.

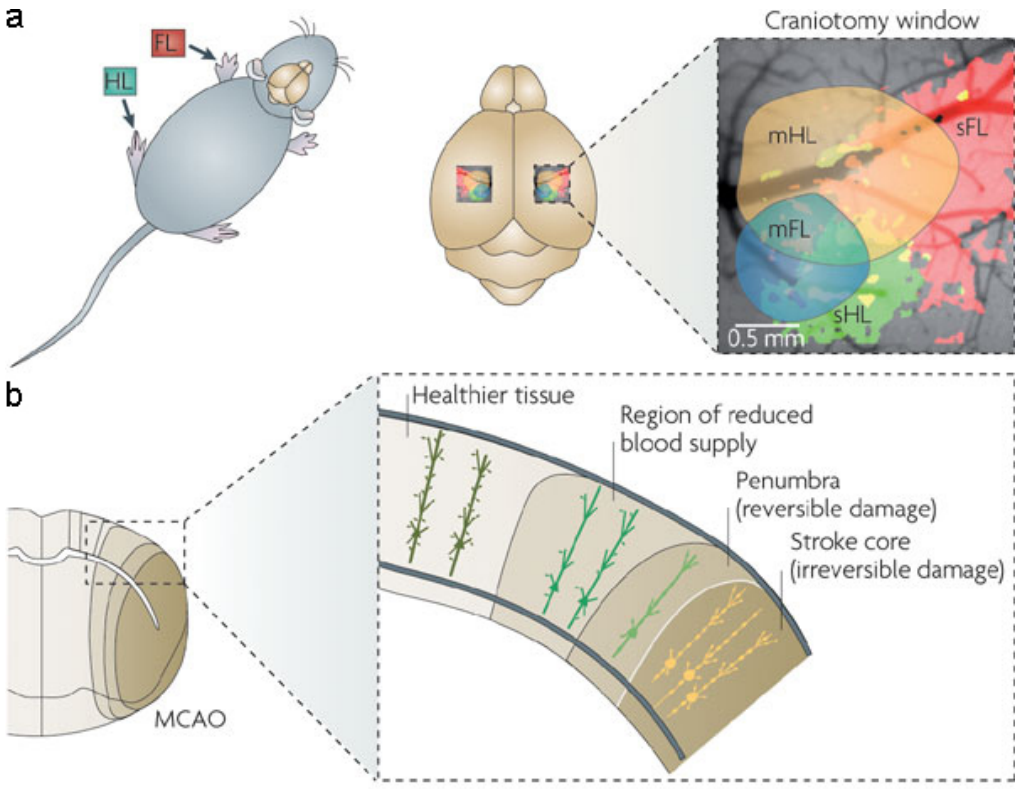


**Figure 28: Stroke-related circuit damage in the sensorimotor cortex**
**a**, Scheme showing the location of the forelimb and hindlimb somatosensory cortex (sFL and sHL, respectively) as well as of the forelimb and hindlimb motor cortex (mFL and mHL, respectively) in the mouse brain. **b**, Cross section through the rodent cortex; occlusion of the middle cerebral artery (MCAO) entails a stroke with a core (darker brown) and a penumbra region (lighter brown); the stroke core features the most pronounced decrease in blood flow, and most neurons and glia in this region will die; in contrast, the partial blood flow in the penumbra allows some cells to survive which then participate in the rewiring of connectivity after stroke. Adapted from Murphy and Corbett (2009).

Then, a small photothrombotic stroke is applied in the M1 forelimb area. During the subsequent weeks, neuronal networks in the penumbra region can be recorded with calcium imaging while the animals are engaged in skilled locomotion and gradually recover their forelimb function. Since a recent study in rodents suggested that neurons in the hindlimb sensory-motor area reorganize to control skilled forelimb movements (Starkey et al., 2012), the penumbra area adjacent to or within the hindlimb area should be targeted. Using our optogenetic mapping

approach and pharmacogenetic silencing in mice with a motor cortex stroke, we already identified respective penumbra regions that are associated with recovery of forelimb function on ladder wheels (Achenbach, 2014). The application of calcium imaging in these regions would then allow to elucidate the following questions:

- How does the population coding of the different forelimb joint angles and hindlimb joint angles evolve in the penumbra region during the recovery phase? Do areas that featured a population coding of hindlimb kinematics before stroke, gradually develop encoding of forelimb kinematics after stroke?
- Do individual neurons, that predicted hindlimb kinematics before stroke, gradually predict forelimb kinematics after stroke?
- Does the relationship between grasp-to-grasp variability and population coding of forelimb joint angles emerge in the penumbra region, and how is this relationship related to recovery of motor function?

More sophisticated questions could be addressed by exploiting the combination of calcium imaging and genetic labelling techniques to dissect the roles of specific cortical projection systems during recovery. For instance, M1 L2/3 neurons projecting to S1 L2/3 and S1 L2/3 neurons projecting to M1 L2/3 can be retrogradely labelled with fluorescent markers. A novel 2-photon microscope that has been developed in the Helmchen lab enables simultaneous imaging of the two labelled projection systems in M1 and S1, if the respective forelimb areas are targeted. Using our paradigm, we are then able to analyse the dynamics of signal transmission between M1 and S1 during the recovery period after stroke. Probing if the brain routes signals from intact forelimb S1 circuits to the penumbra area to shape the emergence of recovery-relevant motor circuits would be interesting in this regard. The next step could involve the application of plasticity-promoting factors such as antibodies against NOGO-proteins (Lindau et al., 2014, Schwab and Strittmatter, 2014, Wahl et al., 2014), and observe their effect on the remodelling of neuronal networks.

In general, identifying links between specific circuit changes and improved behaviour in recovering has been suggested to be one of the most important experimental challenges in the field (Murphy and Corbett, 2009). We believe that our experimental paradigm provides a useful framework to tackle these challenges in future studies.

### 6.3 Concluding remarks: General significance of this study

Coming back to the specific aims of our study (see chapter 1.7), we believe that our study led to the following advances in neuroscience:

- The key finding of our study is that neuronal ensembles in M1 L2/3 encode motion in individual forelimb joints according to contextual relevance. We demonstrated that in a learned movement sequence, the encoding scheme of neuronal networks in M1 does not only refer to the kinematic features of the current discrete grasping action but also incorporates contextual signatures that characterize the whole sequence: The required grasp-to-grasp variability of individual forelimb joints represents such a contextual signature and predicts their encoding in neuronal populations during the whole sequence as well as during discrete grasping actions within the sequence.
- We also demonstrated that the encoding of forelimb angles depends on the type of discrete grasping actions within a sequence. Consistent with the OFC, the representation of motion is strengthened in such joints that are particularly relevant during execution of the respective grasp type. Additionally, grasp types that are associated with an impending hazard such as a fall, feature increased representation in neuronal networks of M1 L2/3 (corrective and digit tip grasps).
- Due to the possibility to combine calcium imaging with genetic labelling of neuronal subtypes or projection systems, we created an experimental framework that allows dissecting the functions of various cortical circuitries with regard to limb movement control. In particular, our experimental paradigm is ideally suited to decode the pathophysiology of cortical circuitries in Parkinson's disease and motor cortex stroke since the moving across rung ladders reveals specific forelimb deficits in rodents modelling these motor disorders (Metz and Whishaw, 2002, Farr et al., 2006).
- Regarding technical advances, we established the combined use of optogenetic stimulation and two-photon calcium imaging in the same animals. The combined application of both techniques enables the identification of specific motor cortex

networks as well as the decoding of their activities without the necessity to mechanically damage the sophisticated neuronal architecture with electrode penetrations.

- We confirmed many results from electrophysiological recordings in monkeys by employing a different technical approach in a different species, namely by investigating the activity of neuronal networks in the mouse motor cortex with calcium imaging. Examples are the complex tuning of individual neurons to several joint angles and the direct prediction of grasp types from neuronal activity.

# 7. Appendix

# CURRICULUM VITAE

NAME: WOLFGANG OMLOR

DATE OF BIRTH: 1983-03-02 IN NEUNKIRCHEN-SAAR, GERMANY

NATIONALITY: GERMAN

## EDUCATION

- 1989-1993: Attendance of the primary school „Maximilian-Kolbe-Schule“ in Neunkirchen
- 1993-1996: Attendance of the grammar school „Johanneum“ in Homburg-Saar
- 1996-2002: Attendance of the grammar school „Goetheschule“ in Essen
- October-December 1999: Attendance of the St. Joseph Highschool in Pine Bluff, Arkansas, U.S.A.
- June 2002: University-entrance diploma
- October 2002 – March 2005: Attendance of medical school at the University of Essen
- April 2005: Research semester to start the experimental medical dissertation “Kortikomuskuläre Kohärenz bei statischen und dynamischen Kräften” at the Neurology Department of the University Clinic of Freiburg
- October 2005 – October 2009: Continuation of medical school at the Eberhard-Karls-University of Tübingen
- August 2007: Elective in neurology at the Mount Sinai Hospital in New York
- August 2008 – July 2009: Practical year at the University Clinic of Tübingen
- October – December 2008: Elective for advanced neurology and elective for pediatric neurology at Harvard Medical School and in the Massachusetts General Hospital in Boston, U.S.A.
- April – May 2009: Elective for surgery at the University of Oxford and in the John Radcliffe Hospital
- November 2009: Final medical exam
- January 2010: Doctoral degree in medicine at the Albert-Ludwigs-University of Freiburg (summa cum laude)

▪ March 2010: Research Assistant in the group of Prof. Helmchen at the Brain Research Institute of Zurich

▪ October 2010: Admission to the MD-PHD-program of the University of Zurich

▪ October 2010: Albrecht-Fleckenstein-Award for the medical dissertation

## AWARDS/SCHOLARSHIPS

▪ 2010: Albrecht-Fleckenstein-Award for the medical dissertation

▪ 2008/09: Scholarships from the German National Academic Foundation to study at Harvard Medical School and at the University of Oxford

▪ 2007-2009: Scholar of the German National Academic Foundation

▪ June 2002: Award for the best university entrance diploma at the Goetheschule in Essen and award from the German physics society for the achievements in the advanced physics course

## HOBBIES

▪ Piano

▪ Athletics

▪ Tennis

## Publication list (peer-review articles)

**Omlor W**, Wahl AS, Lütcke H, Chen I, Sumanovski L, van't Hoff M., Schwab M., Helmchen F. Motor cortex encodes forelimb joint movements according to contextual relevance. *In preparation*

Wahl AS, **Omlor W**, Rubio JC, Chen JL, Zheng H, Schröter A, Gullo M, Weinmann O, Kobayashi K, Helmchen F, Ommer B, Schwab ME. (2014). Neuronal repair. Asynchronous therapy restores motor control by rewiring of the rat corticospinal tract after stroke. Science 344(6189):1250-5.

**Omlor W**, Patino L, Mendez-Balbuena I, Schulte-Mönting J, Kristeva R. (2011). Corticospinal beta-range coherence is highly dependent on the pre-stationary motor state. J Neuroscience 31(22):8037-45.

Chakarov V, Naranjo JR, Schulte-Mönting J, **Omlor W**, Huethe F, Kristeva R. (2009) Beta-range EEG-EMG coherence with isometric compensation for increasing modulated low-level forces. J Neurophysiol. 102(2):1115-20.

Patino L, **Omlor W**, Chakarov V, Hepp-Reymond MC & Kristeva R. (2008). Absence of gamma-range corticomuscular coherence during dynamic force in a deafferented patient. J Neurophysiol. 99(4):1906-16.

Kristeva R, Patino L & **Omlor W**. (2007). Beta-range cortical motor spectral power and corticomuscular coherence as a mechanism for effective corticospinal interaction during steady-state motor output. Neuroimage 36, 785-792.

**Omlor W**, Patino L, Hepp-Reymond MC, Kristeva R. (2007). Gamma-range corticomuscular coherence during dynamic force output. Neuroimage 34(3): 1191-8.

## Acknowledgement

First of all I would like to thank my supervisor Professor Fritjof Helmchen for his great support and for giving me the opportunity to do this project. In particular I would like to thank him for the scientific freedom he granted me.

Additionally I thank Professor Martin Schwab for his helpful advice and for the collaboration with his group. I also would like to thank the third member of my PhD thesis committee, Prof. Giacomo Indiveri, for his inspiring advice.

My sincere thanks go to my collaborator from the Schwab group, Dr. Dr. Anna-Sophia Wahl. Her friendship and scientific support were always an invaluable backup during the entire PHD life. I also want to thank Dr. I-Wen Chen for her constant friendship during the PHD and for her help with regard to the electrophysiological control experiments.

My thanks also go to Dr. Henry Lütcke who supported me in learning Matlab programming and who provided helpful advice in respect of the data analysis. I also thank Balazs Laurenczy for the inspiring discussions regarding Matlab programming.

Moreover, I would like to thank Lazar Sumanovski for his constant support and friendship. I also thank Dr. Marcel van't Hoff, Hans-Jörg Kasper, Martin Wieckhorst, Marco Tedaldi and Stefan Giger for their technical help. My thanks also go to my students, Caroline von Achenbach and Aaron Brändli, who greatly helped in the joint tracking analysis. And many thanks to Dr. Ladan Egolf and Taner Aydinalp for the support regarding various organisational issues.

Last, but not least, my sincere thanks go to my wife, son, parents and siblings, who always provided understanding, love and support during all those years.

## References


Achenbach v (2014) Experimental studies to understand reorganization after stroke in the motor cortex. Masterarbeit.

Aflalo TN, Graziano MS (2006) Partial tuning of motor cortex neurons to final posture in a free-moving paradigm. Proceedings of the National Academy of Sciences of the United States of America 103:2909-2914.

Aflalo TN, Graziano MS (2007) Relationship between unconstrained arm movements and single-neuron firing in the macaque motor cortex. The Journal of neuroscience : the official journal of the Society for Neuroscience 27:2760-2780.

Alaverdashvili M, Whishaw IQ (2008) Motor cortex stroke impairs individual digit movement in skilled reaching by the rat. The European journal of neuroscience 28:311-322.

Alstermark B, Ogawa J (2004) In vivo recordings of bulbospinal excitation in adult mouse forelimb motoneurons. Journal of neurophysiology 92:1958-1962.

Alstermark B, Ogawa J, Isa T (2004) Lack of monosynaptic corticomotoneuronal EPSPs in rats: disynaptic EPSPs mediated via reticulospinal neurons and polysynaptic EPSPs via segmental interneurons. Journal of neurophysiology 91:1832-1839.

Amos A, Armstrong DM, Marple-Horvat DE (1990) Changes in the discharge patterns of motor cortical neurones associated with volitional changes in stepping in the cat. Neuroscience letters 109:107-112.

Anderson CT, Sheets PL, Kiritani T, Shepherd GM (2010) Sublayer-specific microcircuits of corticospinal and corticostriatal neurons in motor cortex. Nature neuroscience 13:739-744.

Arenkiel BR, Peca J, Davison IG, Feliciano C, Deisseroth K, Augustine GJ, Ehlers MD, Feng G (2007) In vivo light-induced activation of neural circuitry in transgenic mice expressing channelrhodopsin-2. Neuron 54:205-218.

Asanuma H (1975) Recent developments in the study of the columnar arrangement of neurons within the motor cortex. Physiological reviews 55:143-156.

Asanuma H, Rosen I (1972) Topographical organization of cortical efferent zones projecting to distal forelimb muscles in the monkey. Experimental brain research 14:243-256.

Asanuma H, Ward JE (1971) Patterns of contraction of distal forelimb muscles produced by intracortical stimulation in cats. Brain research 27:97-109.

Ashe J, Georgopoulos AP (1994) Movement parameters and neural activity in motor cortex and area 5. Cerebral cortex 4:590-600.

Ayling OG, Harrison TC, Boyd JD, Goroshkov A, Murphy TH (2009) Automated light-based mapping of motor cortex by photoactivation of channelrhodopsin-2 transgenic mice. Nature methods 6:219-224.

Baird GS, Zacharias DA, Tsien RY (1999) Circular permutation and receptor insertion within green fluorescent proteins. Proceedings of the National Academy of Sciences of the United States of America 96:11241-11246.

Beaurepaire E, Mertz J (2002) Epifluorescence collection in two-photon microscopy. Applied optics 41:5376-5382.

Beevor C, Horsley V (1890) An experimental investigation into the arrangement of excitable fibres of the internal capsule of the bonnet monkey (Macacus sinicus). Phil Trans R Soc Lond B 49-88.

Beloozerova IN, Sirota MG (1993) The role of the motor cortex in the control of accuracy of locomotor movements in the cat. J Physiol 461:1-25.

Benabid AL, Chabardes S, Mitrofanis J, Pollak P (2009) Deep brain stimulation of the subthalamic nucleus for the treatment of Parkinson's disease. Lancet neurology 8:67-81.

Berndt A, Lee SY, Ramakrishnan C, Deisseroth K (2014) Structure-guided transformation of channelrhodopsin into a light-activated chloride channel. Science 344:420-424.

Bolay H, Gursoy-Ozdemir Y, Sara Y, Onur R, Can A, Dalkara T (2002) Persistent defect in transmitter release and synapsin phosphorylation in cerebral cortex after transient moderate ischemic injury. Stroke; a journal of cerebral circulation 33:1369-1375.

Bortoff GA, Strick PL (1993) Corticospinal terminations in two new-world primates: further evidence that corticomotoneuronal connections provide part of the neural substrate for manual dexterity. The Journal of neuroscience : the official journal of the Society for Neuroscience 13:5105-5118.

Boyden ES, Zhang F, Bamberg E, Nagel G, Deisseroth K (2005) Millisecond-timescale, genetically targeted optical control of neural activity. Nature neuroscience 8:1263-1268.

Boyle MP, Bernard A, Thompson CL, Ng L, Boe A, Mortrud M, Hawrylycz MJ, Jones AR, Hevner RF, Lein ES (2011) Cell-type-specific consequences of Reelin deficiency in the mouse neocortex, hippocampus, and amygdala. The Journal of comparative neurology 519:2061-2089.

Brändli A (2014) Hydroxydopamine mediated Parkinson lesion for chronic calcium imaging of the mouse motor cortex. Semesterarbeit.

Brasted PJ, Wise SP (2004) Comparison of learning-related neuronal activity in the dorsal premotor cortex and striatum. The European journal of neuroscience 19:721-740.

Braun DA, Aertsen A, Wolpert DM, Mehring C (2009) Learning optimal adaptation strategies in unpredictable motor tasks. The Journal of neuroscience : the official journal of the Society for Neuroscience 29:6472-6478.

Breiman L (2001) Random Forests. Machine Learning 45:5-32.

Brinkman C (1981) Lesions in supplementary motor area interfere with a monkey's performance of a bimanual coordination task. Neuroscience letters 27:267-270.

Brown AR, Teskey GC (2014) Motor cortex is functionally organized as a set of spatially distinct representations for complex movements. The Journal of neuroscience : the official journal of the Society for Neuroscience 34:13574-13585.

Brown CE, Aminoltejari K, Erb H, Winship IR, Murphy TH (2009) In vivo voltage-sensitive dye imaging in adult mice reveals that somatosensory maps lost to stroke are replaced over weeks by new structural and functional circuits with prolonged modes of activation within both the peri-infarct zone and distant sites. The Journal of neuroscience : the official journal of the Society for Neuroscience 29:1719-1734.

Brown CE, Li P, Boyd JD, Delaney KR, Murphy TH (2007) Extensive turnover of dendritic spines and vascular remodeling in cortical tissues recovering from stroke. The Journal of neuroscience : the official journal of the Society for Neuroscience 27:4101-4109.

Butts DA, Kanold PO, Shatz CJ (2007) A burst-based "Hebbian" learning rule at retinogeniculate synapses links retinal waves to activity-dependent refinement. PLoS biology 5:e61.

Buzsáki G (2006) Rhythms of the brain. pp 1 online resource (xiv, 448 p.) Oxford: Oxford University Press,.

Cajal R (1888) Estructura de los centros nerviosos de las aves. Rev Trim Histol Norm Pat.

Caminiti R, Johnson PB, Urbano A (1990) Making arm movements within different parts of space: dynamic aspects in the primate motor cortex. The Journal of neuroscience : the official journal of the Society for Neuroscience 10:2039-2058.

Campbell AW (1905) Histological studies on the localisation of cerebral function. Cambridge: University Press.

Capper-Loup C, Burgunder JM, Kaelin-Lang A (2005) Modulation of parvalbumin expression in the motor cortex of parkinsonian rats. Experimental neurology 193:234-237.

Cardin JA, Carlen M, Meletis K, Knoblich U, Zhang F, Deisseroth K, Tsai LH, Moore CI (2009) Driving fast-spiking cells induces gamma rhythm and controls sensory responses. Nature 459:663-667.

Carmichael ST (2003) Gene expression changes after focal stroke, traumatic brain and spinal cord injuries. Current opinion in neurology 16:699-704.

Carmichael ST, Tatsukawa K, Katsman D, Tsuyuguchi N, Kornblum HI (2004) Evolution of diaschisis in a focal stroke model. Stroke; a journal of cerebral circulation 35:758-763.

Carmichael ST, Wei L, Rovainen CM, Woolsey TA (2001) New patterns of intracortical projections after focal cortical stroke. Neurobiology of disease 8:910-922.

Cheatwood JL, Emerick AJ, Schwab ME, Kartje GL (2008) Nogo-A expression after focal ischemic stroke in the adult rat. Stroke; a journal of cerebral circulation 39:2091-2098.

Chen JL, Carta S, Soldado-Magraner J, Schneider BL, Helmchen F (2013) Behaviour-dependent recruitment of long-range projection neurons in somatosensory cortex. Nature 499:336-340.
Chen SX, Kim AN, Peters AJ, Komiyama T (2015) Subtype-specific plasticity of inhibitory circuits in motor cortex during motor learning. Nature neuroscience 18:1109-1115.
Cheney PD, Fetz EE (1985) Comparable patterns of muscle facilitation evoked by individual corticomotoneuronal (CM) cells and by single intracortical microstimuli in primates: evidence for functional groups of CM cells. Journal of neurophysiology 53:786-804.
Cheney PD, Fetz EE, Palmer SS (1985) Patterns of facilitation and suppression of antagonist forelimb muscles from motor cortex sites in the awake monkey. Journal of neurophysiology 53:805-820.
Cheney PD, Griffin DM, Van Acker GM, 3rd (2013) Neural hijacking: action of high-frequency electrical stimulation on cortical circuits. Neuroscientist 19:434-441.
Churchland MM, Cunningham JP, Kaufman MT, Foster JD, Nuyujukian P, Ryu SI, Shenoy KV (2012) Neural population dynamics during reaching. Nature 487:51-56.
Churchland MM, Yu BM, Cunningham JP, Sugrue LP, Cohen MR, Corrado GS, Newsome WT, Clark AM, Hosseini P, Scott BB, Bradley DC, Smith MA, Kohn A, Movshon JA, Armstrong KM, Moore T, Chang SW, Snyder LH, Lisberger SG, Priebe NJ, Finn IM, Ferster D, Ryu SI, Santhanam G, Sahani M, Shenoy KV (2010) Stimulus onset quenches neural variability: a widespread cortical phenomenon. Nature neuroscience 13:369-378.
Churchland MM, Yu BM, Ryu SI, Santhanam G, Shenoy KV (2006) Neural variability in premotor cortex provides a signature of motor preparation. The Journal of neuroscience : the official journal of the Society for Neuroscience 26:3697-3712.
Churchland PS, Sejnowski TJ (1992) The computational brain. Cambridge, Mass.: MIT Press.
Cisek P, Kalaska JF (2005) Neural correlates of reaching decisions in dorsal premotor cortex: specification of multiple direction choices and final selection of action. Neuron 45:801-814.
Cooke DF, Graziano MS (2004a) Sensorimotor integration in the precentral gyrus: polysensory neurons and defensive movements. Journal of neurophysiology 91:1648-1660.
Cooke DF, Graziano MS (2004b) Super-flinchers and nerves of steel: defensive movements altered by chemical manipulation of a cortical motor area. Neuron 43:585-593.
Cooke DF, Padberg J, Zahner T, Krubitzer L (2012) The functional organization and cortical connections of motor cortex in squirrels. Cerebral cortex 22:1959-1978.
Crammond DJ, Kalaska JF (1996) Differential relation of discharge in primary motor cortex and premotor cortex to movements versus actively maintained postures during a reaching task. Experimental brain research 108:45-61.
Crick FH (1979) Thinking about the brain. Scientific American 241:219-232.
d'Avella A, Saltiel P, Bizzi E (2003) Combinations of muscle synergies in the construction of a natural motor behavior. Nature neuroscience 6:300-308.
Dapretto M, Davies MS, Pfeifer JH, Scott AA, Sigman M, Bookheimer SY, Iacoboni M (2006) Understanding emotions in others: mirror neuron dysfunction in children with autism spectrum disorders. Nature neuroscience 9:28-30.
Deisseroth K (2015) Optogenetics: 10 years of microbial opsins in neuroscience. Nature neuroscience 18:1213-1225.
Denk W, Piston DW, Webb WW (1995) Two-photon molecular excitation in laser-scanning microscopy. Handbook of Biological Confocal Microscopy 2nd 445-458.
Denk W, Strickler JH, Webb WW (1990) Two-photon laser scanning fluorescence microscopy. Science 248:73-76.
Desmurget M, Richard N, Harquel S, Baraduc P, Szathmari A, Mottolese C, Sirigu A (2014) Neural representations of ethologically relevant hand/mouth synergies in the human precentral gyrus. Proceedings of the National Academy of Sciences of the United States of America 111:5718-5722.
di Pellegrino G, Fadiga L, Fogassi L, Gallese V, Rizzolatti G (1992) Understanding motor events: a neurophysiological study. Experimental brain research 91:176-180.

Diedrichsen J, Shadmehr R, Ivry RB (2010) The coordination of movement: optimal feedback control and beyond. Trends in cognitive sciences 14:31-39.
Donoghue JP, Leibovic S, Sanes JN (1992) Organization of the forelimb area in squirrel monkey motor cortex: representation of digit, wrist, and elbow muscles. Experimental brain research 89:1-19.
Drew T (1993) Motor cortical activity during voluntary gait modifications in the cat. I. Cells related to the forelimbs. Journal of neurophysiology 70:179-199.
Drew T, Andujar JE, Lajoie K, Yakovenko S (2008) Cortical mechanisms involved in visuomotor coordination during precision walking. Brain research reviews 57:199-211.
Drew T, Jiang W, Kably B, Lavoie S (1996) Role of the motor cortex in the control of visually triggered gait modifications. Canadian journal of physiology and pharmacology 74:426-442.
Drew T, Marigold DS (2015) Taking the next step: cortical contributions to the control of locomotion. Current opinion in neurobiology 33:25-33.
Ethier C, Brizzi L, Darling WG, Capaday C (2006) Linear summation of cat motor cortex outputs. The Journal of neuroscience : the official journal of the Society for Neuroscience 26:5574-5581.
Eusebio A, Pogosyan A, Wang S, Averbeck B, Gaynor LD, Cantiniaux S, Witjas T, Limousin P, Azulay JP, Brown P (2009) Resonance in subthalamo-cortical circuits in Parkinson's disease. Brain : a journal of neurology 132:2139-2150.
Fagg AH, Shah A, Barto AG (2002) A computational model of muscle recruitment for wrist movements. Journal of neurophysiology 88:3348-3358.
Farr TD, Liu L, Colwell KL, Whishaw IQ, Metz GA (2006) Bilateral alteration in stepping pattern after unilateral motor cortex injury: a new test strategy for analysis of skilled limb movements in neurological mouse models. Journal of neuroscience methods 153:104-113.
Fenno L, Yizhar O, Deisseroth K (2011) The development and application of optogenetics. Annual review of neuroscience 34:389-412.
Ferrier D (1873) Experimental Researches in Cerebral Physiology and Pathology. Journal of anatomy and physiology 8:152-155.
Ferrier D (1874) On the Localisation of the Functions of the Brain. British medical journal 2:766-767.
Fetcho JR, Cox KJ, O'Malley DM (1998) Monitoring activity in neuronal populations with single-cell resolution in a behaving vertebrate. The Histochemical journal 30:153-167.
Foerster O (1936) The motor cortex of man in the light of Hughlings Jackson's doctrines. Brain 135-159.
Fogassi L, Gallese V, Fadiga L, Luppino G, Matelli M, Rizzolatti G (1996) Coding of peripersonal space in inferior premotor cortex (area F4). Journal of neurophysiology 76:141-157.
Fogelson N, Williams D, Tijssen M, van Bruggen G, Speelman H, Brown P (2006) Different functional loops between cerebral cortex and the subthalmic area in Parkinson's disease. Cereb Cortex 16:64-75.
Francardo V, Recchia A, Popovic N, Andersson D, Nissbrandt H, Cenci MA (2011) Impact of the lesion procedure on the profiles of motor impairment and molecular responsiveness to L-DOPA in the 6-hydroxydopamine mouse model of Parkinson's disease. Neurobiology of disease 42:327-340.
Franklin DW, Wolpert DM (2011) Computational mechanisms of sensorimotor control. Neuron 72:425-442.
Fritsch G, Hitzig E (1870) Ueber die elektrische Erregbarkeit des Grosshirns. Arch f Anat, Physiol und wissenschaftl Mediz 300-332.
Fu QG, Suarez JI, Ebner TJ (1993) Neuronal specification of direction and distance during reaching movements in the superior precentral premotor area and primary motor cortex of monkeys. Journal of neurophysiology 70:2097-2116.
Fulton J (1935) A note on the definition of the "motor" and "premotor" areas. Brain 311-316.
Fuster JM (1989) The prefrontal cortex : anatomy, physiology, and neuropsychology of the frontal lobe. New York: Raven Press.
Gallese V, Fadiga L, Fogassi L, Rizzolatti G (1996) Action recognition in the premotor cortex. Brain 119 ( Pt 2):593-609.

Gallese V, Keysers C, Rizzolatti G (2004) A unifying view of the basis of social cognition. Trends in cognitive sciences 8:396-403.
Gao TM, Pulsinelli WA, Xu ZC (1999) Changes in membrane properties of CA1 pyramidal neurons after transient forebrain ischemia in vivo. Neuroscience 90:771-780.
Gaymard B, Pierrot-Deseilligny C, Rivaud S (1990) Impairment of sequences of memory-guided saccades after supplementary motor area lesions. Annals of neurology 28:622-626.
Gentilucci M, Fogassi L, Luppino G, Matelli M, Camarda R, Rizzolatti G (1988) Functional organization of inferior area 6 in the macaque monkey. I. Somatotopy and the control of proximal movements. Experimental brain research 71:475-490.
Gentilucci M, Scandolara C, Pigarev IN, Rizzolatti G (1983) Visual responses in the postarcuate cortex (area 6) of the monkey that are independent of eye position. Experimental brain research 50:464-468.
Georgopoulos AP, Ashe J, Smyrnis N, Taira M (1992) The motor cortex and the coding of force. Science 256:1692-1695.
Georgopoulos AP, Kalaska JF, Caminiti R, Massey JT (1982) On the relations between the direction of two-dimensional arm movements and cell discharge in primate motor cortex. The Journal of neuroscience : the official journal of the Society for Neuroscience 2:1527-1537.
Georgopoulos AP, Kettner RE, Schwartz AB (1988) Primate motor cortex and free arm movements to visual targets in three-dimensional space. II. Coding of the direction of movement by a neuronal population. The Journal of neuroscience : the official journal of the Society for Neuroscience 8:2928-2937.
Georgopoulos AP, Schwartz AB, Kettner RE (1986) Neuronal population coding of movement direction. Science 233:1416-1419.
Gerloff C, Corwell B, Chen R, Hallett M, Cohen LG (1997) Stimulation over the human supplementary motor area interferes with the organization of future elements in complex motor sequences. Brain 120 ( Pt 9):1587-1602.
Giszter SF, Mussa-Ivaldi FA, Bizzi E (1993) Convergent force fields organized in the frog's spinal cord. The Journal of neuroscience : the official journal of the Society for Neuroscience 13:467-491.
Gobel W, Kampa BM, Helmchen F (2007) Imaging cellular network dynamics in three dimensions using fast 3D laser scanning. Nature methods 4:73-79.
Gould HJ, 3rd, Cusick CG, Pons TP, Kaas JH (1986) The relationship of corpus callosum connections to electrical stimulation maps of motor, supplementary motor, and the frontal eye fields in owl monkeys. The Journal of comparative neurology 247:297-325.
Goulding M (2009) Circuits controlling vertebrate locomotion: moving in a new direction. Nature reviews Neuroscience 10:507-518.
Gradinaru V, Mogri M, Thompson KR, Henderson JM, Deisseroth K (2009) Optical deconstruction of parkinsonian neural circuitry. Science 324:354-359.
Gradinaru V, Thompson KR, Deisseroth K (2008) eNpHR: a Natronomonas halorhodopsin enhanced for optogenetic applications. Brain cell biology 36:129-139.
Gradinaru V, Zhang F, Ramakrishnan C, Mattis J, Prakash R, Diester I, Goshen I, Thompson KR, Deisseroth K (2010) Molecular and cellular approaches for diversifying and extending optogenetics. Cell 141:154-165.
Graziano M (2006) The organization of behavioral repertoire in motor cortex. Annual review of neuroscience 29:105-134.
Graziano MS (2015) Ethological Action Maps: A Paradigm Shift for the Motor Cortex. Trends in cognitive sciences.
Graziano MS, Aflalo TN (2007) Mapping behavioral repertoire onto the cortex. Neuron 56:239-251.
Graziano MS, Gandhi S (2000) Location of the polysensory zone in the precentral gyrus of anesthetized monkeys. Experimental brain research 135:259-266.
Graziano MS, Hu XT, Gross CG (1997a) Coding the locations of objects in the dark. Science 277:239-241.
Graziano MS, Hu XT, Gross CG (1997b) Visuospatial properties of ventral premotor cortex. Journal of neurophysiology 77:2268-2292.

Graziano MS, Patel KT, Taylor CS (2004) Mapping from motor cortex to biceps and triceps altered by elbow angle. Journal of neurophysiology 92:395-407.
Graziano MS, Reiss LA, Gross CG (1999) A neuronal representation of the location of nearby sounds. Nature 397:428-430.
Graziano MS, Taylor CS, Moore T (2002) Complex movements evoked by microstimulation of precentral cortex. Neuron 34:841-851.
Graziano MS, Yap GS, Gross CG (1994) Coding of visual space by premotor neurons. Science 266:1054-1057.
Graziano MSA (2009) The intelligent movement machine : an ethological perspective on the primate motor system. Oxford ; New York: Oxford University Press.
Grealish S, Mattsson B, Draxler P, Bjorklund A (2010) Characterisation of behavioural and neurodegenerative changes induced by intranigral 6-hydroxydopamine lesions in a mouse model of Parkinson's disease. The European journal of neuroscience 31:2266-2278.
Gremel CM, Costa RM (2013) Premotor cortex is critical for goal-directed actions. Frontiers in computational neuroscience 7:110.
Grienberger C, Konnerth A (2012) Imaging calcium in neurons. Neuron 73:862-885.
Gross CG (1997) Emanuel Swedenborg: A neuroscientist before his time. Neuroscientist 3:142-147.
Grunbaum A, Sherrington C (1903) Observations on the physiology of the cerebral cortex of the anthropoid apes. Proc R Soc Lond 152-155.
Guigon E, Baraduc P, Desmurget M (2007) Computational motor control: redundancy and invariance. Journal of neurophysiology 97:331-347.
Halsband U, Matsuzaka Y, Tanji J (1994) Neuronal activity in the primate supplementary, pre-supplementary and premotor cortex during externally and internally instructed sequential movements. Neuroscience research 20:149-155.
Harris CM, Wolpert DM (1998) Signal-dependent noise determines motor planning. Nature 394:780-784.
Harris KD, Mrsic-Flogel TD (2013) Cortical connectivity and sensory coding. Nature 503:51-58.
Harrison TC, Ayling OG, Murphy TH (2012) Distinct cortical circuit mechanisms for complex forelimb movement and motor map topography. Neuron 74:397-409.
Harvey CD, Coen P, Tank DW (2012) Choice-specific sequences in parietal cortex during a virtual-navigation decision task. Nature 484:62-68.
He SQ, Dum RP, Strick PL (1993) Topographic organization of corticospinal projections from the frontal lobe: motor areas on the lateral surface of the hemisphere. The Journal of neuroscience : the official journal of the Society for Neuroscience 13:952-980.
Hebb DO (1949) The organization of behavior : a neuropsychological theory. New York: Wiley.
Heim N, Griesbeck O (2004) Genetically encoded indicators of cellular calcium dynamics based on troponin C and green fluorescent protein. The Journal of biological chemistry 279:14280-14286.
Helmchen F, Denk W (2005) Deep tissue two-photon microscopy. Nature methods 2:932-940.
Helmchen F, Imoto K, Sakmann B (1996) Ca2+ buffering and action potential-evoked Ca2+ signaling in dendrites of pyramidal neurons. Biophysical journal 70:1069-1081.
Helmchen F, Konnerth A (2011) Imaging in neuroscience : a laboratory manual. Cold Spring Harbor, N.Y.: Cold Spring Harbor Laboratory Press.
Heuer A, Smith GA, Lelos MJ, Lane EL, Dunnett SB (2012) Unilateral nigrostriatal 6-hydroxydopamine lesions in mice I: motor impairments identify extent of dopamine depletion at three different lesion sites. Behavioural brain research 228:30-43.
Hille B (1992) Pumping ions. Science 255:742.
Hira R, Terada S, Kondo M, Matsuzaki M (2015) Distinct Functional Modules for Discrete and Rhythmic Forelimb Movements in the Mouse Motor Cortex. The Journal of neuroscience : the official journal of the Society for Neuroscience 35:13311-13322.
Hires SA, Tian L, Looger LL (2008) Reporting neural activity with genetically encoded calcium indicators. Brain cell biology 36:69-86.

Hocherman S, Wise SP (1991) Effects of hand movement path on motor cortical activity in awake, behaving rhesus monkeys. Experimental brain research 83:285-302.
Holdefer RN, Miller LE (2002) Primary motor cortical neurons encode functional muscle synergies. Experimental brain research 146:233-243.
Hopfield JJ (1982) Neural networks and physical systems with emergent collective computational abilities. Proceedings of the National Academy of Sciences of the United States of America 79:2554-2558.
Hossmann KA (2006) Pathophysiology and therapy of experimental stroke. Cellular and molecular neurobiology 26:1057-1083.
Huber D, Gutnisky DA, Peron S, O'Connor DH, Wiegert JS, Tian L, Oertner TG, Looger LL, Svoboda K (2012) Multiple dynamic representations in the motor cortex during sensorimotor learning. Nature 484:473-478.
Hufschmidt A, Lücking CH (2006) Neurologie compact. Stuttgart u.a.: Thieme.
Iacoboni M, Dapretto M (2006) The mirror neuron system and the consequences of its dysfunction. Nature reviews Neuroscience 7:942-951.
Izawa J, Rane T, Donchin O, Shadmehr R (2008) Motor adaptation as a process of reoptimization. The Journal of neuroscience : the official journal of the Society for Neuroscience 28:2883-2891.
Jaffe DB, Johnston D, Lasser-Ross N, Lisman JE, Miyakawa H, Ross WN (1992) The spread of Na+ spikes determines the pattern of dendritic Ca2+ entry into hippocampal neurons. Nature 357:244-246.
Jenkins IH, Brooks DJ, Nixon PD, Frackowiak RS, Passingham RE (1994) Motor sequence learning: a study with positron emission tomography. The Journal of neuroscience : the official journal of the Society for Neuroscience 14:3775-3790.
Johnson PB, Ferraina S, Bianchi L, Caminiti R (1996) Cortical networks for visual reaching: physiological and anatomical organization of frontal and parietal lobe arm regions. Cerebral cortex 6:102-119.
Kakei S, Hoffman DS, Strick PL (1999) Muscle and movement representations in the primary motor cortex. Science 285:2136-2139.
Kandel ER (2013) Principles of neural science. New York: McGraw-Hill Medical.
Kaneko T, Caria MA, Asanuma H (1994) Information processing within the motor cortex. II. Intracortical connections between neurons receiving somatosensory cortical input and motor output neurons of the cortex. The Journal of comparative neurology 345:172-184.
Kawai R, Markman T, Poddar R, Ko R, Fantana AL, Dhawale AK, Kampff AR, Olveczky BP (2015) Motor cortex is required for learning but not for executing a motor skill. Neuron 86:800-812.
Kenet T, Bibitchkov D, Tsodyks M, Grinvald A, Arieli A (2003) Spontaneously emerging cortical representations of visual attributes. Nature 425:954-956.
Kepecs A, Fishell G (2014) Interneuron cell types are fit to function. Nature 505:318-326.
Komiyama T, Sato TR, O'Connor DH, Zhang YX, Huber D, Hooks BM, Gabitto M, Svoboda K (2010) Learning-related fine-scale specificity imaged in motor cortex circuits of behaving mice. Nature 464:1182-1186.
Kravitz AV, Freeze BS, Parker PR, Kay K, Thwin MT, Deisseroth K, Kreitzer AC (2010) Regulation of parkinsonian motor behaviours by optogenetic control of basal ganglia circuitry. Nature 466:622-626.
Kurtzer IL, Pruszynski JA, Scott SH (2008) Long-latency reflexes of the human arm reflect an internal model of limb dynamics. Current biology : CB 18:449-453.
Kuypers H (1978) The organization of the motor system in primates. Recent advances in primatology 623-634.
Lalo E, Thobois S, Sharott A, Polo G, Mertens P, Pogosyan A, Brown P (2008) Patterns of bidirectional communication between cortex and basal ganglia during movement in patients with Parkinson disease. The Journal of neuroscience : the official journal of the Society for Neuroscience 28:3008-3016.

Langer D, van 't Hoff M, Keller AJ, Nagaraja C, Pfaffli OA, Goldi M, Kasper H, Helmchen F (2013) HelioScan: a software framework for controlling in vivo microscopy setups with high hardware flexibility, functional diversity and extendibility. Journal of neuroscience methods 215:38-52.

Lee D, Quessy S (2003) Activity in the supplementary motor area related to learning and performance during a sequential visuomotor task. Journal of neurophysiology 89:1039-1056.

Lemon RN (2008) Descending pathways in motor control. Annual review of neuroscience 31:195-218.

Lemon RN, Griffiths J (2005) Comparing the function of the corticospinal system in different species: organizational differences for motor specialization? Muscle & nerve 32:261-279.

Lemon RN, Johansson RS, Westling G (1995) Corticospinal control during reach, grasp, and precision lift in man. The Journal of neuroscience : the official journal of the Society for Neuroscience 15:6145-6156.

Li CS, Padoa-Schioppa C, Bizzi E (2001) Neuronal correlates of motor performance and motor learning in the primary motor cortex of monkeys adapting to an external force field. Neuron 30:593-607.

Lindau NT, Banninger BJ, Gullo M, Good NA, Bachmann LC, Starkey ML, Schwab ME (2014) Rewiring of the corticospinal tract in the adult rat after unilateral stroke and anti-Nogo-A therapy. Brain 137:739-756.

Liu D, Todorov E (2007) Evidence for the flexible sensorimotor strategies predicted by optimal feedback control. The Journal of neuroscience : the official journal of the Society for Neuroscience 27:9354-9368.

Luppino G, Matelli M, Camarda RM, Gallese V, Rizzolatti G (1991) Multiple representations of body movements in mesial area 6 and the adjacent cingulate cortex: an intracortical microstimulation study in the macaque monkey. The Journal of comparative neurology 311:463-482.

Lyons MK (2011) Deep brain stimulation: current and future clinical applications. Mayo Clinic proceedings Mayo Clinic 86:662-672.

Maass W, Natschlager T, Markram H (2002) Real-time computing without stable states: a new framework for neural computation based on perturbations. Neural computation 14:2531-2560.

Macpherson JM, Marangoz C, Miles TS, Wiesendanger M (1982) Microstimulation of the supplementary motor area (SMA) in the awake monkey. Experimental brain research 45:410-416.

Mainen ZF, Maletic-Savatic M, Shi SH, Hayashi Y, Malinow R, Svoboda K (1999) Two-photon imaging in living brain slices. Methods 18:231-239, 181.

Mandelblat-Cerf Y, Paz R, Vaadia E (2009) Trial-to-trial variability of single cells in motor cortices is dynamically modified during visuomotor adaptation. The Journal of neuroscience : the official journal of the Society for Neuroscience 29:15053-15062.

Mank M, Griesbeck O (2008) Genetically encoded calcium indicators. Chemical reviews 108:1550-1564.

Mank M, Reiff DF, Heim N, Friedrich MW, Borst A, Griesbeck O (2006) A FRET-based calcium biosensor with fast signal kinetics and high fluorescence change. Biophysical journal 90:1790-1796.

Mante V, Sussillo D, Shenoy KV, Newsome WT (2013) Context-dependent computation by recurrent dynamics in prefrontal cortex. Nature 503:78-84.

Mao T, Kusefoglu D, Hooks BM, Huber D, Petreanu L, Svoboda K (2011) Long-range neuronal circuits underlying the interaction between sensory and motor cortex. Neuron 72:111-123.

Margolis DJ, Lutcke H, Helmchen F (2014) Microcircuit dynamics of map plasticity in barrel cortex. Current opinion in neurobiology 24:76-81.

Margolis DJ, Lutcke H, Schulz K, Haiss F, Weber B, Kugler S, Hasan MT, Helmchen F (2012) Reorganization of cortical population activity imaged throughout long-term sensory deprivation. Nature neuroscience 15:1539-1546.

Marsden JF, Limousin-Dowsey P, Ashby P, Pollak P, Brown P (2001) Subthalamic nucleus, sensorimotor cortex and muscle interrelationships in Parkinson's disease. Brain : a journal of neurology 124:378-388.

Masamizu Y, Tanaka YR, Tanaka YH, Hira R, Ohkubo F, Kitamura K, Isomura Y, Okada T, Matsuzaki M (2014) Two distinct layer-specific dynamics of cortical ensembles during learning of a motor task. Nature neuroscience 17:987-994.

Matsuzaka Y, Aizawa H, Tanji J (1992) A motor area rostral to the supplementary motor area (presupplementary motor area) in the monkey: neuronal activity during a learned motor task. Journal of neurophysiology 68:653-662.

Maturana HR, Lettvin JY, McCulloch WS, Pitts WH (1960) Anatomy and physiology of vision in the frog (Rana pipiens). The Journal of general physiology 43(6)Suppl:129-175.

Messier J, Kalaska JF (2000) Covariation of primate dorsal premotor cell activity with direction and amplitude during a memorized-delay reaching task. Journal of neurophysiology 84:152-165.

Metz GA, Schwab ME, Welzl H (2001) The effects of acute and chronic stress on motor and sensory performance in male Lewis rats. Physiology & behavior 72:29-35.

Metz GA, Whishaw IQ (2002) Cortical and subcortical lesions impair skilled walking in the ladder rung walking test: a new task to evaluate fore- and hindlimb stepping, placing, and co-ordination. Journal of neuroscience methods 115:169-179.

Miller JE, Ayzenshtat I, Carrillo-Reid L, Yuste R (2014) Visual stimuli recruit intrinsically generated cortical ensembles. Proceedings of the National Academy of Sciences of the United States of America 111:E4053-4061.

Mitz AR, Wise SP (1987) The somatotopic organization of the supplementary motor area: intracortical microstimulation mapping. The Journal of neuroscience : the official journal of the Society for Neuroscience 7:1010-1021.

Miyawaki A, Llopis J, Heim R, McCaffery JM, Adams JA, Ikura M, Tsien RY (1997) Fluorescent indicators for Ca2+ based on green fluorescent proteins and calmodulin. Nature 388:882-887.

Moon SK, Alaverdashvili M, Cross AR, Whishaw IQ (2009) Both compensation and recovery of skilled reaching following small photothrombotic stroke to motor cortex in the rat. Experimental neurology 218:145-153.

Moran DW, Schwartz AB (1999) Motor cortical representation of speed and direction during reaching. Journal of neurophysiology 82:2676-2692.

Muakkassa KF, Strick PL (1979) Frontal lobe inputs to primate motor cortex: evidence for four somatotopically organized 'premotor' areas. Brain research 177:176-182.

Muhammad R, Wallis JD, Miller EK (2006) A comparison of abstract rules in the prefrontal cortex, premotor cortex, inferior temporal cortex, and striatum. Journal of cognitive neuroscience 18:974-989.

Müller M (2007) Information Retrieval for Music and Motion. Berlin, Heidelberg: Springer-VerlagBerlinHeidelberg,.

Murakami H, Rubin J, Gabriel P (2011) 1Q84. p 1 online resource (925 p.) New York: Alfred A. Knopf,.

Murata A, Fadiga L, Fogassi L, Gallese V, Raos V, Rizzolatti G (1997) Object representation in the ventral premotor cortex (area F5) of the monkey. Journal of neurophysiology 78:2226-2230.

Murphy TH, Corbett D (2009) Plasticity during stroke recovery: from synapse to behaviour. Nature reviews Neuroscience 10:861-872.

Mushiake H, Inase M, Tanji J (1990) Selective coding of motor sequence in the supplementary motor area of the monkey cerebral cortex. Experimental brain research 82:208-210.

Nachev P, Kennard C, Husain M (2008) Functional role of the supplementary and pre-supplementary motor areas. Nature reviews Neuroscience 9:856-869.

Nagai T, Sawano A, Park ES, Miyawaki A (2001) Circularly permuted green fluorescent proteins engineered to sense Ca2+. Proceedings of the National Academy of Sciences of the United States of America 98:3197-3202.

Nagel G, Szellas T, Huhn W, Kateriya S, Adeishvili N, Berthold P, Ollig D, Hegemann P, Bamberg E (2003) Channelrhodopsin-2, a directly light-gated cation-selective membrane channel. Proceedings of the National Academy of Sciences of the United States of America 100:13940-13945.

Nakai J, Ohkura M, Imoto K (2001) A high signal-to-noise Ca(2+) probe composed of a single green fluorescent protein. Nature biotechnology 19:137-141.

Neafsey EJ, Bold EL, Haas G, Hurley-Gius KM, Quirk G, Sievert CF, Terreberry RR (1986) The organization of the rat motor cortex: a microstimulation mapping study. Brain research 396:77-96.
Nudo RJ (2006) Mechanisms for recovery of motor function following cortical damage. Current opinion in neurobiology 16:638-644.
Nudo RJ (2013) Recovery after brain injury: mechanisms and principles. Frontiers in human neuroscience 7:887.
Nudo RJ, Milliken GW, Jenkins WM, Merzenich MM (1996) Use-dependent alterations of movement representations in primary motor cortex of adult squirrel monkeys. The Journal of neuroscience : the official journal of the Society for Neuroscience 16:785-807.
Obeso JA, Marin C, Rodriguez-Oroz C, Blesa J, Benitez-Temino B, Mena-Segovia J, Rodriguez M, Olanow CW (2008) The basal ganglia in Parkinson's disease: current concepts and unexplained observations. Annals of neurology 64 Suppl 2:S30-46.
Ogawa Y, Tanokura M (1984) Calcium binding to calmodulin: effects of ionic strength, Mg2+, pH and temperature. Journal of biochemistry 95:19-28.
Oheim M, Beaurepaire E, Chaigneau E, Mertz J, Charpak S (2001) Two-photon microscopy in brain tissue: parameters influencing the imaging depth. Journal of neuroscience methods 111:29-37.
Overduin SA, d'Avella A, Carmena JM, Bizzi E (2012) Microstimulation activates a handful of muscle synergies. Neuron 76:1071-1077.
Overduin SA, d'Avella A, Carmena JM, Bizzi E (2014) Muscle synergies evoked by microstimulation are preferentially encoded during behavior. Frontiers in computational neuroscience 8:20.
Palmer AE, Giacomello M, Kortemme T, Hires SA, Lev-Ram V, Baker D, Tsien RY (2006) Ca2+ indicators based on computationally redesigned calmodulin-peptide pairs. Chemistry & biology 13:521-530.
Palmer AE, Tsien RY (2006) Measuring calcium signaling using genetically targetable fluorescent indicators. Nature protocols 1:1057-1065.
Paninski L, Fellows MR, Hatsopoulos NG, Donoghue JP (2004) Spatiotemporal tuning of motor cortical neurons for hand position and velocity. Journal of neurophysiology 91:515-532.
Papadopoulos CM, Tsai SY, Cheatwood JL, Bollnow MR, Kolb BE, Schwab ME, Kartje GL (2006) Dendritic plasticity in the adult rat following middle cerebral artery occlusion and Nogo-a neutralization. Cerebral cortex 16:529-536.
Park MC, Belhaj-Saif A, Cheney PD (2004) Properties of primary motor cortex output to forelimb muscles in rhesus macaques. Journal of neurophysiology 92:2968-2984.
Park MC, Belhaj-Saif A, Gordon M, Cheney PD (2001) Consistent features in the forelimb representation of primary motor cortex in rhesus macaques. The Journal of neuroscience : the official journal of the Society for Neuroscience 21:2784-2792.
Passingham RE (1985) Premotor cortex: sensory cues and movement. Behavioural brain research 18:175-185.
Passingham RE (1986) Cues for movement in monkeys (Macaca mulatta) with lesions in premotor cortex. Behavioral neuroscience 100:695-703.
Passingham RE (1993) The frontal lobes and voluntary action. Oxford ; New York: Oxford University Press.
Passingham RE, Myers C, Rawlins N, Lightfoot V, Fearn S (1988) Premotor cortex in the rat. Behavioral neuroscience 102:101-109.
Passingham RE, Perry VH, Wilkinson F (1983) The long-term effects of removal of sensorimotor cortex in infant and adult rhesus monkeys. Brain 106 (Pt 3):675-705.
Penfield W, Boldrey E (1937) Somatic motor and sensory representation in the cerebral cortex of man as studied by electrical stimulation. Brain 389-443.
Penfield W, Welch K (1951) The supplementary motor area of the cerebral cortex; a clinical and experimental study. AMA archives of neurology and psychiatry 66:289-317.
Peters AJ, Chen SX, Komiyama T (2014) Emergence of reproducible spatiotemporal activity during motor learning. Nature 510:263-267.

Pruszynski JA, Kurtzer I, Scott SH (2008) Rapid motor responses are appropriately tuned to the metrics of a visuospatial task. Journal of neurophysiology 100:224-238.
Ralston DD, Ralston HJ, 3rd (1985) The terminations of corticospinal tract axons in the macaque monkey. The Journal of comparative neurology 242:325-337.
Ramanathan D, Conner JM, Tuszynski MH (2006) A form of motor cortical plasticity that correlates with recovery of function after brain injury. Proceedings of the National Academy of Sciences of the United States of America 103:11370-11375.
Raos V, Umilta MA, Murata A, Fogassi L, Gallese V (2006) Functional properties of grasping-related neurons in the ventral premotor area F5 of the macaque monkey. Journal of neurophysiology 95:709-729.
Rascol O, Payoux P, Ory F, Ferreira JJ, Brefel-Courbon C, Montastruc JL (2003) Limitations of current Parkinson's disease therapy. Annals of neurology 53 Suppl 3:S3-12; discussion S12-15.
Rathelot JA, Strick PL (2006) Muscle representation in the macaque motor cortex: an anatomical perspective. Proceedings of the National Academy of Sciences of the United States of America 103:8257-8262.
Redecker C, Wang W, Fritschy JM, Witte OW (2002) Widespread and long-lasting alterations in GABA(A)-receptor subtypes after focal cortical infarcts in rats: mediation by NMDA-dependent processes. Journal of cerebral blood flow and metabolism : official journal of the International Society of Cerebral Blood Flow and Metabolism 22:1463-1475.
Redgrave P, Rodriguez M, Smith Y, Rodriguez-Oroz MC, Lehericy S, Bergman H, Agid Y, DeLong MR, Obeso JA (2010) Goal-directed and habitual control in the basal ganglia: implications for Parkinson's disease. Nature reviews Neuroscience 11:760-772.
Reimer J, Hatsopoulos NG (2009) The problem of parametric neural coding in the motor system. Advances in experimental medicine and biology 629:243-259.
Reina GA, Moran DW, Schwartz AB (2001) On the relationship between joint angular velocity and motor cortical discharge during reaching. Journal of neurophysiology 85:2576-2589.
Rickert J, Riehle A, Aertsen A, Rotter S, Nawrot MP (2009) Dynamic encoding of movement direction in motor cortical neurons. The Journal of neuroscience : the official journal of the Society for Neuroscience 29:13870-13882.
Rioult-Pedotti MS, Friedman D, Donoghue JP (2000) Learning-induced LTP in neocortex. Science 290:533-536.
Rizzolatti G, Camarda R, Fogassi L, Gentilucci M, Luppino G, Matelli M (1988) Functional organization of inferior area 6 in the macaque monkey. II. Area F5 and the control of distal movements. Experimental brain research 71:491-507.
Rizzolatti G, Craighero L (2004) The mirror-neuron system. Annual review of neuroscience 27:169-192.
Rizzolatti G, Scandolara C, Matelli M, Gentilucci M (1981) Afferent properties of periarcuate neurons in macaque monkeys. II. Visual responses. Behavioural brain research 2:147-163.
Rokni U, Richardson AG, Bizzi E, Seung HS (2007) Motor learning with unstable neural representations. Neuron 54:653-666.
Roland PE, Larsen B, Lassen NA, Skinhoj E (1980a) Supplementary motor area and other cortical areas in organization of voluntary movements in man. Journal of neurophysiology 43:118-136.
Roland PE, Skinhoj E, Lassen NA, Larsen B (1980b) Different cortical areas in man in organization of voluntary movements in extrapersonal space. Journal of neurophysiology 43:137-150.
Rosenblatt F (1958) The perceptron: a probabilistic model for information storage and organization in the brain. Psychological review 65:386-408.
Sanes JN, Donoghue JP (2000) Plasticity and primary motor cortex. Annual review of neuroscience 23:393-415.
Sanes JN, Wang J, Donoghue JP (1992) Immediate and delayed changes of rat motor cortical output representation with new forelimb configurations. Cerebral cortex 2:141-152.
Schaffelhofer S, Agudelo-Toro A, Scherberger H (2015) Decoding a wide range of hand configurations from macaque motor, premotor, and parietal cortices. The Journal of neuroscience : the official journal of the Society for Neuroscience 35:1068-1081.

Schieber MH, Hibbard LS (1993) How somatotopic is the motor cortex hand area? Science 261:489-492.
Schwab ME, Strittmatter SM (2014) Nogo limits neural plasticity and recovery from injury. Current opinion in neurobiology 27:53-60.
Schwartz AB, Kettner RE, Georgopoulos AP (1988) Primate motor cortex and free arm movements to visual targets in three-dimensional space. I. Relations between single cell discharge and direction of movement. The Journal of neuroscience : the official journal of the Society for Neuroscience 8:2913-2927.
Scott SH (2004) Optimal feedback control and the neural basis of volitional motor control. Nature reviews Neuroscience 5:532-546.
Scott SH (2012) The computational and neural basis of voluntary motor control and planning. Trends in cognitive sciences 16:541-549.
Scott SH, Kalaska JF (1995) Changes in motor cortex activity during reaching movements with similar hand paths but different arm postures. Journal of neurophysiology 73:2563-2567.
Scott SH, Kalaska JF (1997) Reaching movements with similar hand paths but different arm orientations. I. Activity of individual cells in motor cortex. Journal of neurophysiology 77:826-852.
Sergio LE, Kalaska JF (2003) Systematic changes in motor cortex cell activity with arm posture during directional isometric force generation. Journal of neurophysiology 89:212-228.
Serrien DJ, Strens LH, Oliviero A, Brown P (2002) Repetitive transcranial magnetic stimulation of the supplementary motor area (SMA) degrades bimanual movement control in humans. Neuroscience letters 328:89-92.
Shenoy KV, Sahani M, Churchland MM (2013) Cortical control of arm movements: a dynamical systems perspective. Annual review of neuroscience 36:337-359.
Shepherd GM (1990) The Synaptic organization of the brain. New York: Oxford University Press.
Sherrington C (1906) Observations on the scratch-reflex in the spinal dog. J Physiol 34:1-50.
Shima K, Mushiake H, Saito N, Tanji J (1996) Role for cells in the presupplementary motor area in updating motor plans. Proceedings of the National Academy of Sciences of the United States of America 93:8694-8698.
Shimazu H, Maier MA, Cerri G, Kirkwood PA, Lemon RN (2004) Macaque ventral premotor cortex exerts powerful facilitation of motor cortex outputs to upper limb motoneurons. The Journal of neuroscience : the official journal of the Society for Neuroscience 24:1200-1211.
Shinoda Y, Kakei S (1989) Distribution of terminals of thalamocortical fibers originating from the ventrolateral nucleus of the cat thalamus. Neuroscience letters 96:163-167.
Sohal VS, Zhang F, Yizhar O, Deisseroth K (2009) Parvalbumin neurons and gamma rhythms enhance cortical circuit performance. Nature 459:698-702.
Squirrell JM, Wokosin DL, White JG, Bavister BD (1999) Long-term two-photon fluorescence imaging of mammalian embryos without compromising viability. Nature biotechnology 17:763-767.
Starkey ML, Bleul C, Zorner B, Lindau NT, Mueggler T, Rudin M, Schwab ME (2012) Back seat driving: hindlimb corticospinal neurons assume forelimb control following ischaemic stroke. Brain 135:3265-3281.
Stellwagen D, Shatz CJ (2002) An instructive role for retinal waves in the development of retinogeniculate connectivity. Neuron 33:357-367.
Steriade M, Gloor P, Llinas RR, Lopes de Silva FH, Mesulam MM (1990) Report of IFCN Committee on Basic Mechanisms. Basic mechanisms of cerebral rhythmic activities. Electroencephalography and clinical neurophysiology 76:481-508.
Stosiek C, Garaschuk O, Holthoff K, Konnerth A (2003) In vivo two-photon calcium imaging of neuronal networks. Proceedings of the National Academy of Sciences of the United States of America 100:7319-7324.
Strick PL, Sterling P (1974) Synaptic termination of afferents from the ventrolateral nucleus of the thalamus in the cat motor cortex. A light and electron microscopy study. The Journal of comparative neurology 153:77-106.

Sul JH, Jo S, Lee D, Jung MW (2011) Role of rodent secondary motor cortex in value-based action selection. Nature neuroscience 14:1202-1208.
Sur M, Leamey CA (2001) Development and plasticity of cortical areas and networks. Nature reviews Neuroscience 2:251-262.
Svoboda K, Denk W, Kleinfeld D, Tank DW (1997) In vivo dendritic calcium dynamics in neocortical pyramidal neurons. Nature 385:161-165.
Svoboda K, Yasuda R (2006) Principles of two-photon excitation microscopy and its applications to neuroscience. Neuron 50:823-839.
Tanji J, Shima K (1994) Role for supplementary motor area cells in planning several movements ahead. Nature 371:413-416.
Tehovnik EJ, Yeomans JS (1987) Circling elicited from the anteromedial cortex and medial pons: refractory periods and summation. Brain research 407:240-252.
Tennant KA, Adkins DL, Donlan NA, Asay AL, Thomas N, Kleim JA, Jones TA (2011) The organization of the forelimb representation of the C57BL/6 mouse motor cortex as defined by intracortical microstimulation and cytoarchitecture. Cerebral cortex 21:865-876.
Theer P, Hasan MT, Denk W (2003) Two-photon imaging to a depth of 1000 microm in living brains by use of a Ti:Al2O3 regenerative amplifier. Optics letters 28:1022-1024.
Tian L, Hires SA, Mao T, Huber D, Chiappe ME, Chalasani SH, Petreanu L, Akerboom J, McKinney SA, Schreiter ER, Bargmann CI, Jayaraman V, Svoboda K, Looger LL (2009) Imaging neural activity in worms, flies and mice with improved GCaMP calcium indicators. Nature methods 6:875-881.
Ting LH, Macpherson JM (2005) A limited set of muscle synergies for force control during a postural task. Journal of neurophysiology 93:609-613.
Todorov E (2004) Optimality principles in sensorimotor control. Nature neuroscience 7:907-915.
Todorov E, Jordan MI (2002) Optimal feedback control as a theory of motor coordination. Nature neuroscience 5:1226-1235.
Torres-Oviedo G, Ting LH (2007) Muscle synergies characterizing human postural responses. Journal of neurophysiology 98:2144-2156.
Townsend BR, Paninski L, Lemon RN (2006) Linear encoding of muscle activity in primary motor cortex and cerebellum. Journal of neurophysiology 96:2578-2592.
Trepel M (2004) Neuroanatomie

Struktur und Funktion ; mit 27 Tabellen. M*unchen u.a.: Urban & Fischer.
Tresch MC, Saltiel P, Bizzi E (1999) The construction of movement by the spinal cord. Nature neuroscience 2:162-167.
Turrigiano GG, Nelson SB (2004) Homeostatic plasticity in the developing nervous system. Nature reviews Neuroscience 5:97-107.
Tye KM, Deisseroth K (2012) Optogenetic investigation of neural circuits underlying brain disease in animal models. Nature reviews Neuroscience 13:251-266.
Van Acker GM, 3rd, Amundsen SL, Messamore WG, Zhang HY, Luchies CW, Cheney PD (2014) Equilibrium-based movement endpoints elicited from primary motor cortex using repetitive microstimulation. The Journal of neuroscience : the official journal of the Society for Neuroscience 34:15722-15734.
Vargas-Irwin CE, Shakhnarovich G, Yadollahpour P, Mislow JM, Black MJ, Donoghue JP (2010) Decoding complete reach and grasp actions from local primary motor cortex populations. The Journal of neuroscience : the official journal of the Society for Neuroscience 30:9659-9669.
Wahl AS, Omlor W, Rubio JC, Chen JL, Zheng H, Schroter A, Gullo M, Weinmann O, Kobayashi K, Helmchen F, Ommer B, Schwab ME (2014) Neuronal repair. Asynchronous therapy restores motor control by rewiring of the rat corticospinal tract after stroke. Science 344:1250-1255.
Weiler N, Wood L, Yu J, Solla SA, Shepherd GM (2008) Top-down laminar organization of the excitatory network in motor cortex. Nature neuroscience 11:360-366.
Weinrich M, Wise SP (1982) The premotor cortex of the monkey. The Journal of neuroscience : the official journal of the Society for Neuroscience 2:1329-1345.

Weinrich M, Wise SP, Mauritz KH (1984) A neurophysiological study of the premotor cortex in the rhesus monkey. Brain 107 ( Pt 2):385-414.

Williams D, Tijssen M, Van Bruggen G, Bosch A, Insola A, Di Lazzaro V, Mazzone P, Oliviero A, Quartarone A, Speelman H, Brown P (2002) Dopamine-dependent changes in the functional connectivity between basal ganglia and cerebral cortex in humans. Brain : a journal of neurology 125:1558-1569.

Williams JH, Whiten A, Suddendorf T, Perrett DI (2001) Imitation, mirror neurons and autism. Neuroscience and biobehavioral reviews 25:287-295.

Winship IR, Murphy TH (2008) In vivo calcium imaging reveals functional rewiring of single somatosensory neurons after stroke. The Journal of neuroscience : the official journal of the Society for Neuroscience 28:6592-6606.

Wise SP, Weinrich M, Mauritz KH (1983) Motor aspects of cue-related neuronal activity in premotor cortex of the rhesus monkey. Brain research 260:301-305.

Woolsey CN, Settlage PH, Meyer DR, Sencer W, Pinto Hamuy T, Travis AM (1952) Patterns of localization in precentral and "supplementary" motor areas and their relation to the concept of a premotor area. Research publications - Association for Research in Nervous and Mental Disease 30:238-264.

Xu T, Yu X, Perlik AJ, Tobin WF, Zweig JA, Tennant K, Jones T, Zuo Y (2009) Rapid formation and selective stabilization of synapses for enduring motor memories. Nature 462:915-919.

Yang G, Pan F, Gan WB (2009) Stably maintained dendritic spines are associated with lifelong memories. Nature 462:920-924.

Yang HW, Lemon RN (2003) An electron microscopic examination of the corticospinal projection to the cervical spinal cord in the rat: lack of evidence for cortico-motoneuronal synapses. Experimental brain research 149:458-469.

Yasuda R, Nimchinsky EA, Scheuss V, Pologruto TA, Oertner TG, Sabatini BL, Svoboda K (2004) Imaging calcium concentration dynamics in small neuronal compartments. Science's STKE : signal transduction knowledge environment 2004:pl5.

Yin HH (2009) The role of the murine motor cortex in action duration and order. Frontiers in integrative neuroscience 3:23.

Yizhar O, Fenno LE, Prigge M, Schneider F, Davidson TJ, O'Shea DJ, Sohal VS, Goshen I, Finkelstein J, Paz JT, Stehfest K, Fudim R, Ramakrishnan C, Huguenard JR, Hegemann P, Deisseroth K (2011) Neocortical excitation/inhibition balance in information processing and social dysfunction. Nature 477:171-178.

Yuste R (2015) From the neuron doctrine to neural networks. Nature reviews Neuroscience 16:487-497.

Yuste R, Peinado A, Katz LC (1992) Neuronal domains in developing neocortex. Science 257:665-669.

Zhang F, Aravanis AM, Adamantidis A, de Lecea L, Deisseroth K (2007a) Circuit-breakers: optical technologies for probing neural signals and systems. Nature reviews Neuroscience 8:577-581.

Zhang F, Gradinaru V, Adamantidis AR, Durand R, Airan RD, de Lecea L, Deisseroth K (2010) Optogenetic interrogation of neural circuits: technology for probing mammalian brain structures. Nature protocols 5:439-456.

Zhang F, Wang LP, Brauner M, Liewald JF, Kay K, Watzke N, Wood PG, Bamberg E, Nagel G, Gottschalk A, Deisseroth K (2007b) Multimodal fast optical interrogation of neural circuitry. Nature 446:633-639.

Zhang S, Murphy TH (2007) Imaging the impact of cortical microcirculation on synaptic structure and sensory-evoked hemodynamic responses in vivo. PLoS biology 5:e119.

Zorner B, Filli L, Starkey ML, Gonzenbach R, Kasper H, Rothlisberger M, Bolliger M, Schwab ME (2010) Profiling locomotor recovery: comprehensive quantification of impairments after CNS damage in rodents. Nature methods 7:701-708.